

# A Hitchhiker's Guide to Click-Chemistry with Nucleic Acids

Nicolò Zuin Fantoni, Afaf H. El-Sagheer, and Tom Brown\*



Cite This: *Chem. Rev.* 2021, 121, 7122–7154



Read Online

ACCESS |

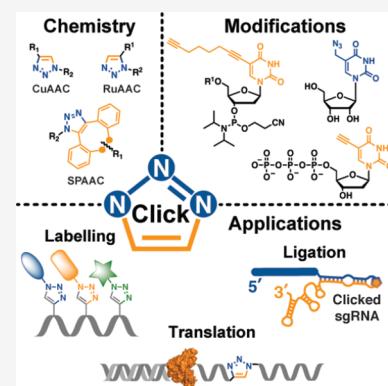


Metrics & More



Article Recommendations

**ABSTRACT:** Click chemistry is an immensely powerful technique for the fast and efficient covalent conjugation of molecular entities. Its broad scope has positively impacted on multiple scientific disciplines, and its implementation within the nucleic acid field has enabled researchers to generate a wide variety of tools with application in biology, biochemistry, and biotechnology. Azide–alkyne cycloadditions (AAC) are still the leading technology among click reactions due to the facile modification and incorporation of azide and alkyne groups within biological scaffolds. Application of AAC chemistry to nucleic acids allows labeling, ligation, and cyclization of oligonucleotides efficiently and cost-effectively relative to previously used chemical and enzymatic techniques. In this review, we provide a guide to inexperienced and knowledgeable researchers approaching the field of click chemistry with nucleic acids. We discuss in detail the chemistry, the available modified-nucleosides, and applications of AAC reactions in nucleic acid chemistry and provide a critical view of the advantages, limitations, and open-questions within the field.



## CONTENTS

1. Introduction	7123	4.3. Click-Chemistry to Assemble Nucleic Acids	7139
2. Chemistry of the Azide Alkyne Cycloaddition	7124	4.3.1. Clicking Nucleobases on the Backbone	7139
2.1. Copper Catalyzed Azide Alkyne Cycloaddition (CuAAC)	7124	4.3.2. Triazole as a Phosphate Linkage Alternative	7139
2.1.1. CuAAC Reaction Mechanism	7124	4.4. Biocompatible Triazole Linkage	7140
2.1.2. Strategies for Cu(I)-Catalyst Generation	7124	4.4.1. Pursuing the Biocompatibility of the Click Backbone	7140
2.1.3. Tailoring the CuAAC Click Reaction	7125	4.4.2. Cellular Biocompatibility of the Triazole Backbone-Modified DNA	7141
2.2. Ruthenium Catalyzed Azide Alkyne Cycloaddition (RuAAC)	7126	4.4.3. Biocompatibility of Triazole-Modified RNA	7142
2.2.1. Ru-Catalysis in Azide Alkyne Cycloadditions	7126	4.4.4. Biophysical Analysis of the Triazole Linkage Trz B	7143
2.2.2. RuAAC Applications for Antibacterial Drug Development	7128	4.5. Antisense Oligonucleotides by Click-Chemistry	7143
2.3. Metal-free Click Chemistry and Strain Promoted Azide Alkyne Cycloaddition (SPAAC)	7128	4.6. Split and Click Approach to Single-Guide RNA Generation	7144
3. Introducing Click-Functional Groups in Nucleic Acid Scaffolds	7130	4.7. Nanomaterials	7145
3.1. Alkyne and Azide Building Blocks for Click Couplings	7130	4.8. Cyclic DNA	7146
3.2. Compatibility of Alkyne Modified dNTPs with PCR	7132	5. Conclusions	7147
4. Applications of the Azide Alkyne Cycloaddition with Nucleic Acids	7132	Author Information	7148
4.1. Small Molecule–DNA Click	7132	Corresponding Author	7148
4.1.1. Fluorophore Labeling	7132	Authors	7148
4.1.2. Other Small-Molecule Labels	7134	Notes	7148
4.2. Cellular Metabolic Labeling of Nucleic Acids	7136		
4.2.1. Metabolic Labeling of DNA	7136		
4.2.2. Metabolic Labeling of RNA	7137		

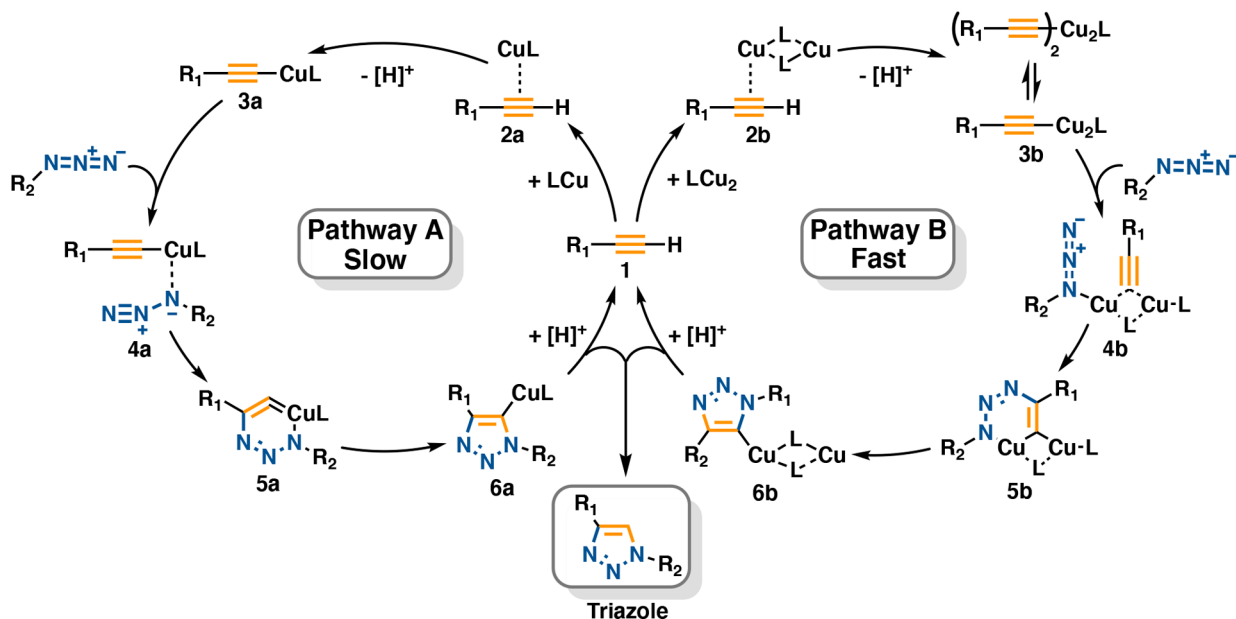
Special Issue: Click Chemistry

Received: August 28, 2020

Published: January 14, 2021



Scheme 1. Two Competitive Pathways for the Cu(I)-Catalyzed Azide–Alkyne Cycloaddition (CuAAC): A Slow Process Catalyzed by a Mononuclear Cu Species (Pathway A) and a More Kinetically Favored Route Promoted by the Formation of a Dinuclear Cu Catalyst (Pathway B)<sup>37</sup>



Biographies	7148
Acknowledgments	7148
Abbreviations	7148
References	7148

## 1. INTRODUCTION

Synthetic methodologies that use modular approaches to efficiently generate biologically relevant constructs are of paramount importance for the fast and high-throughput production of molecular probes, for screening assays, and for the development of pharmaceuticals. In 1999, K. B. Sharpless used the term “click chemistry” to define a set of reactions which are broad in scope, high yielding, stereospecific, and result in few or no byproducts.<sup>1</sup> The name epitomizes chemical transformations that are simple to execute, that involve readily available starting reagents, that are compatible with an aqueous environment or no solvent, and that require simple product separation (*i.e.* chromatographic methods). Currently, four types of reactions follow these criteria and include (i) nucleophilic substitutions; (ii) additions to C–C multiple bonds (*e.g.* Michael addition, epoxidation, dihydroxylation, aziridination); (iii) nonaldol like chemistry (*e.g.* *N*-hydroxysuccinimide active ester couplings); and (iv) cycloadditions (*e.g.* Diels–Adler reaction, Huisgen’s cycloaddition).

For many years Huisgen’s cycloaddition has been applied in various branches of chemistry. It consists of the condensation of organic azides with alkyne groups to form 1,2,3-triazole linkages.<sup>2</sup> Azide and alkyne functionalities can be easily introduced in the scaffold of large organic constructs of biological relevance. These groups are chemically unreactive toward most functional moieties of other biological substrates (such as lipids, proteins, and nucleic acids) and can therefore be considered to be bioorthogonal and biocompatible. However, for more than four decades application of this reaction was limited by the requirement for high temperatures,

long reaction times, and poor regioselectivity (both the 1,4- and 1,5-isomeric adducts are formed). The slow reaction progress is due to the high chemical stability of canonical alkynes. Only electron-deficient alkynes—albeit not bioorthogonal—can be substrates for the autonomous noncatalyzed cycloaddition by conjugate addition mechanisms. Research carried out separately and simultaneously by Meldal<sup>3</sup> and Sharpless<sup>4</sup> addressed these limitations by introducing a copper(I) catalyst. The Cu(I) core has a dual effect in that it activates the slow-reacting alkyne group thus accelerating the azide–alkyne condensation kinetics by  $\sim 10^7$ – $10^8$ -fold,<sup>1</sup> and it organizes the reacting groups by “templation” so that only a regioselective 1,4-disubstituted adduct is formed. This reaction is known as the copper-catalyzed azide alkyne cycloaddition (CuAAC), and its compatibility with a wide range of biological substrates and synthetic conditions makes CuAAC the flagship among click conjugations. Since its discovery, Cu(I)-catalyzed azide alkyne cycloaddition has been widely used within the fields of biology, biochemistry, and biotechnology.<sup>5–8</sup> Researchers have applied azide-alkyne cycloadditions to various biological substrates,<sup>5</sup> developed catalysts of high efficiency and diverse reactivity<sup>9</sup>—some metal complexes favor the production of the 1,5-disubstituted adduct—and investigated “activated” alkyne groups for rapid triazole formation in the absence of metal catalysts.<sup>10–13</sup>

The facile scalability, modularity and biocompatibility of click reactions quickly attracted interest in the application of azide–alkyne cycloadditions (AACs) in the field of nucleic acids,<sup>14–16</sup> enabling the following: (i) facile labeling of oligonucleotides (ODNs) with small-molecular probes;<sup>17</sup> (ii) joining of oligonucleotide sequences (*e.g.* single strands, double strands, including complementary strands);<sup>18,19</sup> (iii) cyclization of oligonucleotides to form circular DNA or RNA constructs;<sup>18,20–22</sup> (iv) metabolic labeling of DNA and RNA;<sup>23</sup> (v) creation of biocompatible nucleic acid scaffolds for applications such as PCR;<sup>23–27</sup> and (vi) generation of

oligonucleotide-functionalized surfaces, DNA nanostructures, nanowires, and nanosensors.<sup>28–32</sup>

This review aims to provide a comprehensive background for both inexperienced and knowledgeable readers about click-chemistry and its recent implementation within the nucleic acid field. An overview of the chemistry of the azide–alkyne cycloaddition will be discussed including the molecular mechanism and the available catalysts. Applications of AAC to nucleic acids will be covered in detail including some of the most recent work conducted to advance the field. We also discuss open questions yet to be addressed.

## 2. CHEMISTRY OF THE AZIDE ALKYNE CYCLOADDITION

The facile formation and high chemical stability of triazole linkages make the azide–alkyne cycloaddition a fascinating strategy for labeling and ligation of nucleic acids. However, direct application of Huisgen's click conversion to oligonucleotides is limited by the requirement for high reaction temperatures which usually results in DNA or RNA degradation. In addition, formation of two regioisomers, the 1,4- and 1,5-disubstituted triazoles, on extended oligonucleotides can result in difficult separation and purification. The introduction of a catalyst accelerates the cycloaddition, increases the reaction yield, and promotes regioselectivity in the final triazole linkage. Various metals and metal complexes have been used for these purposes including copper,<sup>33</sup> ruthenium,<sup>34</sup> silver,<sup>35</sup> and zinc<sup>36</sup> derivatives. Alternatively, “activated” alkynes have been utilized to avoid metal catalysis in the strain promoted azide–alkyne cycloaddition (SPAAC) developed by Bertozzi et al.<sup>10</sup> In the current section, we will focus mainly on the most common strategies used for triazole formation on nucleic acids scaffolds: the copper or ruthenium catalyzed azide–alkyne cycloaddition (CuAAC and RuAAC, respectively) and the metal-free SPAAC reaction.

### 2.1. Copper Catalyzed Azide Alkyne Cycloaddition (CuAAC)

**2.1.1. CuAAC Reaction Mechanism.** The copper catalyzed azide alkyne cycloaddition (CuAAC) represents the best studied and most popular metal ion catalyzed Huisgen reaction. In contrast to the uncatalyzed version, where preference between a concerted or stepwise mechanism depends on the functional group linked to the reactive moiety, in CuAAC the concerted pathway is excluded by the metal center, in favor of the stepwise process.<sup>37</sup> Density-functional theory (DFT) calculations combined with kinetic studies identified two possible competing mechanisms in CuAAC for triazole formation: a slow process catalyzed by a mononuclear Cu species and a more kinetically favored route promoted by the formation of a dinuclear Cu catalyst (Scheme 1).<sup>37–40</sup> In both pathways, the first reaction step is characterized by replacement of a Cu(I) ligand donor with the organic alkyne to form a  $\pi$ -complex (2a and 2b). This step is slightly endothermic in organic solvents ( $\sim 0.6$  kcal/mol) but becomes exothermic in an aqueous environment (by 11.7 kcal/mol). The energy difference further supports the experimental evidence that CuAAC reactions proceed faster in aqueous conditions. Formation of the metal–alkyne adduct reduces the alkyne  $pK_a$  by  $\sim 10$  units making its deprotonation to form the Cu-acetylide adduct (3a and 3b) accessible also in aqueous conditions. This fast reaction step is followed by coordination of the organic azide to the Cu(I) core (or to the second

copper center in the dinuclear catalyzed pathway) which templates the endothermic addition (Figure 1) of the N-3

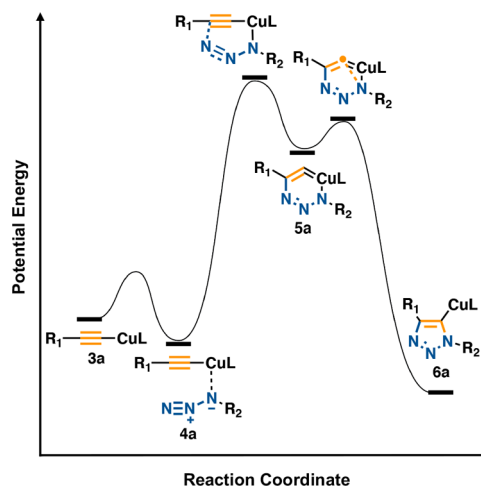


**Figure 1.** Energy profile of the reaction of copper(I) acetylides with organic azide based on DFT studies (L is CH<sub>3</sub>CN or H<sub>2</sub>O) and proposed by K. B. Sharpless.<sup>37</sup>

nitrogen of the azide to the C-2 carbon of the acetylide forming a Cu(III) metallacycle (5a and 5b). The presence of copper plays an essential role in promoting the C–N bond formation by considerably reducing the activation barrier compared to the uncatalyzed reaction (from  $\sim 26$  kcal/mol to either  $\sim 15$  or  $19$  kcal/mol according to the substituents on the copper center). In the final step the ring contracts to form the triazolyl-copper derivative which undergoes protolysis releasing the triazole product and completing the catalytic cycle (6a and 6b).<sup>37</sup> Various reaction mechanisms have been proposed for CuAAC, but recently, a slight variation of the dinuclear catalyzed pathway, suggested first by Fokin et al., was proven by isolating a key dinuclear intermediate from the cycloaddition between Cu-phenylacetylide and benzylazide.<sup>40</sup>

**2.1.2. Strategies for Cu(I)-Catalyst Generation.** Different protocols have been developed to generate and stabilize Cu(I) sources for the Cu-catalyzed cycloaddition reaction.<sup>41</sup> The three main strategies for Cu(I)-catalyst generation involve: (i) direct use of Cu(I) salts or carbene complexes;<sup>42</sup> (ii) oxidation or comproportionation of a Cu(0) source (e.g. from Cu(II) and Cu(0) mixtures) or copper-dressed materials;<sup>43</sup> and (iii) formation of the active catalyst from Cu(II) salts by addition of reducing agents (such as sodium-L-ascorbate (Na-L-asc), tris(2-carboxyethyl)phosphine (TCEP), and hydrazine).<sup>44</sup> Several Cu(I)-salts have been used for click couplings including cuprous iodide, cuprous bromide, CuOTf<sup>+</sup>C<sub>6</sub>H<sub>6</sub>, or CuOAc. When CuAAC is catalyzed by Cu(I) compounds, however, anhydrous degassed organic solvents such as tetrahydrofuran, acetonitrile, dichloromethane, or toluene are required to aid solubilization and to protect the metal center from oxidation. Catalysis directly from Cu(I) sources might however be inefficient and Cu(II)-reductant mixtures can cause degradation of the reacting substrates.<sup>45</sup> In these cases, the active catalyst can be generated by combining Cu(0) (e.g. from elemental copper shavings or nanoparticles) with Cu(II) amine salts. However, reactivity using this strategy is usually slow and high catalyst loading, longer reaction times, and/or microwave irradiation is commonly applied to complete the reaction. As an alternative

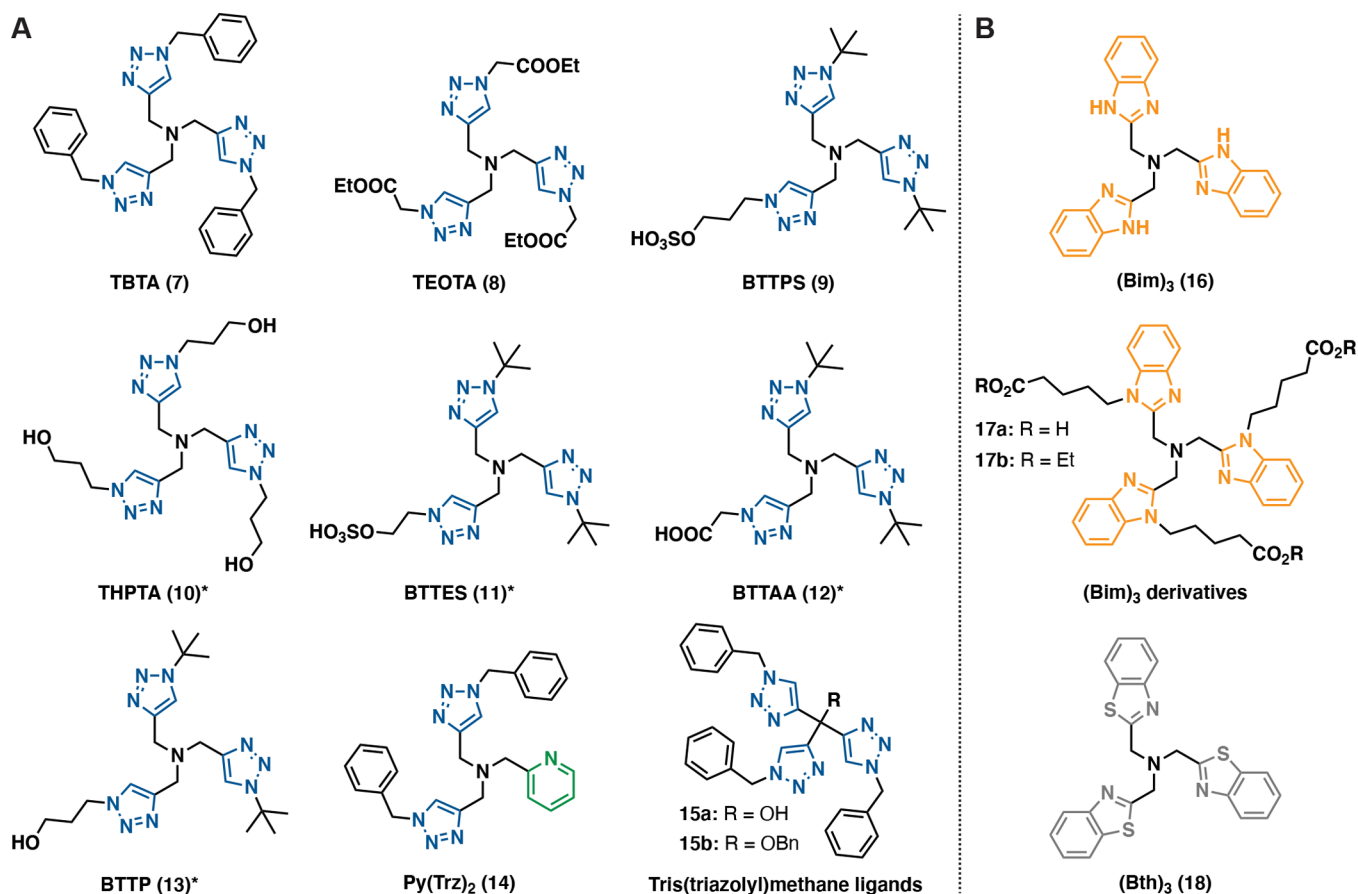


**Figure 2.** Polydentate ligands used to accelerate the CuAAC reaction. (A) Weaker ligands based on the 1,4-triazole ring suitable for environments with high water content: TBTA = tris[(1-benzyl-1H-1, 2, 3-triazol-4-yl)methyl]amine (7); TEOTA = tris[(1-(2-ethoxy-2-oxoethyl)-1H-1, 2, 3-triazol-4-yl)methyl]amine (8); BTTPS = 3-[4-{(bis[(1-*tert*-butyl-1H-1,2,3-triazol-4-yl)methyl]amino)methyl}1H-1,2,3-triazol-1-yl]propyl hydrogen sulfate (9); THPTA = tris[(1-hydroxypropyl-1H-1,2,3-triazol-4-yl)methyl]amine (10); BTTES = 2-[4-{(bis[(1-*tert*-butyl-1H-1,2,3-triazol-4-yl)methyl]amino)methyl}-1H-1,2,3-triazol-1-yl]ethyl hydrogen sulfate (11); BTAA = 2-[4-{(bis[(1-*tert*-butyl-1H-1,2,3-triazol-4-yl)methyl]amino)methyl}-1H-1,2,3-triazol-1-yl]acetic acid (12); BTTP = 3-[4-{(bis[(1-*tert*-butyl-1H-1,2,3-triazol-4-yl)methyl]amino)methyl}-1H-1,2,3-triazol-1-yl]propanol (13); Py = pyridine; Trz = (triazolylmethyl)amine. (B) Strong ligands based on benzimidazole (Bim) or benzothiazole (Bth) rings suitable for reaction environment with high concentration of coordinating organic solvents; \*Ligands biocompatible with cellular conditions.

approach, light can be used to generate a Cu(I) catalyst *in situ* by the photoinduced reduction of Cu(II) salts.<sup>46,47</sup>

In nucleic acid chemistry research, the most pursued strategy involves *in situ* generation of the catalyst by chemical reduction of a Cu(II) salt. The high water solubility of most reductants and cupric compounds makes aqueous conditions biocompatible and therefore highly suitable for nucleotide/oligonucleotide solutions. Various salts (*i.e.* CuSO<sub>4</sub>, Cu(acac)<sub>2</sub>, Cu(OAc)<sub>2</sub>) show high catalytic efficacy when combined with reductants that maintain the Cu(I) oxidation state with Na-L-asc being the most commonly reported.<sup>44</sup> Other reductants such as TCEP<sup>48</sup> and hydrazine<sup>49</sup> have been used for click reactions but various detrimental properties limit their application for CuAAC with biomolecular systems. Hydrazine damages DNA while phosphine reducing agents can sequester copper in solution and reduce azide groups (Staudinger reaction).<sup>50–52</sup> Utilizing these reducing agents might therefore compromise both catalyst and substrate integrity, reducing the reaction speed and yield. Na-L-asc is considered a safer option but its addition to cupric aerobic solutions catalyzes reductant oxidation to dehydroascorbate, causing depletion of the Cu(I) catalyst and side reactions such as the alkyne–alkyne (Glaser) coupling.<sup>50,53</sup> In particular, a

Fenton-type reaction cycle is promoted by the synergistic action of free copper ions, ascorbate, and oxygen which results in generation of reactive oxygen species (ROS). ROS have detrimental effects on nucleic acids in that these species can abstract hydrogen atoms from nucleobases and the (deoxy)-ribose sugar causing oxidative degradation and strand excision.<sup>54,55</sup> For these reasons, excessive catalyst loading should be avoided but inert atmosphere and anaerobic conditions should be used to keep the catalyst in the Cu(I) oxidation state.

**2.1.3. Tailoring the CuAAC Click Reaction.** The low redox potential of the Cu<sup>2+</sup>/Cu<sup>+</sup> couple ( $E_{cu^{2+}/cu^+} = 0.15$  V) makes Cu(II) the most stable oxidation state for free copper ions in aerobic solutions, and Cu(I) salts tend to easily disproportionate to Cu(II) and Cu(0) in aqueous buffers. To further stabilize the catalytically active Cu(I) species, organic additives such as phosphines or tris(triazolyl)amine-based ligands have been included within the catalyst scaffolds.<sup>56</sup> Addition of Cu(I)-binding ligands drives the formation of the active dinuclear Cu<sub>2</sub>L catalyst (*cf.* reaction mechanism in Scheme 1) accelerating the cycloaddition up to several thousand times over the ligand-free reaction. The choice of organic scaffold depends on solvent conditions (*i.e.* strong

Cu(I) coordinating solvents versus weak donors such as water) and on the compatibility of the resulting complex with the system in which CuAAC is applied.<sup>56–58</sup> Complexes with tris(triazolyl)amine-based ligands (Figure 2A) are compatible with nucleic acids and are favored over toxic Cu-phosphine compounds for *in vitro* conjugations. Click couplings with oligonucleotides have been efficiently catalyzed by Cu-TBTA or its water-soluble Cu-THPTA derivative (where TBTA = tris[(1-benzyl-1H-1,2,3-triazol-4-yl)methyl]amine, 7, and THPTA = tris(3-hydroxypropyltriazolylmethyl)amine, 10).<sup>44</sup> Recently, BTES (a sulfonic acid tris(triazolyl)amine-derivative, 11), BTTAA (12), BTTP (13), and a disulfonated bathophenanthroline ligand have also been investigated as nontoxic alternatives to catalyze CuAAC bioconjugations *in vitro* and *in vivo*.<sup>8,44,59</sup>

When Cu-coordinating tris(triazolyl)amine scaffolds are used, high stoichiometric [L]:[Cu] ratios positively affect biochemical click conjugations. In this case, not only is Cu(I) disproportionation prevented but the excess ligand also acts as a sacrificial ROS scavenger and protects the biomolecule from oxidation.<sup>50</sup> However, the performance of tris(triazolyl)amine-derivatives diminishes in coordinating organic solvents (e.g. DMSO) and, in this case, ligands that include two or more pyridine or benzimidazole (Figure 2B, 16–18) groups should be used instead. These ligand scaffolds bind copper more strongly and prevent the solvent from sequestering Cu-ions. The [L]:[Cu] ratio of these ligands needs to be carefully controlled according to the solvent composition as an excessive loading of the organic scaffold in aqueous buffers results in the formation of catalytically inactive Cu<sub>2</sub>L<sub>2</sub> species. In this case, ligand crowding around the metal center prevents access of weakly coordinative organic azides.<sup>56</sup>

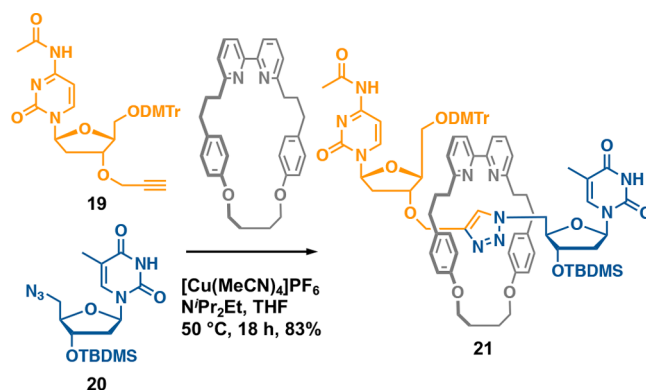
In parallel to tailoring the catalyst, parameters such as buffer choice, additives, concentration, and reaction temperature can be optimized to accelerate CuAAC. Click conjugations can proceed at various pH values, but buffer solutions at neutral pH are usually preferable.<sup>56</sup> Although bases (*i.e.* NEt<sub>3</sub>, 2,6-lutidine, Hünig's base, pyridine) have been reported to improve reaction efficiency by favoring formation of the Cu-acetylide adduct—already a fast process in the reaction mechanism—alkaline conditions disfavor the final reaction step where reprotonation of the Cu-triazolyl intermediate is required to release the clicked triazole. In addition, strong basic environments might cause the formation of insoluble copper-hydroxide and oxide species jeopardizing the click efficiency. Similarly, the presence of highly coordinating anions in the buffer (Tris, phosphate, MOPS, acetate, or HEPES) can compete with organic ligands for Cu(I) binding and inhibit the CuAAC reaction. In this latter case, the copper source can be premixed with the stabilizing tris(triazolyl)amine ligand prior to addition to the buffered solution.<sup>50</sup>

When CuAAC is performed on long nucleic acid polymers, formation of a secondary and tertiary structure can “bury” the reactive groups inhibiting the cycloaddition. Addition of small amounts of organic solvents (DMSO, DMF, NMP) in the aqueous buffer unfolds the macrostructure and exposes the reactive functional moieties permitting the click coupling. Notably, Das and co-workers showed that the use of up to 20% acetonitrile in buffer can be as effective as any ligand in the click labeling of DNA and RNA strands.<sup>22</sup> High percentages of strong coordinating solvents can however sequester the copper ion, preventing Cu<sub>2</sub>L formation and deactivating metal catalysis. Therefore, where an excess of

Cu(I)-coordinating solvent is required (e.g. to solubilize one of the reacting species), stabilizing ligands such as polybenzimidazole scaffolds should be used to release the copper ion from the bound solvent and restore the Cu<sub>2</sub>L active catalyst.<sup>56</sup>

Similar to most click-reactions, CuAAC speed benefits from increased reactant concentration but the small quantities of long nucleic acid sequences that are typically available often limit the feasibility of using concentrated solutions. In this case, the use of excess catalyst (usually present in stoichiometric amounts or slight excess) or templates (*i.e.* nucleic acid splints and macrostructures) augments the local concentration of the reactive moieties and preorganizes the reactants to have the correct relative orientation and directionality for the coupling reaction.<sup>50</sup> In the splint ligation strategy, alkyne and azide modified strands are directed and brought in close proximity by a complementary oligonucleotide (splint) that anneals to the two modified sequences acting as a template.<sup>18,60–62</sup> Alternatively, macrocycles have been used in the active template CuAAC reaction (AT-CuAAC) for the generation of interlocked molecules. Here, a metal ion bound within the macrocycle is used to organize precursor fragments for the click ligation and to template the azide–alkyne cycloaddition that captures the interlocked structure. This strategy has been used to generate several rotaxanes and catenanes<sup>63</sup> and recently also to template the synthesis of mechanically interlocked oligonucleotides (21)<sup>64</sup> by click chemistry (Scheme 2). Finally, gentle heating or use of

**Scheme 2. Synthesis of an Interlocked Dinucleotide from an Alkyne Modified Cytosine (19) and an Azide Modified Thymine (20) Using a Templating Macrocycle (Gray)<sup>64</sup>**



microwaves significantly accelerates the CuAAC reaction by augmenting the reactivity of the substrates and by destabilizing possible Cu(I) species formed with competing coordinating species.

## 2.2. Ruthenium Catalyzed Azide Alkyne Cycloaddition (RuAAC)

### 2.2.1. Ru-Catalysis in Azide Alkyne Cycloadditions.

The 1,4-disubstituted 1,2,3-triazole adduct is the only product formed from the copper(I) catalyzed cycloaddition. However, catalysts capable of yielding 1,5-triazole isomers can be advantageous for placing two substituents adjacent to each other and have potential applications, for example in synthesizing constrained cyclic structures for nanomaterial purposes.

Initially 1,5-regioisomers were obtained by reacting selected metal acetylides with organic azides to generate metallo-

triazoles which are subsequently protonated to yield the 1,5-disubstituted adduct. In this context, Akimova and co-workers scoped several acetylide adducts with various metals to mediate the formation of 4-metalated 1,5-disubstituted triazoles.<sup>65–67</sup> Sharpless and co-workers further revised the reaction and obtained higher yields than earlier reported using bromomagnesium acetylides. In addition, trapping the 4-metalated triazole intermediate with other electrophiles than protons resulted in the regioselective formation of 1,4,5-trisubstituted 1,2,3-triazoles broadening the scope of the reaction.<sup>68</sup> Nonetheless, coupling between metal acetylides and azides is limited by the formation of several types of trace byproducts (Figure 3). Long reaction times in the absence of

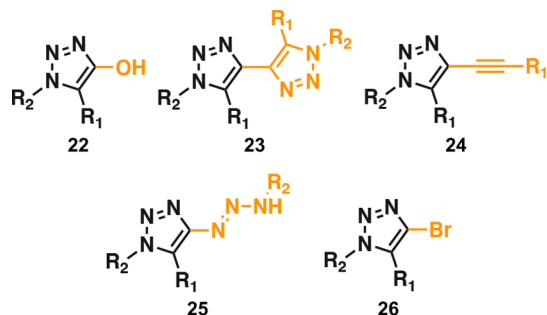


**Figure 3.** Possible byproducts from the reaction between metal acetylides and azides.<sup>68</sup>

strictly anaerobic conditions might result in oxidative couplings and lead to the formation of 4-hydroxy (22), 4-triazol (23), or 4-alkyne (24) 1,2,3-triazole adducts. When excess of the organic azide is used, a byproduct can be formed also by coupling of the organic azide to the C4 position of the triazole (25). Finally, trace amounts of 1,5-disubstituted-4-bromotriazoles (26) are observed when bromomagnesium acetylides are used as substrates.<sup>68</sup>

The development of the ruthenium catalyzed azide alkyne cycloaddition (RuAAC) introduced a more convenient strategy than metal acetylides to promote the formation of

1,5-disubstituted triazoles. The well-known catalytic properties of Ru(II) complexes in several alkyne-reactions<sup>69</sup> quickly spurred interest in the application of these compounds to the cycloaddition reaction. Although some Ru-derivatives (e.g. Ru(OAc)<sub>2</sub>(PPh<sub>3</sub>)<sub>2</sub>, RuCl<sub>2</sub>(PPh<sub>3</sub>)<sub>3</sub>, and RuHCl(CO)(PPh<sub>3</sub>)<sub>3</sub>) favor formation of the 1,4-disubstituted triazole through a similar mechanism to CuAAC,<sup>70</sup> more sterically hindered pentamethylcyclopentadienyl (Cp\*) derivatives, such as [Cp\*<sub>2</sub>RuCl<sub>2</sub>]<sub>2</sub>, Cp\*<sub>2</sub>RuCl(COD), and Cp\*<sub>2</sub>RuCl(NBD) (where COD = cyclooctadiene and NBD = norbornadiene), afford complete conversion to the 1,5-regioisomer and are commonly used in RuAAC.<sup>34</sup>

When ruthenium and copper catalyzed cycloadditions are compared to each other, a different mechanism becomes obvious and apparent from the distinct synthetic conditions required by the two reactions (Figure 4). In contrast to CuAAC, the alkyne in RuAAC couplings is activated by the increased nucleophilicity that originates from its  $\pi$ -interaction with the metal core. The metal-acetylide adduct is not formed during the RuAAC reaction, and this characteristic broadens the applicability of Ru catalyzed conjugations to internal alkyne cycloadditions besides terminal ones.<sup>71,72</sup> Regioselectivity for internal modifications is determined by the propargyl substituents on the unsaturated bond and depends on their electronic properties, steric demand, and ability to form hydrogen bonds.<sup>71,73,74</sup> As a general rule, bulky substituents, propargylic hydrogen bond donors, and heteroatoms are directed to the C5 position in the triazole while electron-deficient groups are placed in the C4 position (Figure 5). Similar to CuAAC, RuAAC is orthogonal to several functional moieties. However, Ru cycloadditions can only proceed in homogeneous aprotic environments since protic solvents (e.g. water, ethyl acetate, methanol, isopropyl alcohol, hexanes, and diethyl ether)—compatible with CuAAC—considerably lower the reaction yields. In an analogous fashion to CuAAC, RuAAC reactions catalyzed by Cp\*<sub>2</sub>RuCl(COD) are performed under an inert atmosphere.<sup>75</sup> In this case, however, the absence of oxygen is required to protect the catalyst from degradation. Alternatively, the Cp\*<sub>2</sub>RuCl(PPh<sub>3</sub>)<sub>2</sub> shows lower

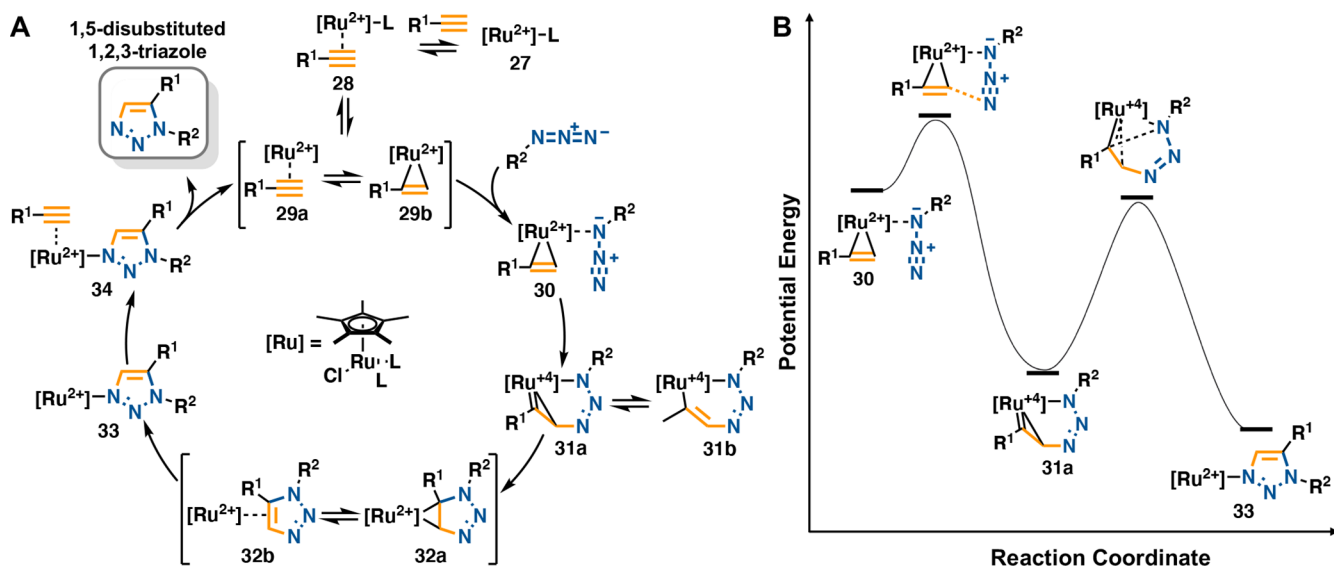


**Figure 4.** (A) Proposed mechanism for the Ru-catalyzed azide-alkyne cycloaddition (RuAAC). (B) Energy profile of the lowest-energy RuAAC pathway based on DFT studies.<sup>71</sup>

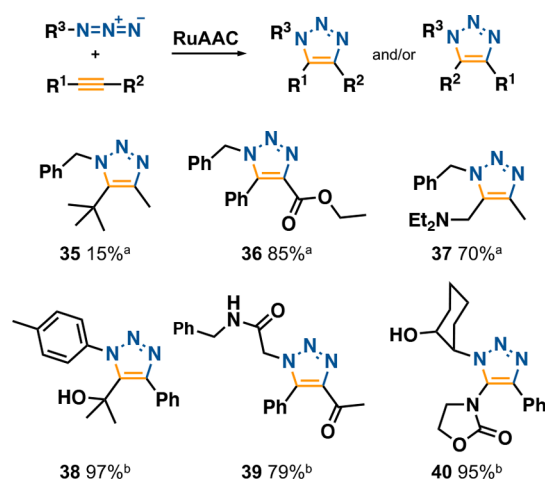


**Figure 5.** Regiochemistry in RuAAC coupling with internal alkynes. (a)  $\text{Cp}^*\text{RuCl}(\text{PPh}_3)_2$  (10 mol %), benzene, 80 °C, 2.5–40 h;<sup>74</sup> (b)  $\text{Cp}^*\text{RuCl}(\text{COD})$  (2 mol %), toluene, rt, 30 min.<sup>71</sup>

sensitivity to atmosphere conditions and yields excellent conversions even when oxygen is present.<sup>71</sup> Finally, the more inert nature of ruthenium catalysts results in the requirement for high temperatures to efficiently promote triazole formation. Otherwise microwaves or catalysts with labile ligands (such as  $[\text{Cp}^*\text{RuCl}]_4$ ) can be used to promote the reaction efficiently even at room temperature.

**2.2.2. RuAAC Applications for Antibacterial Drug Development.** The reduced biocompatibility of RuAAC conditions together with the expensive price of ruthenium complexes has impeded application of this reaction in comparison to the more popular CuAAC. Despite this, Ru catalyzed cycloadditions have recently gained more attention within the nucleic acid field. In particular, RuAAC was used to generate 1,5-triazole adducts of nucleic acids as potential antibacterial drugs. Etheve-Quellejeu and co-workers used the RuAAC and CuAAC reaction to develop a class of aminoacyl-tRNA analogues as Fem-inhibitor antibiotic candidates against Gram-positive bacteria. Fem enzymes are a class of transferases involved in the assembly of the Gram-positive peptidoglycan wall. These proteins use aminoacyl-tRNAs to synthesize pentapeptide side-chains which are the branching points for cross-links among adjacent glycans.<sup>76,77</sup> The triazole ring behaved as a stable analogue of the 3'-aminoacyl bond in tRNA inhibiting the FemXWv protein action, a prototypic enzyme of the Fem family.<sup>78</sup>

### 2.3. Metal-free Click Chemistry and Strain Promoted Azide Alkyne Cycloaddition (SPAAC)

In the previous sections we described a number of possible side reactions promoted by metals when catalyzed AAC conjugations are carried out in the presence of redox-sensitive biomolecules. In addition, performing these types of click reactions *in cellulo* or *in vivo* exposes the organism to exogenous metals that may be toxic or interfere with its metabolism. To circumvent these limitations, various click conversions that do not require metal catalysis have been developed and applied to biochemical and biological systems including: (i) the strain promoted azide alkyne cycloaddition (SPAAC);<sup>10,79,80</sup> (ii) the conjugation between oxanorbornadiene derivatives and azides;<sup>81,82</sup> (iii) the reaction between strained alkenes and tetrazines; and (iv) the alkene–tetrazole photoclick reaction.<sup>83</sup>

The SPAAC reaction pioneered by Bertozzi and Agard is the most widely applied type of metal-free click transformation and involves the cycloaddition between a strained cyclooctyne and an organic azide.<sup>79</sup> Initially used for *in cellulo* ligation with carbohydrates,<sup>84</sup> SPAAC properties have also been harnessed for labeling and ligation of DNA strands. The rigid ring structure of cyclooctyne bends the bond angles of the  $\text{sp}$ -hybridized carbons to  $\sim 160^\circ$  pushing the alkyne geometry toward the cycloaddition transition state. From a molecular orbital perspective, the strain lowers the energy of the alkyne LUMO (lowest unoccupied molecular orbital) bringing it close in reactivity to the azide HOMO (highest occupied molecular orbital) (Figure 6).<sup>85</sup> This hypo-energetic

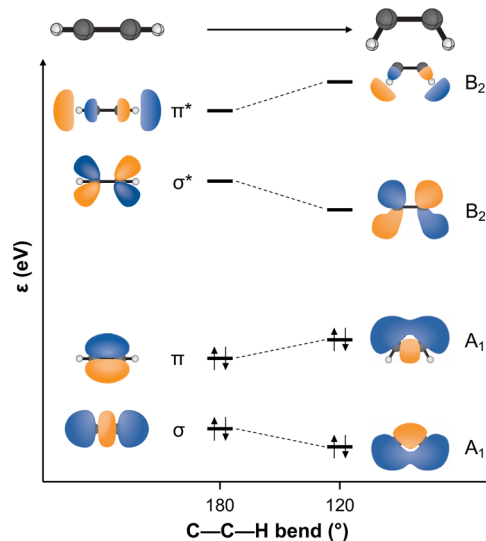


**Figure 6.** Schematic Walsh diagram representing the effect caused by acetylene bending on the orbital relative energies.<sup>85</sup>

shift can be augmented by introducing electron-withdrawing substituents on the cyclooctyne such as halogen atoms or benzyl groups.<sup>86</sup> The strained 8-membered ring provides a compromise between fast reactivity and high stability in aqueous media. Smaller rings are too unstable, and larger rings are not sufficiently reactive.<sup>87</sup> Modification of the cyclooctyne augments the reaction rate and two fluorine atoms in the C3 position of DIFO (difluorinated cyclooctyne) increase the cycloaddition speed by 60-fold compared to the unmodified ring.<sup>12,88</sup> A similar reactivity was reported also for several functionalized derivatives of dibenzocyclooctyne (DIBO). These systems are relatively easy to synthesize and modify at the aryl position with groups that enhance reactivity and solubility.<sup>89–91</sup> In addition, unlike electron deficient terminal alkynes, DIBO is stable in aqueous conditions and survives some common oligonucleotide deprotection conditions therefore being suitable for incorporation into DNA as a phosphoramidite monomer (42, Figure 7A).<sup>90</sup> In the context of nucleic acids, the SPAAC reaction has been employed for oligonucleotide labeling,<sup>91–94</sup> in copper-free DNA strand ligation,<sup>61</sup> and in RNA conjugation in solid phase synthesis.<sup>95</sup> When DIBO and a nonsubstituted cyclooctyne were used to template the click-ligation of DNA strands, the triazole formation occurred very quickly ( $\sim 1$  min at ambient temperature) and it was sensitive to base pairing. The presence of a single base mismatch between the template and

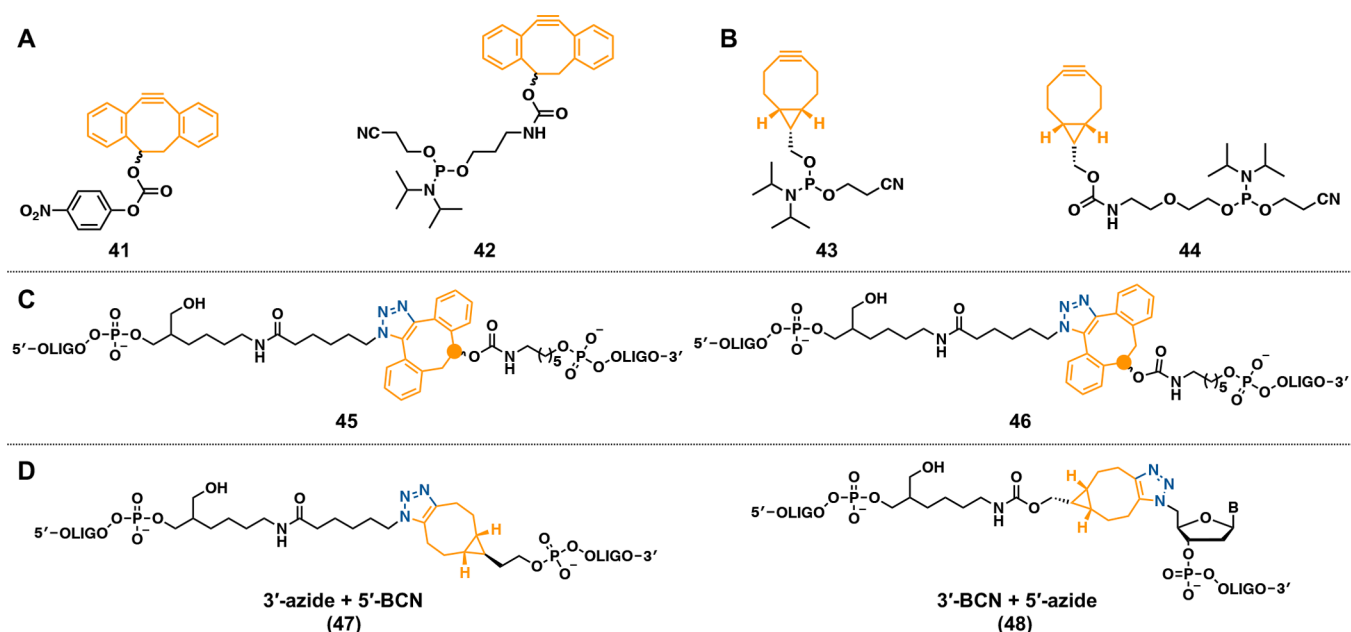


**Figure 7.** (A) Dibenzocyclooctyne (DIBO) oligonucleotide labeling reagents: DIBO p-nitrophenyl carbonate (41) and phosphoramidite monomer (42) for coupling at the 5'-termini of oligonucleotides. (B) Achiral bicyclo[6.1.0]nonyne (BCN) oligonucleotide labeling reagents: BCN-CEP I (43) and BCN-CEP II (44). (C) Click linkage between 3'-azide and 5'-DIBO labeled oligonucleotides. Both regioisomers of the DIBO triazole are shown. (D) Both 3'- and 5'-ends of oligonucleotides can be labeled with BCN, and its click reactions provide single regioisomers.

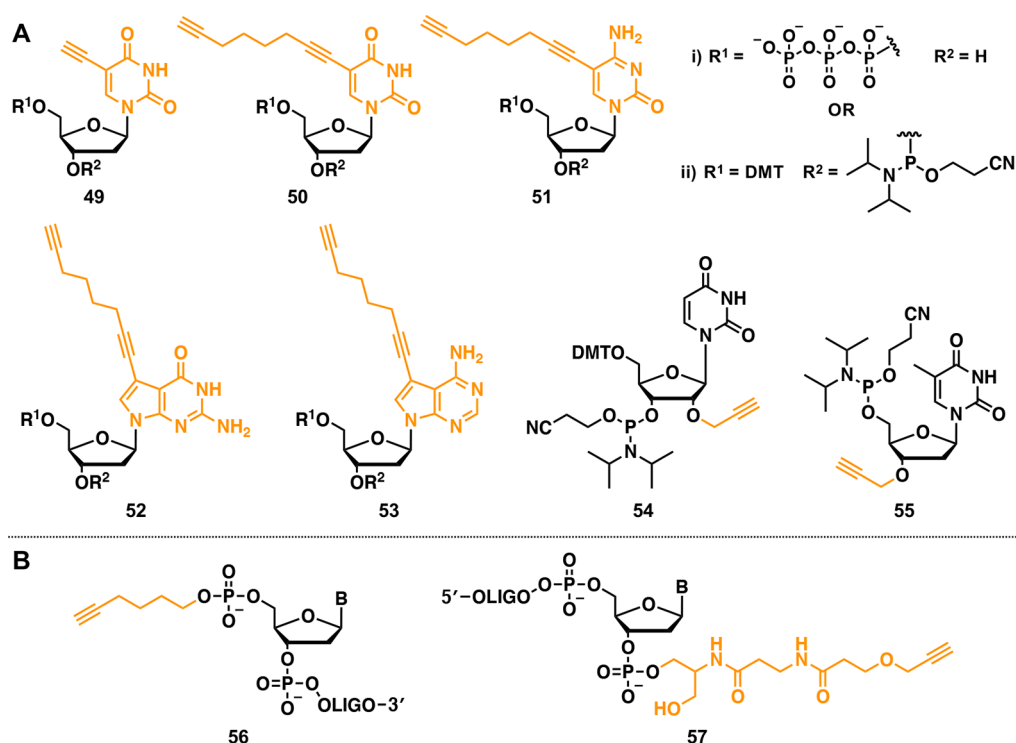


**Figure 8.** (A) Examples of modified nucleosides used to incorporate alkyne groups into oligonucleotides. Modifications 49–53 have been used both as triphosphates (i) and phosphoramidites (ii) monomers for PCR or solid phase synthesis, respectively; Phosphoramidites 54 and 55 have been used to introduce 2'- and 3'-O-propargyl modifications in oligonucleotides by normal and reverse phosphoramidite coupling. (B) Alkyne modifications such as hexynyl (56) and serinol (57) have been introduced through non-nucleosidic alkyne phosphoramidite monomers and solid supports on the 5'- and 3'-ends, respectively.

the alkyne labeled oligonucleotide was sufficient to inhibit the reaction suggesting applications in genetic analysis.<sup>61</sup>

Nonetheless, DIFO and DIBO modifications are asymmetrical with respect to the position of the linker (tether).

Hence, their reaction with azides generates mixtures of stereoisomeric products. Fusion of the cyclooctyne ring with a 3-membered ring yields an achiral system (bicyclo[6.1.0]nonyne (BCN)) that retains the essential reactivity toward

azides (Figure 7B).<sup>96,97</sup> The BCN moiety is simple to synthesize and can be introduced into oligonucleotides as a phosphoramidite monomer (5'-addition) or on the support (3'-addition) during solid-phase oligonucleotide synthesis (43 and 44).<sup>98</sup> However, BCN is unstable to trichloroacetic acid commonly used for the detritylation step, and dichloroacetic acid must be used instead.

Interestingly, an alternative pathway for metal-free click labeling of oligonucleotides was developed by Carell and co-workers.<sup>99</sup> In this strategy a DNA-norbornene hybrid was clicked to organic nitrile oxides both in solution and in solid-phase. The advantages of the reaction include the ready availability of all starting materials and the need for only a 10-fold excess of the nitrile oxide which makes this conversion particularly suitable for DNA labeling with expensive reporter groups. Since the reactivity of nitrile oxides with alkynes was slow in the reported conditions, the reaction was reported to be orthogonal to standard Cu(I) catalyzed azide-alkyne cycloadditions.<sup>99</sup>

### 3. INTRODUCING CLICK-FUNCTIONAL GROUPS IN NUCLEIC ACID SCAFFOLDS

#### 3.1. Alkyne and Azide Building Blocks for Click Couplings

Before the development of rapid and efficient azide-alkyne cycloadditions, chemical modification of oligonucleotides was mostly achieved by coupling amino-functionalized ODNs with active-esters in aqueous buffers. These conjugations are however less efficient than CuAAC, and active esters are easily hydrolyzed. Conversely, organic azides and alkynes have high chemical stability and react only with each other, remaining orthogonal to most functional groups. In addition, inclusion of click modifications in nucleic acid scaffolds is now well-established. The field is also facilitated by the wide commercial availability and well-known synthetic routes to the required modified phosphoramidite monomers<sup>100–106</sup> and nucleoside triphosphates<sup>107–113</sup> for applications in solid phase or enzymatic nucleic acid synthesis, respectively. This section aims to provide a brief overview of the most common strategies that can be pursued to introduce click functional groups into nucleic acid scaffolds.

Nucleosides offer multiple positions that are modifiable with alkyne or azide moieties. The most widely used synthetic routes label either the phosphate group, the 5', 3', or 2'-OH position on the ribose sugar, the C5 position of pyrimidines, or the C7 locus on 7-deazapurines (Figure 8). In one of the earliest oligonucleotide-labeling studies, an azide group on the 5' position of a M13-40 universal forward sequencing primer was clicked with alkynyl 6-carboxyfluorescein (FAM) in near quantitative yield.<sup>114</sup> The azide modification was introduced by reacting 5'-aminohexyl oligonucleotides with an excess of succinimidyl 5-azidovalerate. In this case, a large excess of the alkynylamido-fluorophore (150 fold relative to the azide), high temperature (80 °C), and a long reaction time were required to complete the cycloaddition in the absence of the Cu(I) catalysts. The complicated chemistry required for the labeling spurred researchers to develop alternative strategies and building blocks for facile insertion during the solid phase synthesis cycles (Figure 8). Currently the most common approach reverses the chemistry by conjugating alkyne modified DNA to azide-probes. This alternative strategy is justified by the high reactivity between organic azides and P(III) groups (Staudinger reaction) which makes it very

difficult to prepare and purify azide-containing phosphoramidites. Alternatively, azide groups can be introduced into oligonucleotides during solid-phase synthesis through substitution of functional groups such as alkyl iodides, bromides, or mesylates by sodium azide.<sup>115</sup> In addition, the 3'-end of oligonucleotides can be modified with the azide moiety prior to solid phase synthesis by incorporating an azide modified nucleoside or through other azide modified linkers attached to the solid support.<sup>116</sup> These types of azide modifications are stable to oligonucleotide synthesis conditions even though the coupling steps use a large excess of the phosphoramidite monomers. The stability arises from the protonation of the phosphoramidite group by the mildly acidic coupling reagent (e.g., tetrazole) which prevents reaction of the phosphorus lone pair with the azide. This approach is defined as “reverse click labeling” as it is less common compared to the use of alkyne-modified oligonucleotides. However, reverse click chemistry is advantageous when alkyne modified labels are more readily accessible than the azide-derivatives (*i.e.* some Cy dyes).<sup>115</sup>

Owing to their facile synthesis, 2'-deoxyuridine derivatives such as 5-ethynyl-dU (dU<sup>°</sup>) (49) and 5-(1,7-octadiynyl)-dU (dU<sup>°</sup>) (50) are the most used alkyne modified building blocks (Figure 8A). Carell and co-workers used the phosphoramidite derivatives of these two nucleosides to label multiple positions of 16-mer ONs by solid phase synthesis. The monomers were prepared first by Sonogashira coupling of the alkyne group to the C5 position of a deoxyuridine and then by reacting the 5'-dimethoxytrityl-nucleoside with 2-cyanoethyl *N,N,N',N'*-tetraisopropylphosphorodiamidite. The efficiency of the click labeling reaction was assessed using various azide modified reporter groups (Figure 9, 58–60). High density oligonucleo-

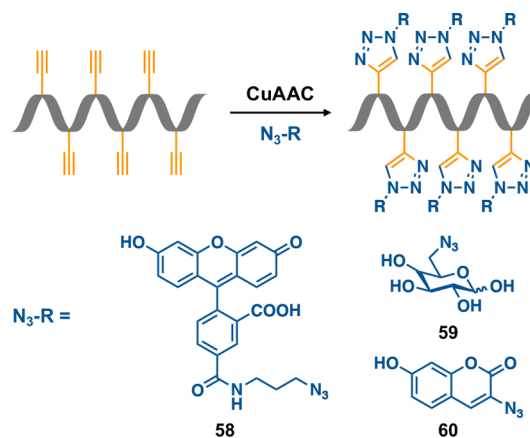


**Figure 9.** Strategy for high-density postsynthetic labeling of alkyne-modified DNA primers and azide labels (fluorescein azide, 58; azido-sugar, 59; and coumarin azide, 60) used in the click coupling by Carell et al.<sup>17</sup>

tide modification with flexible octadiynyl linkers provided reliable triazole formation whereas clustering of ethynyl monomers resulted, instead, in incomplete click reactions due to steric shielding of the alkyne by the DNA backbone.<sup>17</sup> The validity of click chemistry for DNA postfunctionalization was also confirmed on extended sequences (up to 2000 bp) produced by PCR using the alkyne modified ODNs as primers. Here, the observation of a single fluorescent band after gel electrophoresis of the fluorescein-clicked products

confirmed the labeling. There are applications of this CuAAC reaction in the functionalization of DNA macro-structures.

The low reactivity of dU<sup>ε</sup> was later confirmed by Hocke et al. in a study that reported only 36% average of triazole formation using mild CuAAC conditions for the reaction between a heavily dU<sup>ε</sup>-modified amplicon (339 bp) and an organic azide.<sup>117</sup> In addition, the application of ethynyl modified phosphoramidites to solid phase oligonucleotide synthesis is limited by the poor stability of the alkyne in acidic and basic conditions. In contrast to octadiynyl modified nucleobases, the 5-ethynyl group requires silyl protection during phosphoramidite oligonucleotide synthesis in order to prevent its partial hydration and conversion to acetyl side-products during the deprotection cycles.<sup>118</sup> The real advantage of dU<sup>ε</sup> is when this modification is used for PCR experiments. In fact, dU<sup>ε</sup> triphosphate (dU<sup>ε</sup>TP) is a very good substrate for DNA polymerases (comparable to natural dNTPs) and is superior to octadiynyl-dU (dU<sup>ε</sup>TP) when used for the replication/amplification of long DNA templates. The presence of extended hydrophobic linkers such as octadiynyl can cause oligonucleotide aggregation in water and low yields in the PCR amplification of long genes. For this and other reasons, dU<sup>ε</sup>TP and its derivatives have been used also as efficient metabolic labels to track DNA and RNA synthesis *in cellulo* and *in vivo* in animal tissue models.<sup>23,119,120</sup> This contrast between the octadiynyl and ethynyl spacer reactivity underlines the importance of “choosing the right alkyne for the right job” to achieve efficient triazole formation.

Alkyne and azide modified nucleosides have also been utilized in enzymatic approaches to modify RNA with clickable groups for CuAAC and SPAAC labeling (Figure 10). Das and co-workers modified the 5'- and 3'-end of RNA using a synthesized 5'-azidoguanosine (61) or a commercially

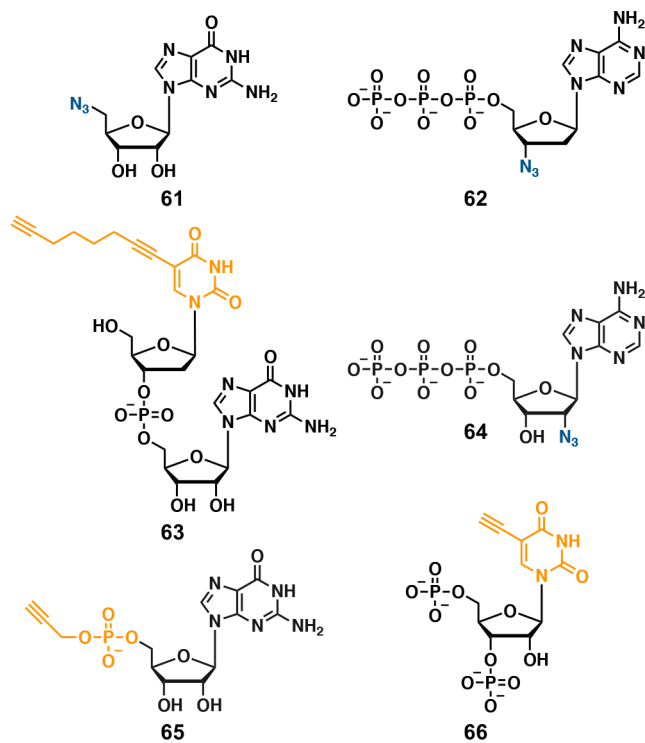
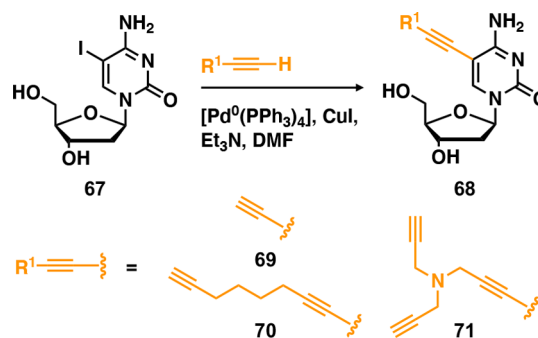


**Figure 10.** Alkyne and azide building blocks introduced into RNA enzymatically.

available 3'-azido-2',3'-dideoxyadenosine (62) in combination with T7 RNA polymerase or poly(A) polymerase (PAP), respectively. The azide-labeled RNA was then used for templated and nontemplated click-ligation to generate two different artificial RNA backbones.<sup>22</sup> Jäschke and co-workers further advanced the field by enzymatically labeling the 5'- and 3'-ends of RNA using commercially available dU<sup>ε</sup>pG dinucleotide (63) or C-2' azido-modified nucleotide (64), respectively.<sup>121,122</sup> dU<sup>ε</sup>pG can be prepared by custom solid-phase synthesis, and it can be incorporated near-quantitatively by various bacteriophage RNA polymerases (RNAPs).<sup>121</sup> In addition, the C-2' azido-modified nucleotide can be incorporated at the 3'-end of RNA by PAP enzymes.<sup>122</sup> Interestingly, in these two strategies the click labels are placed either on the nucleobase or at the C-2' site of the ribose ring. Therefore, the 5'- and 3'-OH groups are available for further enzymatic manipulations (e.g. splinted ligation to other RNA sequences, addition of poly(A)-tails, and 3'-adapter ligation). In an alternative strategy, *O*-propargyl-guanosine-5'-monophosphate (65) and alkynylated 3',5'-uridine bisphosphate (66) were synthesized and used for the chemoenzymatic labeling of RNA termini with FAM (fluorescein) and dabcy azides. While 65 was introduced at the 5'-end of RNA by *in vitro* transcription prior to CuAAC click with dabcy azide, 66 was first clicked to FAM azide and then incorporated at the 3'-end of RNA using T4 RNA ligase. This strategy was extended to label RNA site-specifically at internal positions as exemplified by the synthesis of several pre-miRNA hairpin loop probes up to 79 nt in length.<sup>123</sup>

Significant and extensive work on alkyne nucleobase derivatives has also been carried out by the Seela group. In addition to thymine, cytosine and two 7-deazapurines were labeled with the octadiynyl group starting from the iodo-precursors using palladium-assisted Sonogashira cross-coupling (Scheme 3). Melting experiments on a DNA duplex

### Scheme 3. Synthesis of Alkyne-Modified Nucleosides by Sonogashira Coupling<sup>124–127</sup>

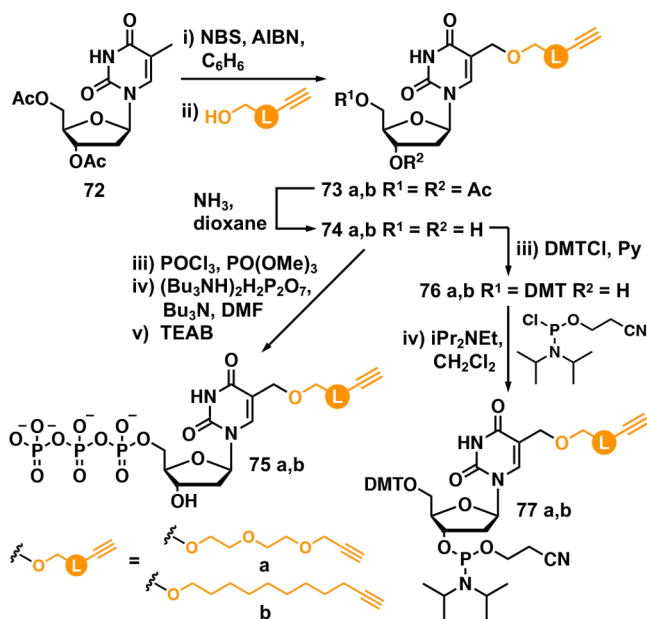


modified with these nucleosides revealed that the octadiynyl modification stabilizes the helix structure more than the ethynyl group.<sup>124,125</sup> The same researchers used octadiynyl linkers to prepare clickable derivatives of a pyrrolo dC analogue and 7-alkynyl-7-deaza-2'-deoxyinosine. The latter case is of particular interest because the lack of the guanine 2-amino group in the hypoxanthine nucleobase provides deoxyinosine with the capability to base pair to all the canonical nucleobases. In addition, the stability of 7-deazapurines to acidic pH—in contrast to canonical purine nucleosides—makes these modifications suitable for footprinting experiments. Seela and co-workers expanded the

nucleobase modifications beyond ethynyl (69) and octadiynyl (70) functional linkers. Using Sonogashira coupling, a tripropargylamine-dU phosphoramidite was prepared for postsynthetic labeling of oligonucleotides with two 3-azido-7-hydroxycoumarin fluorophores. In this case, oligonucleotides clicked only to one coumarin were more fluorescent than bis-labeled oligonucleotides due to self-quenching between the two dyes in the latter case. The presence of a branched alkyne group provided nonetheless a slight stabilization of the duplex base pair and a convenient methodology to introduce multiple functionalization on terminal triple bonds.<sup>126,127</sup>

In a recent work Hocek and co-workers reported a new methodology for the introduction of alkyne groups that avoids the use of Sonogashira coupling with expensive 5-iodo-2'-deoxyuridine. In their strategy a natural thymidine nucleoside was coupled to flexible alkynes such as a hydrophilic propargyl-diethylene glycol (PEG) or a hydrophobic undecyne (UN) linker (Scheme 4). Radical bromination of 3',5'-

**Scheme 4. Alternative Strategy to Sonogashira Coupling for the Modification of Nucleosides with Alkyne Functionalities**<sup>128</sup>



di-*O*-acetyl protected thymidine with *N*-bromosuccinimide (NBS) and azobis(isobutyronitrile) (AIBN), followed by *in situ* treatment with the alcohol derivatives of propargyl-PEG (a) or undecyne (b) released the protected alkyne functionalized nucleoside (73a,b). The monomer was then deprotected with  $\text{NH}_3$  (74a,b) and converted by standard procedures to its triphosphate form ( $\text{dU}^{\text{PEG}}\text{TP}$  and  $\text{dU}^{\text{UN}}\text{TP}$ ) (75a,b) or phosphoramidite ( $\text{dU}^{\text{PEG}}$  and  $\text{dU}^{\text{UN}}$ ) (77a,b). Both  $\text{dU}^{\text{PEG}}$  (77a) and  $\text{dU}^{\text{UN}}$  (77b) monomers were compatible with solid phase synthesis conditions and were successfully introduced in oligonucleotides. In the case of the triphosphates, the new monomers were recognized by various DNA polymerases (i.e., KOD XL DNA, BST large fragment, vent(exo-), and PWO) giving full length products in primer extension experiments using a 19-mer template. However, in the case of longer PCR amplicons (235 bp) only  $\text{dU}^{\text{PEG}}\text{TP}$  was efficiently incorporated outperforming the control  $\text{dU}^{\text{O}}\text{TP}$  whereas  $\text{dU}^{\text{UN}}\text{TP}$  completely inhibited the PCR reaction.  $\text{dU}^{\text{PEG}}$

modified DNA reacted with azides 2-fold faster compared to oligonucleotides with pendant octadiynyl groups, emphasizing the potential of this modification for biological *in vivo* and *in vitro* applications where fast cycloaddition rates are crucial to monitor rapid metabolic processes.<sup>128</sup>

To label the internal positions of the phosphate backbone, Caruthers and co-workers introduced an ethynylphosphonate internucleotide linkage at specific sites by solid phase phosphoramidite synthesis. The alkyne linker was then coupled by CuAAC to various organic azide prior to oligonucleotide deprotection and cleavage from the solid support. The modified oligonucleotide had therefore one of the nonbridging oxygen atoms replaced by a 1,2,3-triazole. Using this methodology, multiple, high density functionalization of the phosphate backbone can be achieved. In addition, modifications on the phosphate can in some cases be more advantageous than those on the nucleobase as the base-pairing and hybridization should not be compromised once the triazole is formed.<sup>129</sup>

### 3.2. Compatibility of Alkyne Modified dNTPs with PCR

The compatibility of C5-modified pyrimidine dNTPs with DNA polymerases is explained by X-ray analysis of the ternary complex between KlenTaq—the N-terminally truncated form of Taq polymerase—a primer/template duplex and the triphosphate derivative. The crystal structure illustrates the plasticity of the enzyme emphasizing the relevance of flexible regions in the dNTP binding pocket that can adapt to the modified substrates.<sup>130</sup> The advantage of modifications at the C5 position of pyrimidines is explained by the minor disruption caused not only to the DNA duplex but also to the ternary complex. The adaptability of KlenTaq underpins the idea that the enzyme is able to accommodate the incoming triphosphate by interacting with the modified substrates. Studies on rigid and nonpolar modifications revealed that additional interactions arise when aromatic rings are included. In this case, recognition of the functionality occurred through cation- $\pi$  contacts formed with the positively charged side chains of amino acid residues such as arginine or lysine (Figure 11). This explains the efficient enzymatic incorporation of  $\text{dT}^{\text{deb}}\text{TP}$  (78) and  $\text{dC}^{\text{deb}}\text{TP}$  (79) (7-fold reduction in incorporation compared with dTTP; deb = 1,4-diethynylbenzene) and, in comparison, the ineffective processing of previously reported thymidine analogues lacking aromatic rings in their modifications (2500-fold lower than dTTP).<sup>130,131</sup> When flexible and polar regions were introduced in the C5 position of the dNTP, extra hydrogen bonds were formed between the modification and the enzyme. These additional contacts enhance the interaction with KlenTaq and might explain the higher compatibility of  $\text{dU}^{\text{PEG}}$  compared to hydrophobic dNTPs described above.<sup>128,131</sup>

## 4. APPLICATIONS OF THE AZIDE ALKYNE CYCLOADDITION WITH NUCLEIC ACIDS

### 4.1. Small Molecule–DNA Click

**4.1.1. Fluorophore Labeling.** Strategies to chemically modify genetic material with small molecules are invaluable resources in several research fields and have been studied ever since solid phase oligonucleotide synthesis was first developed. Although various molecular probes have been conjugated to nucleic acids, labeling with fluorescent dyes represents the main application due to its impact in the fields of DNA and

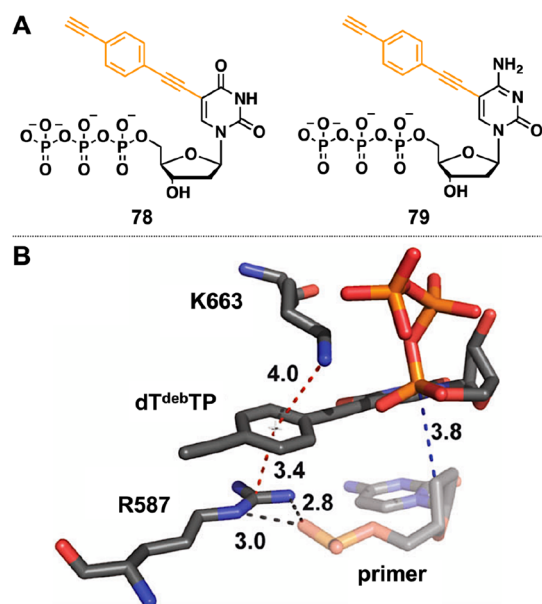


**Figure 11.** (A) Structure of  $dT^{debTP}$  (78) and  $dC^{debTP}$  (79). (B) Close-up view of the interaction pattern between the modified  $dT^{debTP}$  and the enzyme side chains R587 and K663 (red dashed lines indicate cation– $\pi$  interaction; Adapted with permission from ref 130. Copyright 2012, Royal Society of Chemistry).<sup>130</sup>

RNA sequencing, diagnostics, forensics, and genetic analysis.<sup>132–134</sup> Chemical modification of oligonucleotides with fluorophores was initially achieved by coupling amino groups to carboxylic acids via active esters. However, as described above (*cf.* section 3), this coupling reaction has some limitations when compared to azide–alkyne cycloadditions. In the particular case of DNA labeling, active esters are unstable in the alkaline buffers (pH > 8) used for the reaction and compared to AAC building blocks they tend to decompose in the presence of moisture or over prolonged storage periods. Similarly, Michael-type reactions between maleimide or iodoacetamide modified fluorophores and thiol-labeled DNA are limited by the electrophile instability and the predisposition of thiols to dimerize. By contrast AAC conjugation of fluorophores to DNA or RNA is high yielding and the reactive partners are stable in the aqueous buffers used for the coupling. The small quantities required for efficient triazole formation (usually <1 mg) are particularly advantageous when expensive and valuable dyes are conjugated. In addition, the stability of the alkyne group to solid phase synthesis conditions allows postsynthetic labeling of oligonucleotides. This feature is particularly relevant when oligonucleotides are conjugated to dyes that are easily degradable under the strong basic conditions required for DNA and RNA cleavage and deprotection. In this case, CuAAC is the most viable method for the coupling and has opened the field of DNA and RNA labeling to various dyes that were otherwise inaccessible.

Wagenknecht and co-workers used CuAAC to couple two fluorescent dyes—blue phenoxazinium azide (80, 81) and red coumarin azide (82)—postsynthetically to alkyne modified oligonucleotides (Figure 12). Both fluorophores are unstable in a basic environment and cannot be incorporated as phosphoramidite monomers during solid phase synthesis. Several DNA duplexes were modified, attaching blue phenoxazinium either at the 2'-position of uridine or using

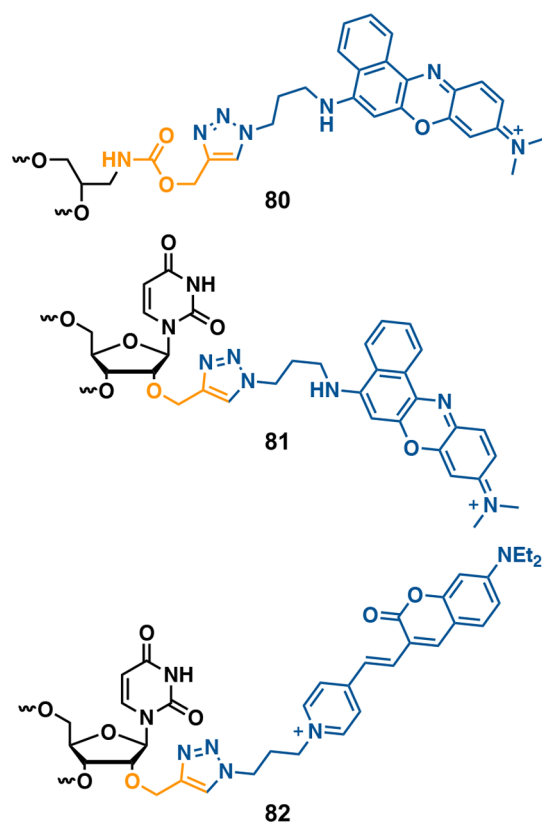


**Figure 12.** Fluorescent modifications (phenoxazinium azide, 80, 81; and red coumarin azide, 82) introduced through CuAAC by Wagenknecht and co-workers.<sup>135</sup>

an acyclic glycol linker as a non-nucleosidic DNA base surrogate. In this case the modification site did not influence the fluorescent properties of the dye and the 2'-fluorophore-modified uridine was still able to base-pair to adenine without reducing the thermal stability of the duplex compared to the unmodified control. The oligonucleotides modified with the coumarin dye at the 2'-position of uridine were characterized by a significant Stokes' shift of ~100 nm and good quantum yields, making this chromophore accessible for fluorescent labeling of nucleic acids in various assays and in cell biology.<sup>135</sup> The same group used dual emitting DNA probes to develop the concept of "DNA traffic lights".<sup>136</sup> These fluorophore combinations allow readout otherwise not achievable with the conventional fluorophore-quencher or exciton-based dye pairs. Here thiazole orange (TO) (83) and thiazole red (TR) (85) were used as an energy transfer (ET) combination that allows fluorescence shifts between red and green dependent on the ET efficiency. The CuAAC reaction advances the DNA traffic lights concept by introducing the energy donor dye TO via click reaction at the 2'-position of uridine. This strategy is more advantageous than the previous approach in that the postsynthetic labeling through the triazole simplifies the synthesis of one of the dsDNA strands. In addition, the U–A base pair at the site of modification was effective in blocking undesired excitonic (ground state) interactions between TO and TR. Different dye combinations can be quickly investigated using this approach; as an example the energy donor TO was replaced by the significantly more photostable CyIQ dye (Figure 13, 84).<sup>137</sup>

The utility of CuAAC for oligonucleotide tagging with multiple small molecules is limited as the introduction of

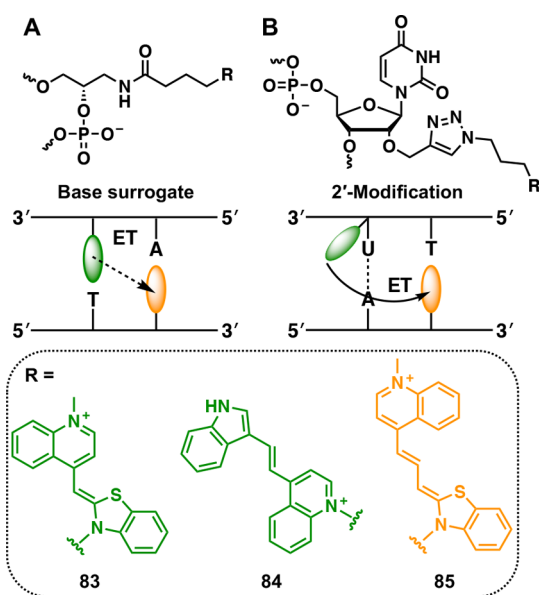
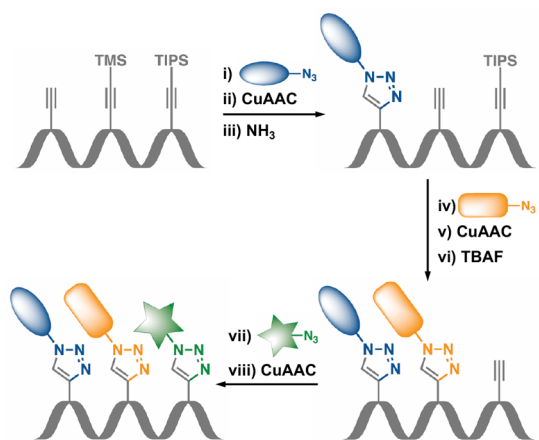


**Figure 13.** (A) TO (83) and TR (85) as two base surrogates allow excitonic interactions that interfere with energy transfer (ET). (B) For TO (or CyIQ, 84) as the 2'-modification, the U–A base pair blocks excitonic interactions (green, TO or CyIQ; orange, TR).<sup>137</sup>

different labels at specific alkyne-modified positions cannot be controlled using standard approaches. To direct fluorophore incorporation to predefined loci, a DNA sequence was modified with an unprotected and two orthogonally protected octadiynyl groups (Scheme 5). The alkyne modifications were

#### Scheme 5. Click-Click-Click Strategy Developed by Carell and Co-workers for the Sequential Labeling of Oligonucleotides with up to Three Different Probes<sup>102</sup>



introduced in the oligonucleotides by standard solid phase synthesis, and three different fluorescent dyes were efficiently incorporated into oligonucleotides directly on the resin or in solution after oligonucleotide deprotection. The free alkyne was first conjugated to a stable azide-modified fluorophore directly on the resin. Following cleavage of the trimethylsilyl (TMS) protecting group from the second alkyne by ammonia treatment, a second fluorophore could be added in specific positions of the modified strand. This approach left the third and remaining alkyne group protected with triisopropylsilyl (TIPS) and therefore available for its deprotection by tetrabutylammonium fluoride and labeling with a third

fluorophore. Recently a similar strategy was used to introduce multiple different fluorophores at predetermined loci of an oligonucleotide strand.<sup>102</sup>

Besides canonical DNA and RNA constructs, click chemistry has been used to introduce dyes into other nucleic acid derivatives. The 2'-amino position of 2'-amino-locked nucleic acid (2'-amino-LNA) monomers was modified with a 2'-*N*-alkynyl group and clicked to various probes (xanthene, cyanine, and a polyaromatic hydrocarbon) by CuAAC. The combination between LNA/DNA strands and click chemistry allowed the efficient generation and screening of a wide library of fluorescent oligonucleotides. Several probes with high target binding and specificity were identified and found to have possible applications in various fluorescence assays including, but not limited to, live-cell nucleic acid imaging, aptasensing, and nucleic acid diagnostics. In addition, the 2'-*N*-alkynyl group in the LNA/DNA strands is available for tagging with other modifications such as carbohydrates, lipids, cofactors, and cell-penetrating peptides. Therefore these clickable LNA/DNA probes offer an appealing strategy for the development of biosensors, therapeutics, and nanoconstructs.<sup>138</sup>

**4.1.2. Other Small-Molecule Labels.** In addition to fluorophores, nucleic acids have been clicked to other small-molecules such as metal complexes or modifications aimed to improve their cellular uptake. Alkyne-modified RNA was conjugated to different azide modified receptor-binding molecules including 3'-cholesterol (86), 3'-folate (87), and 3'-anandamide (88) (Figure 14). The anandamide-RNA

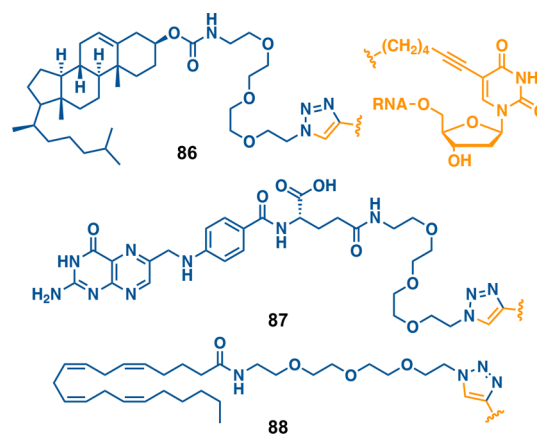


**Figure 14.** Clicked RNA-hybrids with receptor-binding molecules.<sup>139</sup>

hybrids had surprisingly high transfection capability, and the modification enabled the efficient delivery of siRNA into difficult-to-transfect RBL-2H3 cells that are models for neuronal transfection. Application of this system to human immune cells (BJAB) demonstrated silencing effects similar to those provided by cationic transfection reagents, representing a nontoxic alternative to the latter class. Thereby, the application of siRNA-based gene silencing was extended to neuronal and immune cells.<sup>139</sup>

Click labeling of nucleic acid derivatives with metal complexes has enabled researchers to efficiently produce libraries of hybrids with diverse functionalities dependent on the metal center and the shape of the coordinating scaffold. The interest in these click-conjugates arises from the advantage that oligonucleotide base pairing can provide in targeting the biochemical activity of metal complexes to selected sequences. Using this strategy, highly specific

chimeric probes can be generated with possible applications as gene-targeted biosensors, nucleases, and fluorescent and radioactive probes. Hüsken et al. used the CuAAC reaction to form a small library of ferrocenyl bioconjugates with peptide nucleic acids (PNA) (Figure 15A). In this work,

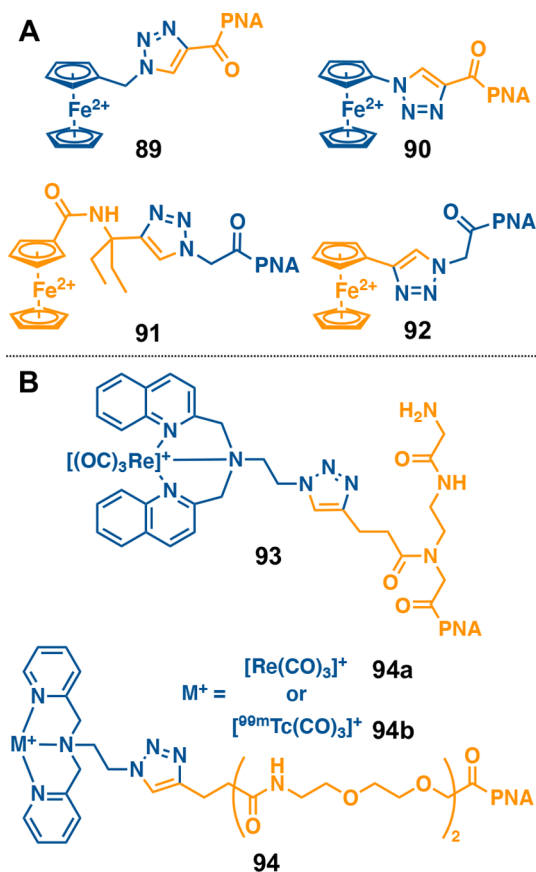


**Figure 15.** Clicked PNA–metal complex hybrids as electrochemical (A),<sup>140</sup> fluorescent,<sup>141</sup> or radioactive<sup>142</sup> (B) sensors.

different electrochemical potentials—provided by distinct ferrocene derivatives (89–92)—could be encoded into PNA oligomer sequences using the same synthetic conditions. The four clicked ferrocenyl-PNA hybrids exhibited potential differences bigger than 60 mV, distinguishable by electrochemical methods such as differential pulse voltammetry. This “four-potential” labeling with electrochemical probes corresponds to the “four-colour” detection with different fluorophores in classical DNA analysis and opens potential applications for PNA in the field of electrochemical nucleic acid biosensors.<sup>140</sup> The same workers exploited click chemistry to attach a  $[\text{Re}(\text{CO})_3(\text{L-N}_3)]^+$  (93) (where  $\text{L-N}_3 = (2\text{-azido-}N,N\text{-bis}((\text{quinolin-2-yl})\text{methyl})\text{ethanamine})^{141}$  and a  $[\text{Tc}(\text{CO})_3(\text{DPA-N}_3)]^+$  (94b) (where  $\text{DPA-N}_3 = di(2\text{-picolyl)amine}^{142}$  complex to PNA as a fluorescent or radioactive probe, respectively (Figure 15B). The rhenium hybrid (93) was an effective bioimaging agent and was detectable in living cells at a concentration of 10  $\mu\text{M}$  using fluorescent microscopy. In addition, eGFP expression in genetically modified HeLa cells decreased by 18% after incubation with the Re–PNA conjugate targeting the eGFP sequence, suggesting that the hybrid might be used as an antisense agent. The specific antisense effect is further supported by the absence of a change in protein expression

observed for a conjugate containing a mismatched PNA sequence.<sup>141</sup> Biodistribution analysis of 94b in Wistar rat or mouse models (NMRI nu/nu) identified fast blood clearance and low accumulation in the kidneys.<sup>142</sup>

The CuAAC reaction is an efficient tool to generate wide libraries of targeted compounds and quickly evaluate their structure–activity relationships. In recent work on targeted chemical nucleases, Cu-Clip-Phen complexes (95) (where Phen = 1,10-phenanthroline) were conjugated to various alkyne-modified triplex forming oligonucleotides (TFOs) by click chemistry (Figure 16, 95a–g).<sup>143</sup> In the presence of

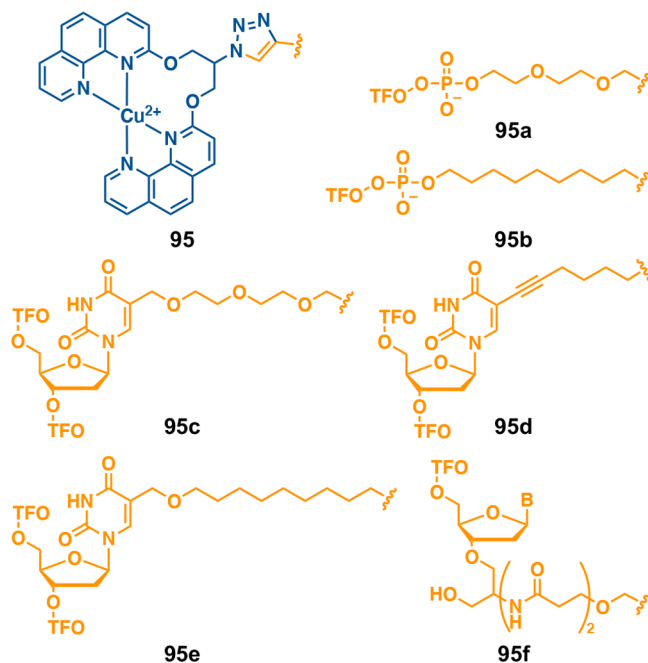


**Figure 16.** Clicked AMN–TFO hybrids with Clip-Phen developed by Hocek and co-workers.<sup>143</sup>

oxygen and reductant, copper-phenanthrene compounds cause the production of ROS and copper-oxo species capable of oxidatively damaging nucleic acids ultimately leading to strand excision.<sup>144,145</sup> Therefore, tagging copper chemical nucleases to TFOs provides a strategy to develop targeted dsDNA-cleaving agents where sequence specific recognition arises from Hoogsteen base pairing. The artificial nuclease Clip-Phen machinery was coupled to different positions (*i.e.* 5'-end, 95a and 95b; internal, 95c–e; or 3'-end, 95f) of the TFO probe using various linkers differing in length, flexibility, and polarity (Figure 16). Damage by the hybrids was assessed on a target and an *off*-target—noncomplementary by Hoogsteen base pairing—dsDNA sequences. Under optimized conditions significant cleavage of the target duplex (up to 34%) with no *off*-target effects was generated when Clip-Phen was linked internally or at the 5'-end of TFOs through a flexible linker. The absence of clear footprinting cleavage suggested that strand-excision does not proceed with single-nucleotide precision but that the target dsDNA sequence is degraded in close proximity to the copper source by the produced diffusible free radicals.<sup>143</sup>

In two studies carried out by Kellett and co-workers TFOs of various length were conjugated by click chemistry to either phenanthrene (96–100)<sup>146</sup> or *tris*(2-pyridylmethyl)amine (TPMA) (101–102)<sup>147</sup> derivatives (Figure 17). The

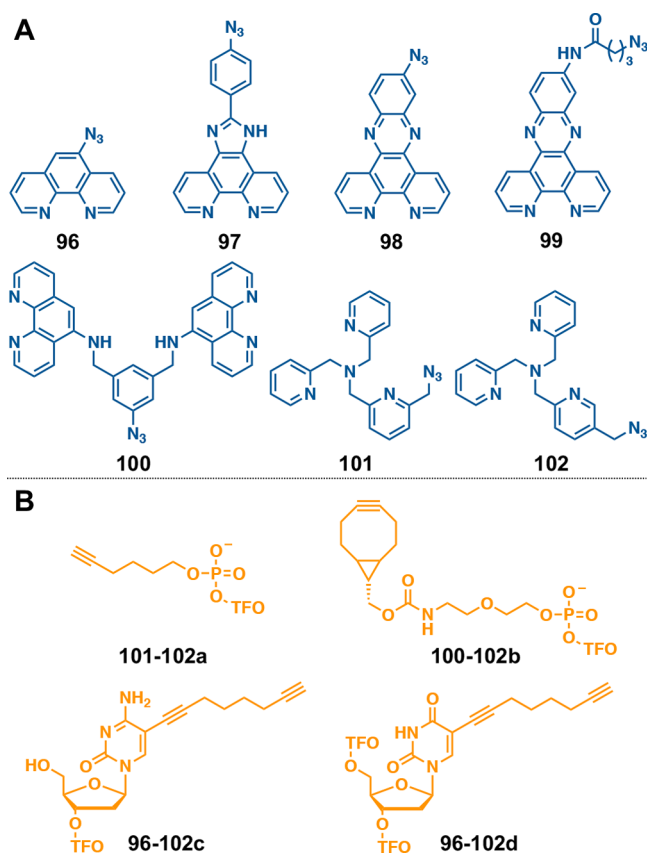


**Figure 17.** AMN-TFO hybrids developed by Kellett et al. and formed by the click reaction between phenanthrene<sup>146</sup> (96–100) or TPMA<sup>147</sup> (101, 102) derivatives (A) with various alkyne modified triplex forming oligonucleotides (B).

extended aromatic structure of phenanthrene dsDNA intercalating ligands significantly stabilized binding by the TFO to the target duplex and increased the triplex melting temperature with  $\Delta T_M$  up to 22 °C. Although oxidative damage of a fluorophore-labeled dsDNA target by one Cu-AMN-TFO (including 98 as AMN) was to a small extent sequence-specific, high-resolution cleavage at the single nucleotide level was not, at this point, achieved. To enhance cleavage selectivity, a bis-Phen di-copper compound (100) was conjugated to three of the studied TFOs and cleavage was assessed also when an ancillary intercalator (Phen; dipyrido[3,2-f:2',3'-h]quinoxaline, DPQ and dipyrido[3,2-a:2',3'-c]-phenazine, DPPZ) was coordinated to the copper centers. Although cleavage discrimination between an *on*- and *off*-target sequence was modest in the presence of only Cu(NO<sub>3</sub>)<sub>2</sub>, damage markedly increased upon complexation of 100 to Cu-Phen or Cu-DPQ. The presence of the ancillary intercalator positively affected AMN activity, and the target duplex was completely ablated without any apparent damage of the *off*-target sequence.<sup>146</sup> Promising sequence selectivity was also achieved when Cu-TPMA complexes were conjugated by CuAAC reaction to TFOs (101–102). In good agreement with the Clip-Phen hybrids, the best sequence discrimination was achieved when TPMA was linked to an internal position of the TFO sequence (102d). In this case, the target duplex was depleted faster than the *off*-target sequence (analyzed by gel densitometry 72% versus 24% knockdown at 100 equiv of Na-L-asc, respectively). Interestingly, analysis of dsDNA cleavage activity by real time

PCR identified damage promoted by the clicked AMN in the absence of exogenous reductant. Conversely, no effect on duplex integrity was observed when this was treated with free Cu-TPMA in the absence of reductant. In addition, the oxidative damage mechanism was studied on a larger DNA construct—the closed circular pCSanDI-HYG plasmid, 6389 bp—containing the target sequence of one of the AMN-TFOs under study. Cleavage experiments in the absence or presence of ROS scavengers showed that the supercoiled (SC) plasmid is converted to the nicked open circular (OC) and linear (L) form through an oxidative cutting mechanism that relies (primarily) on the generation of superoxide type (O<sub>2</sub><sup>•-</sup>) radicals. Although polypicolyl ligands do not afford the same stabilization effect provided by phenanthrene derivatives, a similar increase in stability ( $\Delta T_M$  up to 18.4 °C) was achieved in this case by modifying the AMN with the duplex binder thiazole orange (TO).<sup>147</sup>

Despite the reduced specificity of AMN-TFOs compared to enzymatic constructs, the extent and oxidative nature of their damage could make these artificial nucleases efficient sequence-selective knockdown agents. Further DNA backbone or ribose modifications aimed to increase TFO stability to endo- or exo-nucleases might advance this technology for future cellular applications.

#### 4.2. Cellular Metabolic Labeling of Nucleic Acids

Nucleic acid labeling by click chemistry is particularly advantageous when applied for the *in vitro* and *in vivo* study of cell cycle kinetics, DNA and RNA synthesis, and cellular proliferation. Initially analysis of cellular DNA synthesis was performed by incorporating labeled DNA precursors such as [<sup>3</sup>H]thymidine and 5-bromo-2'-deoxyuridine (BrdU) into the genome during the S phase of the cell cycle. Upon penetrating the cell membrane, these monomers are converted to their triphosphate forms by cellular kinases and subsequently incorporated into genomic material. Nucleic acids embedding [<sup>3</sup>H]thymidine or BrdU can then be visualized by autoradiography or by immuno-staining with BrdU-specific antibodies and turnover can be detected using the ribonucleoside derivatives [<sup>3</sup>H]uridine or 5-bromouridine (BrU).<sup>150,151</sup> However, the applicability of these methods suffers from several limitations. The radioactivity of [<sup>3</sup>H]-nucleosides makes their handling cumbersome, and autoradiography is a slow technique not suitable for high-throughput studies. In addition, the microscopic images of radiolabeled nucleic acids have usually low spatial-resolution and low signal-to-noise ratios. Staining with BrdU (or BrU) is instead limited by antibody diffusion in the specimen which often requires sectioning of the tissue and long incubation times with the antibody. In the specific case of DNA labeling, access of the anti-BrdU antibody to the BrdU epitope is also hindered by nucleobase pairing in double stranded DNA. Strong denaturing conditions are therefore required to expose the BrdU subunits resulting in degradation of the specimen structure and making the staining intensity dependent on the experimental setup.

**4.2.1. Metabolic Labeling of DNA.** Initial work by Mitchison and co-workers focused on developing an alternative technique for DNA labeling in the context of preserved cellular and chromatin ultrastructure. In their strategy, 5-ethynyl-2'-deoxyuridine (EdU, 103) was used to label cellular DNA prior to CuAAC reaction with fluorescent

organic azides.<sup>23</sup> Similar to BrdU, EdU is first phosphorylated (104) in the cell by kinases and then introduced into the genome by DNA polymerases (Figure 18). In contrast to

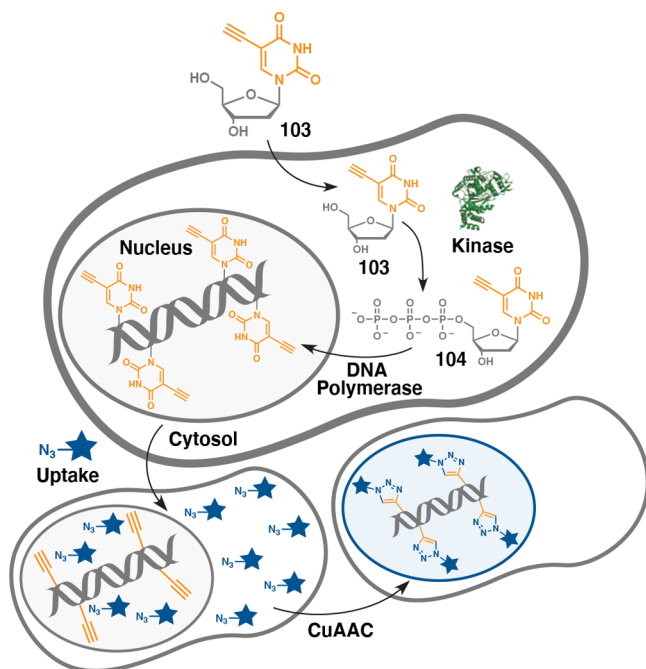


**Figure 18.** dU\* (103) is phosphorylated into cells (104) and integrated within the genome by polymerase enzymes. The exposed alkynes can then be labeled by CuAAC with organic azide probes.

BrdU, however, the reporter group—the alkyne—of the incorporated EdU is localized in the major groove of the double helix. Here, the alkyne is not affected by any steric hindrance, and it can undergo CuAAC staining without requirement for prior sample fixation or DNA denaturation. For this reason, CuAAC coupling of EdU-labeled DNA to various fluorescent azides proceeded smoothly and with high reproducibility among the fluorophores. In addition, upon injection into mice, EdU allowed the rapid and sensitive whole-mount imaging of cellular turnover in small intestine villi offering an easier and more efficient strategy for the study of organ and tissue dynamics compared to previous methods.

Despite the several advantages of EdU over BrdU-staining, EdU has higher cytotoxicity and its inclusion in cellular DNA represents a chemical insult that causes DNA instability, necrosis, and cell-cycle arrest.<sup>152</sup> The intrinsic toxicity and alteration of biological function imposed by EdU represent therefore a critical constraint in metabolic labeling studies where subsequent tissue survival is required. To prevent cellular toxicity while preserving metabolic DNA incorporation, Luedtke and co-workers analyzed a series of arabinofuranosyl-ethynyluracil derivatives (Figure 19A) and identified selective DNA labeling by (2'S)-2'-deoxy-2'-fluoro-5-ethynyluridine (F-ara-EdU, 104) with minimal impact on genome function.<sup>120</sup> The lower toxicity of F-ara-EdU compared to both BrdU and EdU enables detection by CuAAC fluorescent staining with greater sensitivity in pulse-chase experiments and in other metabolic labeling studies where long-term cell survival is required (60 days or more). As an example, usage of F-ara-EdU in combination with BrdU in pulse-chase experiments allowed birth dating of DNA *in vivo*, identification of quiescent/senescent cells, and thus

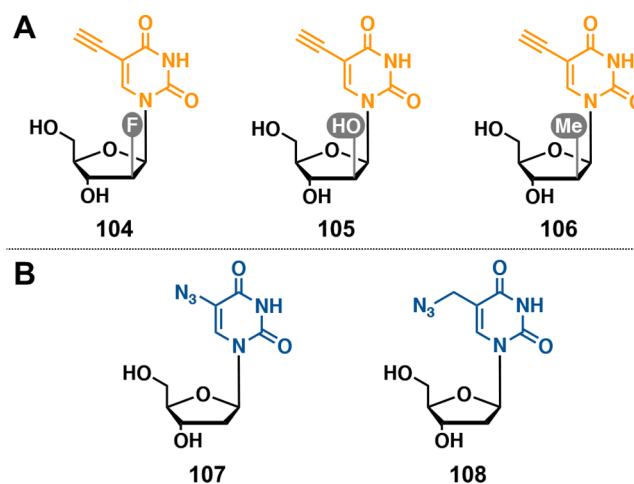


**Figure 19.** (A) Arabinofuranosyl-5-ethynyluridine derivatives studied for cellular metabolic labeling of DNA: F-ara-EdU (104); ara-EU (105); and Me-ara-EdU (106).<sup>120</sup> (B) Azide modified uridine derivatives AdU (107) and AmdU (108) used for cellular metabolic labeling of DNA.<sup>23,153</sup>

timing of tissue development and differentiation in Zebrafish embryos.<sup>120</sup>

The methods hitherto described involve labeling of DNA with alkyne reporter groups followed by CuAAC labeling with fluorescent organic azides. Reversing the chemistry by incorporating azido nucleoside analogues (Figure 19B) expands click labeling capability also to the strain-promoted azide–alkyne cycloaddition (SPAAC) where cytotoxic Cu(I) catalyst are not required. Although initial studies with 5-azido-2'-deoxyuridine (AdU, 107) were unsuccessful reporting poor labeling results,<sup>23</sup> more recent work with 5-(azidomethyl)-2'-deoxyuridine (AmdU, 108) showed strong nuclear staining.<sup>153</sup> Interestingly, an in-depth study of SPAAC versus CuAAC fluorescent staining revealed a bias in SPAAC detection of AmdU, and preferential labeling occurred at sites of single-stranded DNA. SPAAC staining prejudice is probably imposed by the larger bulk of the cyclooctyne modification compared to terminal alkynes, and it was suggested to be a useful method for probing variable chromatin and/or secondary structures of DNA in cells. In addition, AmdU labeling is bioorthogonal to other available methods (*i.e.* F-ara-EdU and BrdU) and allowed the time-resolved, three-color analysis of DNA synthesis in single cells.<sup>153</sup>

**4.2.2. Metabolic Labeling of RNA.** It is important to note that the above-described deoxynucleotide precursors are specific only for DNA incorporation as no labeling was detected in cells where DNA synthesis was selectively inhibited.<sup>23,120,153</sup> To label RNA, a similar strategy can be exploited by using labeled nucleosides (Figure 20)—instead of the deoxynucleosides—for incorporation by RNA polymerases during gene transcription.

Salic and co-workers showed that the ribonucleoside 5-ethynyluridine (EU, 109) is integrated into RNA transcripts generated in cells by polymerases I, II, and III.<sup>154</sup> To be integrated into RNA, EU enters the ribonucleoside salvage pathway and is first phosphorylated to form the 5'-ribonucleoside phosphates—EUMP, EU DP, and EUTP. However, ribonucleotide reductase can convert EU DP to its deoxyribonucleoside diphosphate EdUDP which can be readily incorporated into DNA, thus limiting the utility of

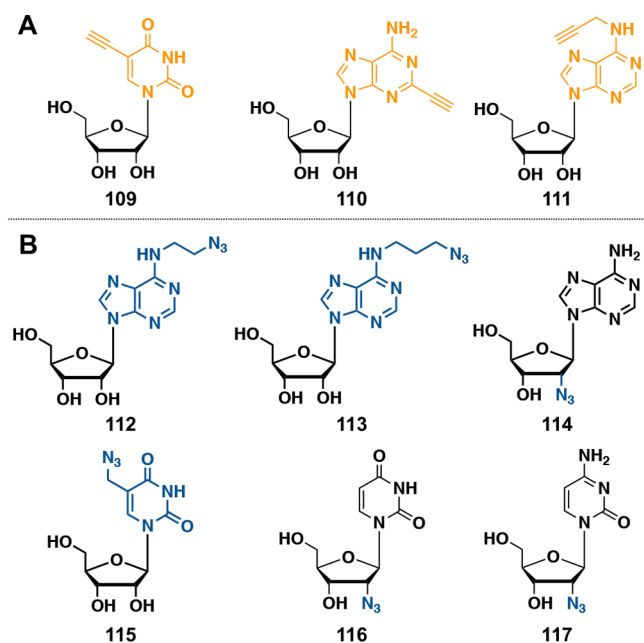


**Figure 20.** (A) Alkyne modified nucleosides used for cellular metabolic labeling of RNA: EU (109);<sup>154</sup> EA (110);<sup>155</sup> and N<sup>6</sup>pA (111).<sup>156</sup> (B) Azide modified purine (112–114)<sup>158</sup> and pyrimidine (115–117)<sup>158,161,162</sup> derivatives used for cellular metabolic labeling of RNA.

EU as a specific transcriptional label. Treating cells with EU in the presence of hydroxyurea or thymidine—two ribonucleotide reductase inhibitors—revealed no difference in EU staining whereas, in a parallel experiment, DNA incorporation of EdU was abolished by the same inhibitors.<sup>154</sup> The authors therefore suggested that EU is a poor substrate for ribonucleotide reductase and can be used as a specific label for cellular RNA. In animals EU allowed intense staining of four different organs (small intestine, kidney, liver, and spleen) with low background staining on control sections. In the small intestine, the high sensitivity of EU staining enabled detection of significant transcription not only in the highly proliferative crypt-cells but, at a lower extent, also in villar cells. Notably, the transcriptional activity in villar cells was not identified in previous studies which used tritiated-uridine as a label.<sup>150</sup>

In addition to EU, other alkyne-modified ribonucleosides have been synthesized and used for tracking of transcription in cells. Alkyne-modified adenosine precursors—such as 2-ethynyl adenosine (EA, 110)<sup>155</sup> and N<sup>6</sup>-propargyladenosine (N<sup>6</sup>pA, 111)<sup>156</sup>—are particularly interesting RNA metabolic labels as they can be used to monitor poly(A) tail dynamics beyond being an efficient tool for CuAAC-mediated fluorescence imaging and affinity enrichment of nascent transcripts. RNA transcripts from cells treated with EA and actinomycin D (ActD)—a cellular transcription inhibitor that does not interfere with polyadenylation pathways—were reacted with biotin-azide and measured by streptavidin-alkaline phosphatase blotting. ActD reduced but did not block EA labeling of RNA indicating a transcription independent pathway for incorporation of the alkyne nucleoside in the transcripts. Treatment of cells with EA in the presence of both ActD and cordycepin—a cellular polyadenylation inhibitor—completely prevented EA-labeling, altogether confirming incorporation of the alkyne nucleoside into RNA both by

transcription and polyadenylation.<sup>155</sup> Studies on (N<sup>6</sup>pA) identified its efficient and selective incorporation in RNA by all three mammalian RNA polymerases I, II, and III. In HEK293 cells, it was shown that N<sup>6</sup>pA is incorporated also into poly(A) tails by the “canonical” poly(A) polymerase, PAP $\alpha$ —although the authors state that further studies are required to determine if N<sup>6</sup>pA can be a potential substrate for “noncanonical” poly(A) polymerases involved in a variety of alternative polyadenylation pathways.<sup>156</sup> A strategy involving pulse-labeling with EU or N<sup>6</sup>pA prior to chase with media lacking modified nucleoside allowed observation of metabolism of RNAs transcripts from endogenous promoters in the absence of general inhibitors which often have pleiotropic effects. In this method bulk poly(A) tails can be detected after a short labeling pulse enabling the analysis of poly(A) dynamics in transcripts synthesized within a 2 h window, thereby reducing the length heterogeneity of poly(A) tails which arises over time.<sup>156</sup>

The introduction of alkyne nucleosides into RNA limits labeling to CuAAC coupling where copper-induced radicals can be generated leading to RNA degradation and deleterious effects on downstream analyses such as RNA sequencing.<sup>157</sup> Similar to the “reverse” metabolic labeling of DNA, azido-nucleosides can be robustly introduced into RNA for posttranscriptional SPAAC coupling.<sup>158</sup> Efficient metabolic labeling was detected with three adenosine analogues bearing azide handles at both the N6- (112–113) and 2'-positions (114). Interestingly, 112 and 113 were predominantly introduced during transcription whereas 114 was incorporated also during polyadenylation. This labeling bias was suggested to offer a potential strategy to analyze nascent RNA synthesis and poly(A) elongation differentially inside living cells. Although the same work reported that 5-methylazidouridine (5-AmU, 115) is not incorporated into cellular RNA,<sup>158</sup> the triphosphate form of 5-AmU was later shown to be readily recognized and integrated by RNA polymerases.<sup>159</sup> This difference is caused by the incompatibility of 5-AmU with the uridine-cytidine kinase, UCK2—the enzyme generating pyrimidine monophosphates from nucleosides in the pyrimidine salvage pathway. An engineered version of UCK2 developed by Kleiner and co-workers was able to convert 5-AmU to 5-AmU monophosphate *in vitro*.<sup>160</sup> Upon transfection of the plasmid expressing the mutant enzyme into HeLa cells, 5-AmU was efficiently incorporated into cellular transcripts. In combination with 5-EU in pulse-chase experiments, 5-AmU allowed analysis of RNA synthesis and turnover during cellular stresses with high temporal resolution. Similar work by Spitale and co-workers on UCK2 identified that the poor metabolic label 2'-azidouridine (2'-AzU, 116) can become a highly stringent nontoxic approach for cell-specific RNA metabolic labeling when used together with wild-type UCK2 overexpression.<sup>161</sup> Other nonspecific metabolic labels (such as 5-EU and 2'-azidocytidine, 2'-AzC, 117) reduced cell viability, and 5-AmU treatment caused complete cell detachment leading to loss of membrane integrity and reduced proliferation.<sup>161</sup> Nonetheless, a 2'-AzC/deoxycytidine kinase (dCK) pair was later reported to be 10-fold more efficient in promoting RNA labeling than the 2'-AzU/UCK2 combination with negligible effects on viability after a 3-day treatment.<sup>162</sup>

Alternatively, reporter groups for CuAAC or SPAAC couplings can be introduced into RNA strands site-specifically using natural or engineered methyltransferases.<sup>163–166</sup> In

combination with *S*-adenosyl-L-methionine (AdoMet or SAM) analogues, these enzymes can transfer the sulfur-bound alkynyl chain of the adenosyl *co*-factor to specific nitrogen sites on nucleobases (Figure 21). As an example,

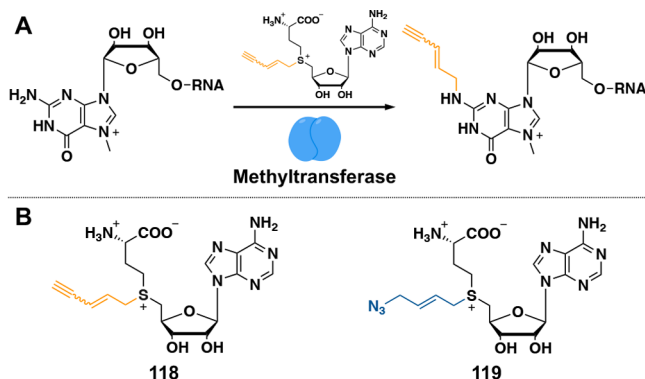


**Figure 21.** (A) General strategy for the metabolic labeling of RNA where a click reporter group is transferred to the N2 of m7G by a methyltransferase. (B) AdoMet derivatives used for the metabolic labeling with methyltransferases AdoEnYn (118) and AbSAM (119).<sup>165,166</sup>

tRNA:methyltransferase (Trm1) was used to transfer the pent-2-en-4-ynyl (EnYn) chain from AdoEnYn (118) to the N2 of guanosine 26 in tRNA<sup>Phe</sup>.<sup>163</sup> The posttranscriptional alkyne modification can then be coupled by CuAAC reaction to various reporter molecules (e.g. fluorescent organic azides, biotin azide, etc.) enabling imaging or enrichment of RNA. A similar chemoenzymatic technique developed by Rentmeister and co-workers was used to site-specifically introduce various alkyne or azide reporter groups at the 5'-cap of eukaryotic mRNA for posttranscription CuAAC and SPAAC labeling.<sup>165,166</sup> Here, an engineered trimethylguanosine synthase from *Giardia lamblia* (GlaTgs2) recognizes and site-specifically modifies the N2 position of the m7G-triphosphate cap at the 5'-end of eukaryotic mRNA. Used in combination with AdoEnYn (118)<sup>166</sup> or Ab-SAM (119),<sup>165</sup> the engineered GlaTgs2 variant transfers the click-“tag” labels—EnYn or 4-azidobut-2-enyl (Ab), respectively—to the N2 position of the m7G-cap. Labeling of the 5'-cap of eukaryotic mRNA with 4-azidobut-2-enyl has particular relevance because it enables labeling both by CuAAC and SPAAC chemistries.<sup>165</sup> Importantly in both strategies fluorescent labeling of the cap was achieved also in the complex environment of the eukaryotic cellular lysate.<sup>165,166</sup>

#### 4.3. Click-Chemistry to Assemble Nucleic Acids

**4.3.1. Clicking Nucleobases on the Backbone.** The biocompatibility of click chemistry has been used in the synthesis of several DNA and RNA analogues in which the structural features of nucleic acids were substituted with triazole units. Obika and co-workers synthesized an oligonucleotide containing 1-ethynyl-2-deoxy- $\beta$ -D-ribofuranose and clicked the alkyne group to various modifications forming artificial triazole nucleobases (Figure 22A). Although none of the oligonucleotides incorporating the artificial modification formed stable DNA duplexes, similar  $T_M$  values obtained from 1-(phenyl-thio)methyl-1*H*-1,2,3-triazole (120g) paired to the four canonical nucleosides suggested that this functionality could behave as an universal nucleobase.<sup>167</sup> A reverse approach was implemented by Seela's group who reacted *N*-

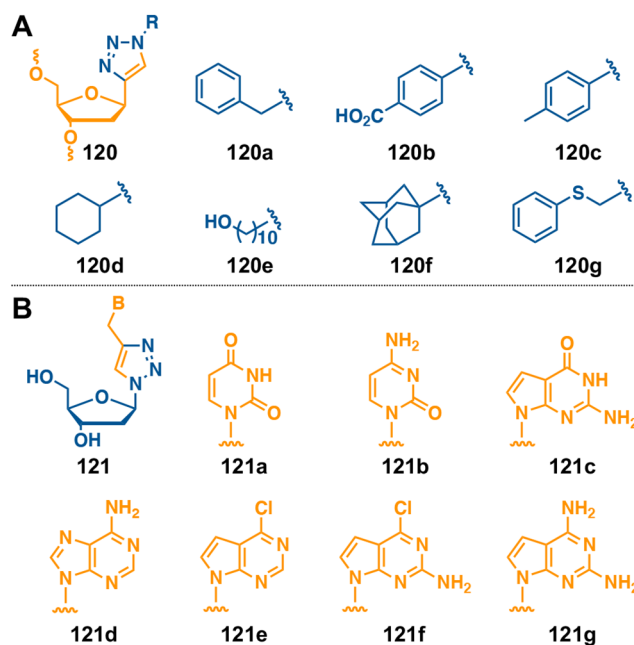


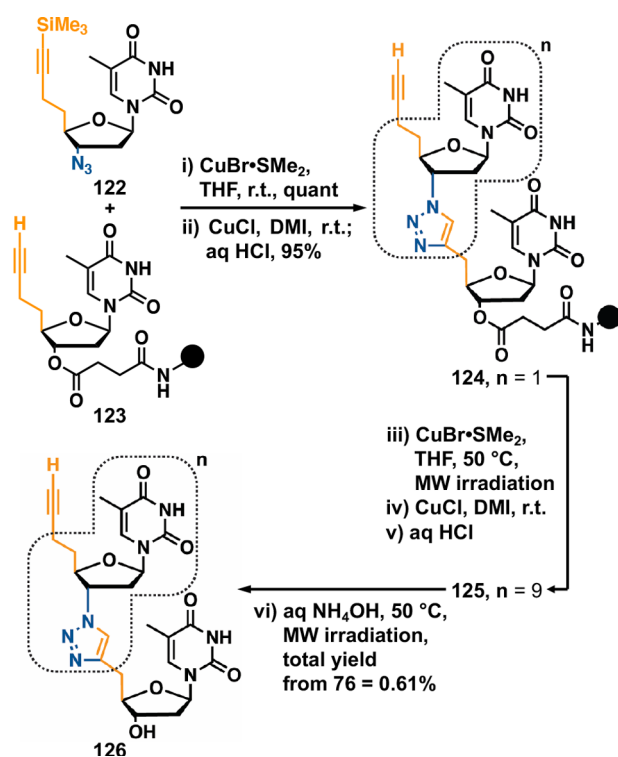
**Figure 22.** (A) Clicked artificial nucleobases (R) by Obika and co-workers.<sup>167</sup> (B) Reverse-clicked nucleobases (B) and nucleobase derivatives by Seela and co-workers.<sup>168</sup>

9 propargylpurines or *N*-1 propargylpyrimidines with toluoyl protected 1-azido-2-deoxyribofuranose (Figure 22B). The clicked nucleosides were then deprotected with sodium methoxide and studied either as potential antiviral agents or as artificial nucleobases when introduced in dsDNA. Both clicked derivatives of uridine (121a) and adenine (121d) destabilized dsDNA, behaving as an abasic site, and stability was retained only when these modifications were placed at the termini of the duplex.<sup>168</sup>

**4.3.2. Triazole as a Phosphate Linkage Alternative.** A major benefit of click chemistry lies in using triazole formation as a strategy to chemically synthesize long nucleic acids analogues. Chemical ligation of nucleosides has several advantages over routinely used enzymatic methods. The synthesis of long genetic constructs requires multiple cycles of PCR amplification, mismatch repair, cloning, sequencing, and selection. Inclusion of high-fidelity proofreading polymerases minimizes the number of mistakes during the amplification cycles by incorporating the enzymatic mismatch repair in the workflow. Nonetheless, repair, cloning, and sequencing steps together with the low quantities yielded by PCR can represent an obstacle to the production of large amounts of DNA and RNA strands for research and industrial purposes. In addition, epigenetic modifications (i.e. 5-methylcytosine (mC), 5-hydroxymethylcytosine (hmC), 5-formylcytosine (fC), and 5-carboxylcytosine (caC))—important for tuning the expression of specific genes—are incorporated randomly against G by DNA polymerases (i.e. guanine does not discriminate between them), precluding the synthesis of site-specific modified epigenomes by traditional enzymatic methods. Specific epigenetic mutations can be introduced in limited numbers through nucleobase-modified PCR primers or by the templated ligation of synthetic nucleic acid chains by ligase enzymes. However, pure chemical DNA synthesis is limited by the maximum oligonucleotide length achievable on solid phase supports (coupling reactions are inefficient beyond ~200 nt) and by the high error rates during phosphoramidite coupling

reactions (up to 1–10 errors per kilobase).<sup>169</sup> A chemical ligation method capable of efficiently joining short and pure oligonucleotides could broaden the application of synthetic DNA strategies to the production of large genomes. Some progress in chemical ligation of oligonucleotides was made by using cyanogen bromide as the coupling agent<sup>170,171</sup> or by templating the reaction between 3'-phosphorothioate and 5'-tosylate (or iodide) modified oligonucleotides. Nevertheless, compared to other chemical ligations such as CuAAC, these strategies require the use of toxic compounds or functional groups which are unstable in aqueous media. Application of triazoles as alternatives to the phosphate linkage was initially investigated by Nuzzi et al. In this work, two types of triazole DNA backbones were formed by clicking together nucleotides with 3'- or 5'-terminal alkynes or azides.<sup>172</sup> Isobe et al. further advanced the field by producing a fully backbone modified decamer strand (126, <sup>TL</sup>DNA) from sequential steps of CuAAC reaction with 122 followed by deprotection of the silyl alkyne-protecting group (Scheme 6).<sup>26,173</sup> The molecular

Scheme 6. Solid Phase Synthesis of 10-mer <sup>TL</sup>DNA<sup>26</sup>



design encompassed a methylene bridge at the pseudo-5'-position of the sugar backbone to retain the five-bond spacer length and flexibility of the phosphodiester linkage in natural oligonucleotides (Trz C, Figure 23). The modified chain annealed to a complementary sequence forming a duplex structure more stable ( $T_M = 61.1$  °C) than the one yielded from the unmodified control ( $T_M = 20$  °C). In this case, the lack of repulsive interactions of the triazole backbone with the anionic phosphate backbone was essential to enhance the stability of dsDNA, but the spacer length was also thought to aid duplex stabilization. In contrast, an 11-mer backbone-modified RNA analogue (<sup>TL</sup>RNA) provided less stable RNA:RNA duplexes when compared to the natural RNA control.<sup>174</sup> A detailed thermodynamic analysis of modified and unmodified duplexes revealed that <sup>TL</sup>RNA:RNA structure had

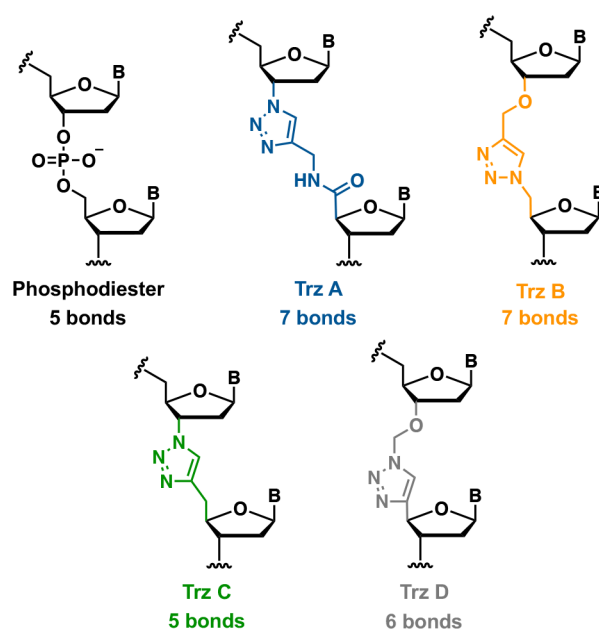


Figure 23. Canonical phosphodiester linkage and first-generation triazole linkage A (Trz A), second generation triazole linkage B (Trz B), and triazole linkage C (Trz C) in <sup>TL</sup>DNA reported by Isobe et al. and triazole linkage D (Trz D) reported by Varizhuk et al. The number of bonds between the C3' and C4' atoms of adjacent sugar rings is indicated.

a much lower association enthalpy ( $\Delta H = -52$  kcal mol<sup>-1</sup>) compared to the control ( $\Delta H = -87$  kcal mol<sup>-1</sup>). Structural studies associated this reduction in association enthalpy with triazole/2'-OH interactions which inevitably constrain the triazole orientations, causing a mismatch in the internucleoside distance between the two strands. Noticeably, this interaction is not present in the case of <sup>TL</sup>DNA duplexes (no 2'-OH present).<sup>174</sup>

Although consecutive Trz C modifications in <sup>TL</sup>DNA apparently stabilize the duplex structure, isolated triazole modifications reduce the stability of the dsDNA helix (average  $\Delta T_M$  per modification  $\sim -4$  °C). Computational analysis of 12 structures—differing in the position of the triazole relative to the duplex axis—identified a longer helical pitch which may arise from a lesser twist of the triazole compared to the phosphodiester linkage.<sup>175</sup>

A similar destabilization was noted also in the case of DNA and RNA duplexes made with oligonucleotide modified at single backbone positions with triazoles differing in spacer length (Figure 23). A single modification with the 7-bond linker Trz B reduces oligonucleotide binding affinity toward target DNA and RNA compared to an unmodified control ( $\Delta T_M \sim -4$  to  $-8$  °C/modification).<sup>176,177</sup> Nonetheless, the cooperative UV-melting transitions with similar hyperchromicity for both the modified and unmodified structures demonstrate a fully base-paired double helical structure. The best results are usually achieved in the case of flexible 6 bond modifiers (Trz D) where little destabilization is caused per modification (average  $\Delta T_M \sim -1.4$  °C/modification).<sup>178,179</sup>

#### 4.4. Biocompatible Triazole Linkage

**4.4.1. Pursuing the Biocompatibility of the Click Backbone.** As described above, triazoles have outstanding chemical properties that render these linkages interesting analogues of the phosphodiester backbone. This analogy raises



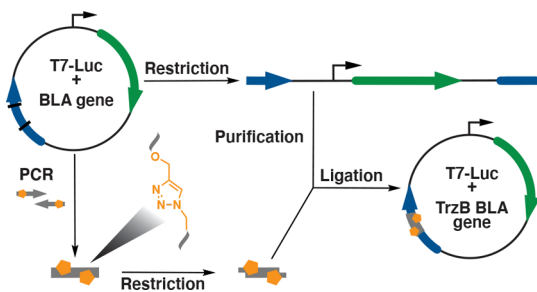


**Figure 25.** Triazole B is inserted into the BLA gene (blue) of plasmid DNA followed by transformation and growth of *E. coli*. The insert is gray, and the triazole linkages are orange.<sup>24</sup>

nucleotide excision repair (NER) mechanism. This result excludes any DNA repair mechanism that might lead to substitution of the triazole by a canonical phosphodiester linkage and further supports the triazole biocompatibility in the delicate metabolic balance of living organisms.<sup>24</sup>

Interestingly, **Trz B** is an effective phosphodiester surrogate also when used to generate clicked DNA templates for RNA transcription.<sup>181</sup> In this work, *in vitro* RNA synthesis was carried out using T7 RNA polymerase (T7-RNAP)—an enzyme commonly used in biotechnology to produce small RNAs and in expression of cloned genes. Two templates transcribing the 54-mer DicF sequence—an *E. coli* growth inhibitor—were designed and synthesized to include **Trz B** either at the +4/5 position of the essential T7 promoter locus or within the coding sequence (CDS) of the gene. In the former case, no RNA product was obtained due to a possible disruption of the required DNA–protein complex caused by the triazole. In contrast, the clicked CDS analogue yielded ~80% of RNA compared to a native DNA control, and accurate transcription was confirmed by mass spectrometry.<sup>181</sup> This was the first report of RNA transcription from a purely synthetic DNA analogue that included an artificial backbone linkage.

To exclude any influence of selective pressure on *E. coli* transfected with the modified BLA gene, the biocompatibility of **Trz B** was re-evaluated on a nonessential gene encoding for the red-fluorescent protein mCherry.<sup>27</sup> Errors in replication or transcription of the **Trz B**-BLA gene can result in an inactive  $\beta$ -lactamase variant. Hence, the host organisms with the

improper gene are suppressed on ampicillin containing media. The mCherry coding region was therefore modified with two triazole linkers introduced 4-bp apart to investigate also the effect of proximity on biocompatibility. The modified mCherry gene was faithfully and efficiently expressed in *E. coli* colonies thus eliminating the possibility of selective pressure in this system.<sup>27</sup> Interestingly, expression of triazole modified mCherry was observed also upon transfection in the more metabolically complex context of eukaryotic cells. Here, single cell analysis of fluorescent protein expression identified correct transcription and translation of the gene in human MCF-7 breast cancer cells.<sup>182</sup>

Following the above discoveries, a 335 base pair gene encoding the *iLOV* green fluorescent protein was synthesized using a one-pot click ligation strategy from 10 oligonucleotides modified at the 5'- and 3'-ends with azide and alkyne groups, respectively (Figure 26).<sup>183</sup> The resulting *click-iLOV* gene had eight **Trz B** modifications and similar structure to the natural gene—the melting temperature was only 3 °C lower than the unmodified control. Although qPCR analysis showed that strand extension is slowed down at the modification sites, the multiple triazoles were correctly read-through by *Taq* DNA polymerase. Expression of the *click-iLOV* was faithful also when the plasmid incorporating the gene was transfected into *E. coli*. Interestingly, the genes replicated from the *click-iLOV* template had in this case a lower amount of genetic mutations compared to a natural analogue produced by enzymatic ligation of 10 canonical oligonucleotides. This is probably due to a higher synthetic purity of the starting oligonucleotides. All the above results emphasize the possibility of an alternative chemical approach to gene synthesis with applications in synthetic biology and industrial biotechnology.

**4.4.3. Biocompatibility of Triazole-Modified RNA.** The remarkable compatibility of the triazole backbone with DNA polymerases encouraged investigations in the RNA context. Two RNA templates were prepared with an internal dC<sup>Me</sup>-triazole-U linkage (dC<sup>Me</sup>tU, dC<sup>Me</sup> = 5-methyl-2'-deoxycytidine) prepared by CuAAC, and a SPAAC modification made by coupling 5'-BCN oligonucleotides with 2'-azide oligonucleotides. Three different sets of primers were designed so that reverse transcription was initiated either before, next to, or after (bridged-primer) the triazole linkage. Reverse tran-

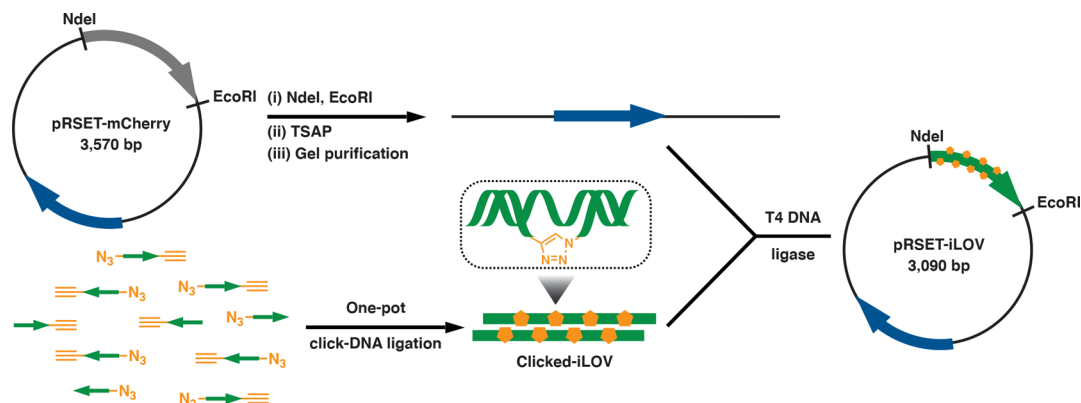


**Figure 26.** ILOV gene was assembled using templated CuAAC ligation from alkyne/azide oligonucleotides; a plasmid vector (pRSET-mCherry) was cleaved with *NdeI* and *EcoRI* restriction nucleases to remove the mCherry gene (encoding for a red fluorescent protein). The sticky ends of the linearized plasmid and artificial gene were then ligated using T4 DNA ligase to form the pRSET-iLOV plasmid (encoding for a green fluorescent protein).<sup>183</sup>

scription of the two modified templates—dC<sup>Me</sup>tU or clicked-BCN—by M-MLV RT (Moloney Murine Leukemia Virus reverse transcriptase) was successful when initiated before or next to the triazole. However, in both cases one nucleotide was omitted. Conversely when bridged primers were used on the SPAAC-clicked template, transcription was complete only if the duplex formed with the primer was stabilized (*i.e.* by changing the buffer salt from Mg<sup>2+</sup> to Mn<sup>2+</sup>). This result suggests that it is easier for M-MLV to read-through the SPAAC modification when it has a “running start” from a strand of unmodified RNA than to start on top of the bulky BCN linker.<sup>184</sup>

#### 4.4.4. Biophysical Analysis of the Triazole Linkage

**Trz B.** The geometry and charge of the triazole linkage significantly differ from those of the canonical nucleic acid phosphodiester backbone, and a deep analysis of the biophysical properties of the two backbones is essential to understand the basis of the triazole biocompatibility with the polymerase machinery. The X-ray structure of Taq polymerase bound to DNA provided a useful guide, showing that 12 nucleotides interacts with the enzyme mainly through hydrogen bonding with the phosphodiester backbone.<sup>185</sup> Substituting one of the phosphates with a triazole linkage would prevent only one or two of these interactions and might explain the ability of polymerases to correctly read through triazoles during PCR amplification. Nuclear magnetic resonance analysis of a 13 bp dsDNA including one unit of **Trz B** afforded further insights showing that, in comparison to a natural backbone, the triazole induced local structural changes without affecting the B-DNA duplex and Watson–Crick base pairing (Figure 27). In addition, some similarities

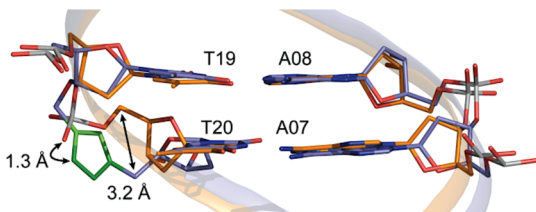


**Figure 27.** Close-up showing the overlaid average structures of a duplex containing the triazole (in purple 13merTAL, PDB: 2L8I) and an unmodified DNA duplex (in orange 13merRef, PDB: 2KUZ). The triazole modification is highlighted in green (Adapted with permission from ref 176. Copyright 2011, John Wiley & Sons).<sup>176</sup>

are evident between the two backbones in that the large dipole moment of the N(3)-atom together with its location in a similar position to one of the phosphate-branching oxygen atoms makes it a suitable hydrogen bond acceptor for DNA polymerase.<sup>176,186</sup> As a proof of concept, a methylated (N(3)-blocked) **Trz B** derivative was used as a template for PCR amplification. In this case, polymerase readthrough of the N(3)-cationic triazole was slowed down and the yield of PCR amplicons was severely reduced compared to the neutral **Trz B** template. This contrasting behavior suggests an electrostatic repulsion with the positively charged amino-acidic side chains in the polymerase–DNA template recognition site.

The presence of **Trz B** increases the opening rates of the flanking base pairs compared to a natural duplex and causes a destabilization of the four neighboring base-pairs. The Gibbs free-energy for the dissociation of the two adjoining base-pairs was diminished by 11 kJ mol<sup>-1</sup> in total with a stronger

perturbation on the 5'-side (7.2 kJ mol<sup>-1</sup>) than on the 3'-side (3.4 kJ mol<sup>-1</sup>). Nonetheless, the triazole linkage fits within the canonical B-DNA helical structure and induces only minor distortion to the major and minor grooves.<sup>176</sup>

As described above (*cf.* section 4.2.2), DNA duplexes made with the **Trz B** modified strand are slightly destabilized ( $\Delta T_M = -8$  °C) by the modification. Interestingly, the presence of one mismatched site at the triazole lowered the duplex melting temperature by  $-10.9$  °C on average, closely resembling the loss in stability ( $-11.6$  °C) in the unmodified control. However, the combination of the triazole linkage with the mismatched site generated a more significant decrease in hyperchromicity for the modified duplex than for the native control (18.8% versus 7.5%, respectively) indicating a greater loss of base stacking caused by **Trz B**.<sup>176</sup> This suggests a replication model where only correct dNTPs are selected and incorporated by the template–polymerase complex to form the desired base paired dsDNA. Triazoles in this case might introduce a further advantage compared to the canonical phosphate backbone. The significant duplex destabilization caused by incorporation of mismatched dNTPs near **Trz B** exposes the rogue nucleotides to the proofreading action of DNA polymerases and promotes their removal by the 3'-exonuclease domain of the polymerase enzyme.

#### 4.5. Antisense Oligonucleotides by Click-Chemistry

Antisense oligonucleotides (ASOs) are short nucleic acids that bind to specific mRNA sequences or other cellular RNAs, modulating gene expression by affecting translation. The sequence-specificity of ASOs renders them particularly interesting in the therapeutic field where targeted activity is essential to selectively inhibit genes, to prevent toxic side-effects and to develop personalized drugs. Although several ASOs have been recently approved by the FDA for the treatment of various genetic diseases,<sup>187–189</sup> advancement of the field is limited by the difficult and inefficient delivery of oligonucleotides to targeted tissues, unknown long-term toxicities, and *off-target* effects of oligonucleotides. Modification of the sugar–phosphate backbone or nucleobases can improve the therapeutic properties of ASOs, and in this context, triazoles are interesting candidates for antisense technologies. They increase stability toward nuclease degradation and reduce the anionic charge of oligonucleotides, potentially aiding cellular uptake. However, triazole modifications alone usually destabilize duplex structures representing a potential limitation to sequence-specific RNA targeting and binding. To understand how triazole linkages affect the hybridization properties of oligonucleotides, 1,4-triazoles (**Trz B–D**) together with a 1,5-adduct (Triazole E, **Trz E**) formed by the RuAAC reaction have recently been studied for their capability to form double helices with complementary DNA and RNA strands. 1,5-Triazole modified backbones are one bond shorter than the 1,4-analogues placing the substituents 3.2 Å apart (instead of 4.9 Å) with the same bond spacing as the thermally stable **Trz D**. Duplexes with the 6-bond spacers 1,4-triazole **Trz D** and 1,5-triazole **Trz E** (Figure 28) were the least destabilized structures, displaying a UV thermal melting value close to the unmodified helix (for DNA  $\Delta T_M = -3.2$  °C and  $-2.9$  °C, respectively; for RNA  $\Delta T_M = -0.8$  °C and  $-3.3$  °C, respectively). Among the triazoles, the 1,4-**Trz D** was the best at adopting the A-conformation required for RNA recognition and is therefore a good candidate for use in antisense oligonucleotides.

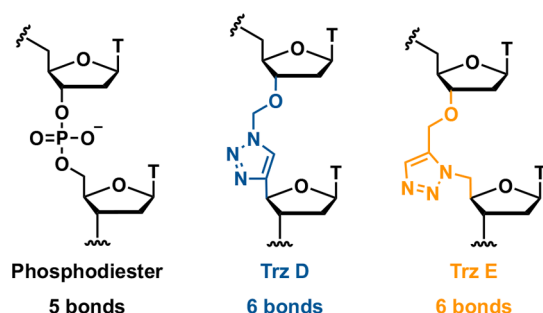


**Figure 28.** Canonical phosphodiester linkage beside the 1,4-disubstituted triazole D (Trz D) and the 1,5-disubstituted triazole E (Trz E).

To strengthen base pairing around the click modification, the aminoethylphenoxazine nucleobase (G-clamp, **132**) can be introduced at the 3'-side of the triazole (Figure 29). G-

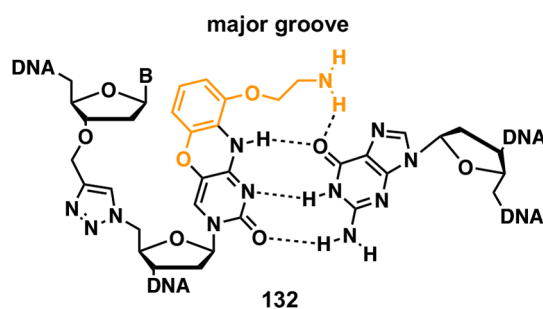


**Figure 29.** Structure of the triazole G-clamp base paired with guanine in complementary DNA. The additional steric bulk of the nucleobase derivative of cytosine is highlighted in orange.<sup>177</sup>

clamp mimics the guanine binding mode of cytosine but provides higher pairing stability through an extra hydrogen bond and enhances base stacking. UV melting analysis on various DNA:DNA and DNA:RNA duplexes, including both G-clamp and the triazole modification, showed that the stability of the duplex was increased beyond that of the native control. Interestingly the introduction of a mismatch at or near the modification strongly destabilized the duplex making this backbone/nucleobase combination a potent mismatch sensor.<sup>177</sup>

As an alternative to G-clamp, the sugar moiety of the DNA backbone adjacent to triazoles has been modified with ribose analogues such as morpholino<sup>190</sup> and conformationally restricted locked nucleic acids (LNA) (Figure 30).<sup>191–193</sup> The advantage of this strategy lies in its independence with

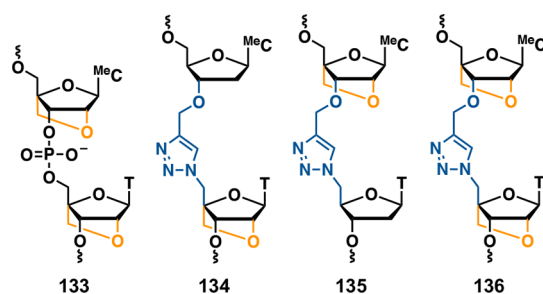


**Figure 30.** Structures of phosphodiester and triazole linked LNA backbones analyzed for DNA and RNA binding.<sup>191</sup>

respect to the nature of the neighboring nucleobases; it broadens stabilization to encompass all sequence contexts. Triazole-linked morpholino ODNs were shown to bind RNA targets with slightly enhanced stability compared to strands incorporating only the triazole modification but lower affinity in comparison to the native control.<sup>190</sup> Alternatively, inclusion of an LNA sugar modification at the 3'-side of the triazole (**134**) considerably strengthens oligonucleotide binding and one or two of these linkages were sufficient to provide DNA:RNA duplexes with stability close to that of an unmodified control. The affinity arises from the constraint that LNA imposes on the nucleic acid backbone, locking the sugar pucker in the 3'-endo conformation and inducing the A-form helical structure required in DNA:RNA duplexes. Positioning LNA on the 5'-side does not afford the same stabilizing effect (**135**), suggesting that the reduced backbone flexibility originates only when LNA is directly attached to a phosphodiester group and not to a nonoptimal triazole linkage.<sup>191</sup> Significantly, DNA strands containing both G-clamp and LNA modifications in combination with triazole were successfully read-through (replicated) by polymerase enzymes to produce complementary unmodified DNA. Therefore, the biocompatibility of these modifications also provides a potential solution in PCR where duplex stability might be necessary for correct DNA amplification by polymerases lacking 3'-exonuclease activity.

#### 4.6. Split and Click Approach to Single-Guide RNA Generation

Click chemical ligation was recently utilized in the emerging field of CRISPR-Cas (Clustered Regularly Interspaced Palindromic Repeats) gene editing, to generate pools of single guide RNAs (sgRNAs). CRISPR-Cas is the leading technology in the field of genome editing and allows genomic manipulation and modification with single-nucleotide precision.<sup>194</sup> CRISPR systems comprise a sgRNA that recognizes and binds to specific DNA sequences, programming and directing the cleaving action of the Cas (CRISPR associated protein) enzyme.<sup>195</sup> Since its discovery in 2012—made by Emmanuelle Charpentier and Jennifer Doudna, who shared the Nobel prize in 2020—CRISPR-Cas has been the subject of intensive study which often requires production of large sgRNA libraries. However, the enzymatic production of RNA is limited in scope and is not suitable for the production of the kind of complex chemically modified RNA that is increasingly used in CRISPR gene editing and related CRISPR applications. Ligation of short chemically synthesized RNA strands by CuAAC coupling was instead shown to offer a valid and efficient strategy for the generation of large, chemically modified RNA constructs (e.g. ribozymes).<sup>21</sup>

In an effort to simplify sgRNA production, Smith and co-workers prepared a bimolecular guide RNA system by conjugating a 5'-hexyne tracrRNA (65-mer) to a 3'-azide crRNA component (34-mer) using CuAAC chemistry (Figure 31A and B).<sup>196</sup> The new triazole linked sgRNA (**137**) had an additional 20-atom spacer replacing the phosphate linkage, and the modification was placed at the loop structure of the upper stem (Figure 31A)—suggested to be nonessential for CRISPR-Cas9 activity. The same loop was modified also by Brown and co-workers with triazole linkages of various length. In this work, a 37-mer crRNA and a 66-mer tracrRNA were conjugated to form the sgRNA construct either by SPAAC or CuAAC reaction (Figure 31C, **138–141**).<sup>197</sup> Independently

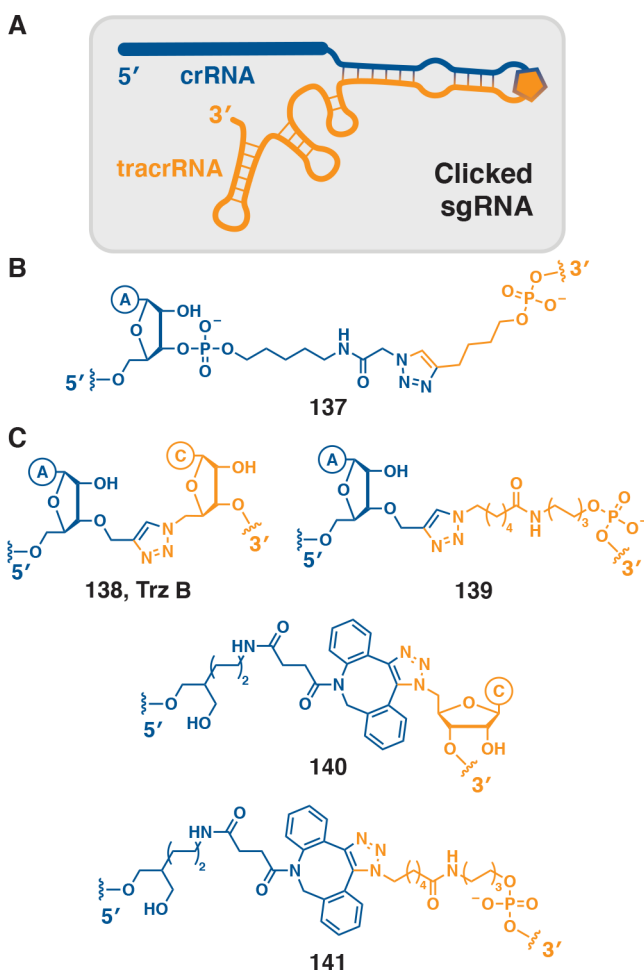


**Figure 31.** A 3'-azide (or alkyne) modified crRNA and a 5'-alkyne (or azide) modified Cas9-binding RNA are clicked together at the upper stem to generate a chemically ligated sgRNA construct (A) where a natural phosphate linkage is substituted by the triazole. (B) Type of triazole linkage used by Smith and co-workers.<sup>196</sup> Type of triazole linkages used by Brown and co-workers.<sup>197</sup>

from the spacer length and bulk, in both sgRNA designs gene editing in cells was efficient and comparable to a natural dual crRNA/tracrRNA system.<sup>196,197</sup> The similar result from the two researches is a further proof that the upper stem loop is a suitable position to host chemical modifications.

In a different approach, Brown and co-workers modified the sgRNA close to the protospacer adjacent motif (PAM) (Figure 32) by conjugating 5'-azide-modified 79mer tracrRNAs to a 20mer crRNA oligonucleotide functionalized with either a 3'-propargyl group (138) or a 5'-C6-NH<sub>2</sub> and 3'-serinol-alkyne (142). In addition, valuable sugar modifications—such as 2'-OMe groups or chimeric deoxyribonucleotide units—were incorporated to improve the yield during oligonucleotide solid-phase synthesis.<sup>197</sup> Although all sgRNAs with the biocompatible TrzB linkage directed gene editing *in vitro* with efficiencies comparable to *in vitro* transcribed (IVT) sgRNA, the sgRNA construct with the long linker (142) significantly impaired Cas9-mediated cleavage of DNA. This result further demonstrates the importance of the biocompatible TrzB linkage at positions close to the PAM site. *In cellulo*, the hybrid guides formed by chimeric RNA-DNA completely inhibited gene editing. In this case the difference from the *in vitro* result was attributed to RNase H nuclease activity that, in

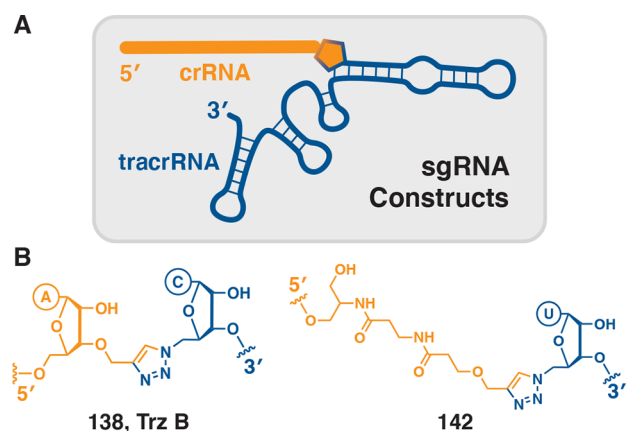


**Figure 32.** (A) 3'-Alkyne modified variable RNA (20mer) and a 5'-azide modified Cas9-binding RNA (79mer) are clicked together at the PAM site to make the chemically ligated sgRNA construct. (B) Structures of the artificial linkages used to conjugate the two RNA strands.<sup>197</sup>

cells, might induce cleavage of the RNA strand in the sgRNA-DNA construct.<sup>197</sup> These modular split-and-click approaches reduce the synthetic burden of sgRNA production and allow the potential screening of numerous, short crRNAs. In this way pools of sgRNAs can be quickly generated by chemical conjugation of variable DNA-targeting RNAs—prepared on demand—to an invariant Cas9-binding RNA domain made cost-effectively on large scale.

#### 4.7. Nanomaterials

The highly selective assembly properties and addressability of DNA make it an invaluable substrate for the development of nanomaterials and nanotechnologies. The base-pairing recognition together with the backbone flexibility of nucleic acids allowed nanostructures of great diversity and complexity to be built for various applications (e.g., DNA origami, crystalline arrays, aptamers, nanomechanical devices, etc.).<sup>198</sup> However, assembly and stability of these nanoarrays depend on precise hydrogen-bonding as well as base stacking, and the non-covalent interactions make the system thermodynamically fragile unless they are stored in controlled buffers at ambient temperature. The purification of complex nanostructures can therefore be a complicated or even impossible task and might limit the use of these constructs. A click-fixation technology based on CuAAC chemistry was shown to solve the problem allowing stable DNA nanoarrays to be produced and subsequently purified under denaturing conditions.<sup>31</sup> Using this strategy much larger DNA nanoscaffolds can be built in a hierarchical manner.

Besides DNA duplexes, the CuAAC reaction was used to assemble other nucleic acid tertiary structures such as triplexes and quadruplexes. Triplex recognition elements have been used in nanotechnology as external stimuli that control the chemical reactivity in DNA-directed reactions. Efficient double click reactions in the presence of triplex specific binders (i.e., naphthylquinoline) allowed three-way branched nonsymmetrical DNA nanostructures to be made.<sup>199</sup> In addition, click chemistry was used to trap conformational isomers of G-quadruplexes (Figure 33). In this strategy the oligonucleotide termini of the four-stranded structure were clicked together trapping the G-quadruplex structure and enabling its direct identification in a complex solution.

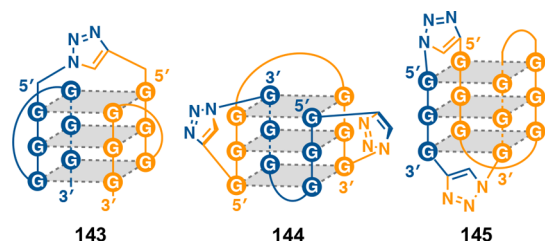


**Figure 33.** Conformational isomers of G-quadruplexes trapped by click chemistry.<sup>200</sup>

The click approach demonstrated that G-quadruplexes can be formed by various human telomeric DNA and RNA sequences.<sup>200</sup> To efficiently cross-link strands of DNA, Seela and co-workers developed a template-free technique where two oligonucleotide strands were clicked onto a bifunctional azide linker (Figure 34A).<sup>201,202</sup> The so-called “bis-click”

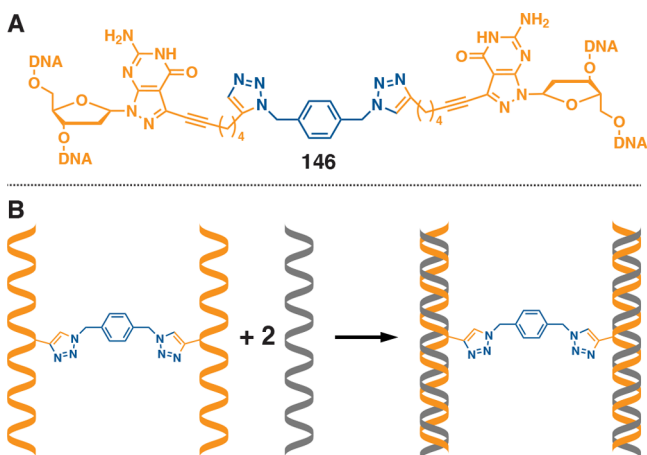


**Figure 34.** Bis-click strategy where an interstrand click cross-linker (A) was used by Seela and co-workers to generate a four-stranded DNA structure consisting of two cross-linked duplexes (B).<sup>201</sup>

protocol can be applied to generate single-stranded DNA, duplexes, and multistranded structures.<sup>31,201–204</sup> As an example, hybridization of a bis-click construct with the complementary strands yielded a four-stranded DNA structure consisting of two cross-linked duplexes (Figure 34B).<sup>201</sup>

#### 4.8. Cyclic DNA

Click chemistry has been used to synthesize small cyclic DNA scaffolds for applications in drug–DNA binding analysis and as potential therapeutics. The 5′-alkyne and the 3′-azide group of hairpin oligonucleotides—where the hairpin has a hexaethylene glycol loop—were coupled using the CuAAC reaction to form an artificial mini-duplex structure (Figure 35).<sup>20</sup> From UV melting analysis the artificial duplex had very high thermodynamic stability and the presence of stable base pairing was shown by an NMR study of a cyclic GC dinucleotide. Conversely, a single base pair duplex failed to form interbase hydrogen bonds probably due to the absence of stabilization by base stacking. Mini-duplexes are very informative in studies on DNA–drug interaction. The binding of a novel threading intercalator was explained using a click-ligated cyclic duplex with both ends sealed to prevent entry of the molecule from the mini-duplex termini.<sup>205</sup>

Cyclic mini-duplexes have also been studied as potential therapeutic agents as they benefit from superior resistance to

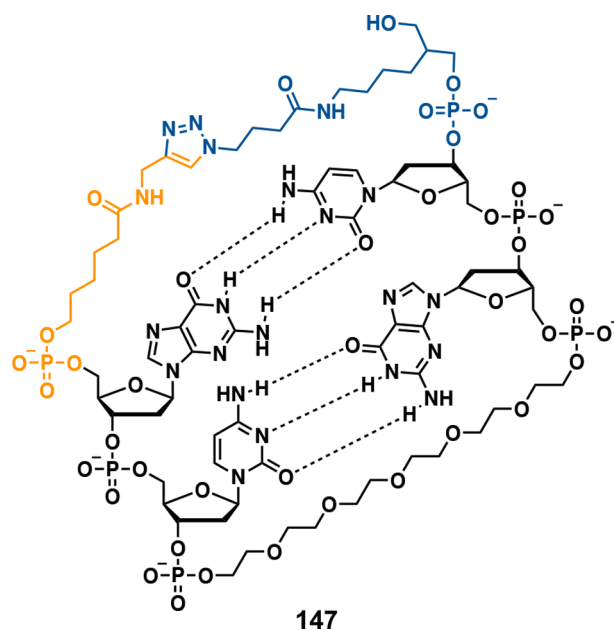


**Figure 35.** Chemical structure of a stable cyclic GC/GC dinucleotide mini-duplex.

nucleases, high thermal stability, and a small-size that might aid cell penetration when compared to canonical duplexes. Within the cell these constructs can behave as decoys that target the DNA binding site of cellular transcription factors.<sup>206</sup> Cyclic dumbbell oligonucleotides—synthesized by CuAAC coupling of the hairpin loops—were able to bind to the nuclear factor (NF)-κB p50 homodimer similar to the unmodified control decoy. The binding affinity of the dumbbell oligonucleotide was directly dependent on the number of thymidine residues constituting the loop region, and the triazole structure did not prevent the cyclic duplex from binding to the nuclear transcription factor. In addition, the constructs had high melting temperatures and were resistant to degradation by DNase enzymes, exemplified by snake venom phosphodiesterase.<sup>207</sup>

Smaller cyclic DNA structures such as cyclic dinucleotides also have therapeutical relevance in that they can control various biological pathways such as signal transduction, biofilm formation, or quorum sensing.<sup>208,209</sup> 2′3′-cGAMP is an uncanonical cyclic dinucleotide—produced by a cGAS cyclase—where an adenosine and a guanosine are connected via a 3′-5′ and a unique 2′-5′ linkage. cGAMP activates stimulator of interferon gene (STING) proteins, a potent pathway of innate immunity in eukaryotic organisms. Recently, a cGAMP derivative with the 3′-5′ linkage substituted by a triazole was synthesized with the aim of developing an efficient cell-penetrating and immune-regulatory pharmaceutical agent. The clicked analogue has a more open conformation than the natural active dinucleotide as the two nucleobases are not parallel to each other. This open structure compromised the binding affinity of the compound, and no interaction with the STING proteins was detected. Despite the negative result, the authors suggested that the clicked-cGAMP might have a more favorable interaction with cyclase cGAS.<sup>210</sup>

Finally, the CuAAC reaction has also been applied to the formation of large dsDNA catenanes by conjugation of two complementary oligonucleotides (Figure 36). The catenane

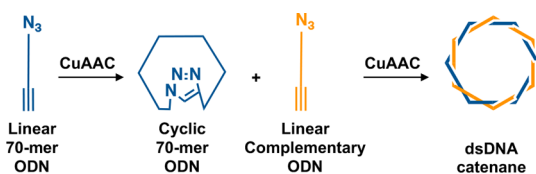


**Figure 36.** Generation of a dsDNA catenane by the templated click ligation of a linear ODN on a complementary cyclic oligonucleotide.<sup>18</sup>

was made of six helical turns, each one consisting of 10 base pairs flanked by T-T mismatches. The base mismatches were used as hinges that allow the duplex to be flexible and adopt a cyclic structure. The macrostructure was synthesized through a stepwise process from two strands labeled with a 5'-alkyne and a 3'-azide. The first oligonucleotide was cyclized using nontemplated CuAAC chemistry and was used as a template for the click ligation and cyclization of the second oligonucleotide.<sup>18</sup>

## 5. CONCLUSIONS

The azide alkyne cycloaddition is the flagship among click chemistry conversions due to its modularity, wide applicability, and compatibility with various synthetic conditions and reacting substrates. The introduction of metal catalysts such as copper (CuAAC)<sup>4,44</sup> and ruthenium (RuAAC)<sup>34</sup> overcomes the limitations of the Huisgen reaction, increasing coupling speed and yielding regiospecific products. A metal-free variant—the strain-promoted azide alkyne cycloaddition (SPAAC)—was developed by Bertozzi and co-workers through careful design and modification of the alkyne group.<sup>13</sup> Here, the cycloaddition is promoted by the ring strain and the absence of metal catalysis broadens the application of AAC also to cellular systems where metals might interfere with the viability of the organism.

This progress in click-chemistry methodology has positively impacted on several research areas; in recent years, it has been widely used within the fields of biology, biochemistry, and biotechnology. The potential and versatility of AAC chemistry is particularly evident when this reaction is applied to nucleic acids. Click-chemistry with oligonucleotides has recently become a well-established area with a wide range of protocols and useful modifications currently available. The field is also facilitated by the wide commercial availability of modified nucleoside phosphoramidites<sup>100–106</sup> and nucleoside triphosphates<sup>107–113</sup> for solid phase and enzymatic synthesis, respectively. The synthetic routes to introduce azide and alkyne modifications into these monomers are well established and usually involve the following: (i) simple Sonogashira coupling between alkynes and iodo-precursors, (ii) nucleophilic substitution of alkyl halides and mesylates by sodium azide, (iii) incorporation of the reactive group through linkers prior to or during solid phase synthesis, or (iv) metabolic labeling of nucleic acids through inclusion of modified nucleosides by DNA and RNA polymerases. New synthetic pathways are also being developed with the aim of expanding the library of available modifications. In this context, flexible and polar alkynes are attracting interest as they are more easily recognized by DNA polymerases and are capable of faster cycloaddition reaction rates.<sup>128</sup>

All this has enabled the development of a wide variety of nucleic acid-based tools and techniques. Among these, AAC labeling of oligonucleotides with fluorophores remains a major

application due to its impact in the fields of DNA sequencing, genomics, and forensic and genetic analysis. Click chemistry has also been used to label oligonucleotides with other small-organic compounds that increase the cellular uptake of nucleic acids. It has enabled targeting of reactive inorganic compounds to specific genomic sequences. The application of the AAC reaction has expanded beyond simple labeling of oligonucleotides, and the modularity provided by azide alkyne cycloadditions has been studied as a method for the assembly of nucleic acids for applications in biology and nanotechnology. The efficiency and ability to template triazole formation using the base pair recognition provided by nucleic acids has facilitated the ligation of DNA strands allowing long sequences to be assembled using purely synthetic chemistry methods. Careful design and analysis of the triazole linkage as a phosphate backbone surrogate in the context of DNA replication has shown that the click modification is successfully recognized and read-through by polymerase machinery both *in vitro* and in cells.<sup>180</sup> This constitutes a competitive strategy for the chemical synthesis of stretches of genomic DNA, particularly those containing modified and epigenetic bases. The genes assembled with this approach are functional in both prokaryotic and eukaryotic systems.<sup>182,183</sup> In addition, click-ligation of oligonucleotides is a potent tool to generate antisense oligonucleotides. In this context the presence of the triazole increases oligonucleotide stability toward nuclease degradation and reduces the anionic charge of oligonucleotides, possibly aiding cellular uptake. Chemical synthesis and click ligation of ASOs has been used to introduce base modifications and nucleoside derivatives (*i.e.* locked nucleic acids, G-clamp) that enhance target binding and mismatch sensitivity. Applications of click chemistry in the highly topical and biologically important field of CRISPR-Cas gene editing has been explored for the fast and high-throughput generation of libraries of single guide RNAs. Here a split and click approach was used to conjugate different variable crRNA to a constant tracrRNA sequence by triazole formation.<sup>197</sup>

The wide variety of applications discussed in this review demonstrates the huge impact that azide–alkyne cycloadditions have made in the nucleic acid field. Future advancements in click chemistry with nucleic acids are anticipated to involve in-depth studies on modified CRISPR/Cas systems for gene editing and the development of new artificial nucleic acid analogues. Chemical ligation of oligonucleotides by click chemistry has many potential applications as it can be used to synthesize large DNA or RNA constructs that contain highly modified artificial sugars, bases, and backbone linkages. Unlike enzymatic nucleic acid ligation, click ligation is not inhibited by extreme modifications. Furthermore, it is scalable, and it can be used to generate large quantities of linear and cyclic oligonucleotide analogues compatible with emerging therapeutic applications. This is particularly exciting as oligonucleotide therapeutics promise to deliver entirely new classes of medicines for “hard to treat” diseases. Such constructs will also have important uses in biotechnology, nanotechnology, and materials chemistry.

## AUTHOR INFORMATION

## Corresponding Author

**Tom Brown** – Department of Chemistry, University of Oxford, Oxford OX1 3TA, U.K.; [orcid.org/0000-0002-6538-3036](https://orcid.org/0000-0002-6538-3036); Email: [tom.brown@chem.ox.ac.uk](mailto:tom.brown@chem.ox.ac.uk)

## Authors

**Nicolò Zuin Fantoni** – Department of Chemistry, University of Oxford, Oxford OX1 3TA, U.K.; [orcid.org/0000-0003-3161-0656](https://orcid.org/0000-0003-3161-0656)

**Afaf H. El-Sagheer** – Department of Chemistry, University of Oxford, Oxford OX1 3TA, U.K.; Chemistry Branch, Department of Science and Mathematics, Faculty of Petroleum and Mining Engineering, Suez University, Suez 43721, Egypt; [orcid.org/0000-0001-8706-1292](https://orcid.org/0000-0001-8706-1292)

Complete contact information is available at:  
<https://pubs.acs.org/10.1021/acs.chemrev.0c00928>

## Notes

The authors declare no competing financial interest.

## Biographies

Nicolò Zuin Fantoni was born in Padova, Italy. Nicolò studied chemistry at the University of Padova receiving his MSc degree in 2014 for work in bioinorganic chemistry. In 2015, Nicolò joined the Kellett group at Dublin City University (DCU) as a Marie Curie Ph.D. student within the ClickGene ITN project. Here, he worked on developing copper–polypyridyl complexes as stabilized artificial metallo nucleases (AMN) and linking them to triplex forming oligonucleotides by CuAAC and SPAAC reactions. In 2019 Nicolò joined the Brown group at the University of Oxford where he is working on the biocompatible triazole linkage.

Afaf H. El-Sagheer is a Professor of Bioorganic/Nucleic Acid Chemistry at Suez University—currently on long sabbatical—and research fellow at Oxford University. Afaf studied chemistry at Suez Canal University (Egypt) and did her Ph.D. at Southampton University with Professor John Mellor and then moved back to Egypt to become a lecturer. She was promoted to associate Professor in 2009 and then Professor in 2014 at Suez University. Afaf is on a long term sabbatical working at the chemistry department in Oxford on the use of click chemistry to assemble novel long modified biocompatible DNA and RNA constructs for gene synthesis and on new methods of DNA synthesis and their applications in biology and medicine (diagnostics and therapeutics). Some of the reagents she developed are commercially available. Afaf has more than 150 publications in high impact factor journals in addition to several patents and book chapters. She has been invited to give talks at scientific meetings in UK, Europe, USA, and China.

Tom Brown is Professor of Nucleic Acid Chemistry in the Departments of Chemistry and Oncology at Oxford University. His research interests center on oligonucleotide synthesis and applications of oligonucleotide chemistry in biology and medicine (diagnostics and therapeutics). He is coinventor of several technologies for genetic analysis and cofounder of three Biotech companies including ATDBio (synthesis of modified oligonucleotides). He has published over 400 research papers and many patents. Awards including the Royal Society of Chemistry (RSC) Josef Loschmidt prize, the RSC award for Nucleic Acid Chemistry, the RSC prize for Interdisciplinary Research, Chemistry World entrepreneur of the year for 2014, and UK BBSRC research council Innovator of the Year for 2016. He was also presented with a lifetime

award for external engagement and promoting impact by Oxford University. Tom is a Fellow of the Royal Society of Edinburgh and a Fellow of the Royal Society of Chemistry. He is former President of the Chemistry Biology Interface Division of the RSC, Editor-in-Chief of the RSC Book series on Chemical Biology, and was co-Chair of the 2018 EuCheMS congress in Liverpool, UK. He is currently Associate Head of the Chemistry Department at Oxford University with responsibility for Research.

## ACKNOWLEDGMENTS

This work was supported by UK BBSRC grant BB/R008655/1 (New and versatile chemical approaches for the synthesis of mRNA and tRNA).

## ABBREVIATIONS

Acac	acetylacetate
OAc	acetate
BCN	bicyclo[6.1.0]nonyne
CuAAC	copper catalyzed azide alkyne cycloaddition
CRISPR	clustered regularly interspaced short palindromic repeats
DIBO	dibenzocyclooctyne
dNTP	deoxynucleoside triphosphate
dU <sup>c</sup>	5-ethynyl-dU
dU <sup>o</sup>	5-octadynyl-dU
FAM	6-carboxyfluorescein
ODN	oligonucleotide
RuAAC	ruthenium catalyzed azide alkyne cycloaddition
SPAAC	strain promoted azide alkyne cycloaddition

## REFERENCES

- (1) Kolb, H. C.; Finn, M. G.; Sharpless, K. B. Click Chemistry: Diverse Chemical Function from a Few Good Reactions. *Angew. Chem., Int. Ed.* **2001**, *40*, 2004–2021.
- (2) Huisgen, R. 1,3-Dipolar Cycloadditions. Past and Future. *Angew. Chem., Int. Ed. Engl.* **1963**, *2*, 565–598.
- (3) Tornøe, C. W.; Christensen, C.; Meldal, M. Peptidotriazoles on Solid Phase: [1,2,3]-Triazoles by Regiospecific Copper(I)-Catalyzed 1,3-Dipolar Cycloadditions of Terminal Alkynes to Azides. *J. Org. Chem.* **2002**, *67*, 3057–3064.
- (4) Rostovtsev, V. V.; Green, L. G.; Fokin, V. V.; Sharpless, K. B. A Stepwise Huisgen Cycloaddition Process: Copper(I)-Catalyzed Regioselective “Ligation” of Azides and Terminal Alkynes. *Angew. Chem., Int. Ed.* **2002**, *41*, 2596–2599.
- (5) Pickens, C. J.; Johnson, S. N.; Pressnall, M. M.; Leon, M. A.; Berkland, C. J. Practical Considerations, Challenges, and Limitations of Bioconjugation via Azide-Alkyne Cycloaddition. *Bioconjugate Chem.* **2018**, *29*, 686–701.
- (6) Thirumurugan, P.; Matosiuk, D.; Jozwiak, K. Click Chemistry for Drug Development and Diverse Chemical-Biology Applications. *Chem. Rev.* **2013**, *113*, 4905–4979.
- (7) *Click Chemistry: A Universal Ligation Strategy for Biotechnology and Materials Science*; Lahann, J., Ed.; John Wiley & Sons Ltd: Chichester, United Kingdom, 2009.
- (8) Besanceney-Webler, C.; Jiang, H.; Zheng, T. Q.; Feng, L.; del Amo, D. S.; Wang, W.; Klivansky, L. M.; Marlow, F. L.; Liu, Y.; Wu, P. Increasing the Efficacy of Bioorthogonal Click Reactions for Bioconjugation: A Comparative Study. *Angew. Chem., Int. Ed.* **2011**, *50*, 8051–8056.
- (9) Wang, C. L.; Ikhlef, D.; Kahlal, S.; Saillard, J. Y.; Astruc, D. Metal-Catalyzed Azide-Alkyne “Click” Reactions: Mechanistic Overview and Recent Trends. *Coord. Chem. Rev.* **2016**, *316*, 1–20.
- (10) Agard, N. J.; Prescher, J. A.; Bertozzi, C. R. A Strain-Promoted [3 + 2] Azide-Alkyne Cycloaddition for Covalent Modification of

Biomolecules in Living Systems. *J. Am. Chem. Soc.* **2004**, *126*, 15046–15047.

(11) Ramil, C. P.; Lin, Q. Bioorthogonal Chemistry: Strategies and Recent Developments. *Chem. Commun.* **2013**, *49*, 11007–11022.

(12) Agard, N. J.; Baskin, J. M.; Prescher, J. A.; Lo, A.; Bertozzi, C. R. A Comparative Study of Bioorthogonal Reactions with Azides. *ACS Chem. Biol.* **2006**, *1*, 644–648.

(13) Jewett, J. C.; Bertozzi, C. R. Cu-Free Click Cycloaddition Reactions in Chemical Biology. *Chem. Soc. Rev.* **2010**, *39*, 1272–1279.

(14) Merkel, M.; Peewasan, K.; Arndt, S.; Ploschik, D.; Wagenknecht, H. A. Copper-Free Postsynthetic Labeling of Nucleic Acids by Means of Bioorthogonal Reactions. *ChemBioChem* **2015**, *16*, 1541–1553.

(15) El-Sagheer, A. H.; Brown, T. Click Chemistry - a Versatile Method for Nucleic Acid Labelling, Cyclisation and Ligation. In *DNA Conjugates and Sensors*; Fox, K. R., Brown, T., Eds.; Royal Society of Chemistry: Cambridge, United Kingdom, 2012; pp 119–139.

(16) El-Sagheer, A. H.; Brown, T. Click chemistry with DNA. *Chem. Soc. Rev.* **2010**, *39*, 1388–1405.

(17) Gierlich, J.; Burley, G. A.; Gramlich, P. M. E.; Hammond, D. M.; Carell, T. Click Chemistry as a Reliable Method for the High-Density Postsynthetic Functionalization of Alkyne-Modified DNA. *Org. Lett.* **2006**, *8*, 3639–3642.

(18) Kumar, R.; El-Sagheer, A.; Tumpene, J.; Lincoln, P.; Wilhelmsson, L. M.; Brown, T. Template-Directed Oligonucleotide Strand Ligation, Covalent Intramolecular DNA Circularization and Catenation Using Click Chemistry. *J. Am. Chem. Soc.* **2007**, *129*, 6859–6864.

(19) Kocalka, P.; El-Sagheer, A. H.; Brown, T. Rapid and Efficient DNA Strand Cross-Linking by Click Chemistry. *ChemBioChem* **2008**, *9*, 1280–1285.

(20) El-Sagheer, A. H.; Kumar, R.; Findlow, S.; Werner, J. M.; Lane, A. N.; Brown, T. A Very Stable Cyclic DNA Miniduplex with Just Two Base Pairs. *ChemBioChem* **2008**, *9*, 50–52.

(21) El-Sagheer, A. H.; Brown, T. New Strategy for the Synthesis of Chemically Modified RNA Constructs Exemplified by Hairpin and Hammerhead Ribozymes. *Proc. Natl. Acad. Sci. U. S. A.* **2010**, *107*, 15329–15334.

(22) Paredes, E.; Das, S. R. Click Chemistry for Rapid Labeling and Ligation of RNA. *ChemBioChem* **2011**, *12*, 125–131.

(23) Salic, A.; Mitchison, T. J. A Chemical Method for Fast and Sensitive Detection of DNA Synthesis *in Vivo*. *Proc. Natl. Acad. Sci. U. S. A.* **2008**, *105*, 2415–2420.

(24) El-Sagheer, A. H.; Sanzone, A. P.; Gao, R.; Tavassoli, A.; Brown, T. Biocompatible Artificial DNA Linker that is Read Through by DNA Polymerases and is Functional in *Escherichia Coli*. *Proc. Natl. Acad. Sci. U. S. A.* **2011**, *108*, 11338–11343.

(25) Fujino, T.; Yamazaki, N.; Isobe, H. Convergent Synthesis of Oligomers of Triazole-Linked DNA Analogue ((TL)DNA) in Solution Phase. *Tetrahedron Lett.* **2009**, *50*, 4101–4103.

(26) Isobe, H.; Fujino, T.; Yamazaki, N.; Guillot-Nieckowski, M.; Nakamura, E. Triazole-Linked Analogue of Deoxyribonucleic Acid (TLDNA): Design, Synthesis, and Double-Strand Formation with Natural DNA. *Org. Lett.* **2008**, *10*, 3729–3732.

(27) Sanzone, A. P.; El-Sagheer, A. H.; Brown, T.; Tavassoli, A. Assessing the Biocompatibility of Click-Linked DNA in *Escherichia Coli*. *Nucleic Acids Res.* **2012**, *40*, 10567–10575.

(28) Rozkiewicz, D. I.; Gierlich, J.; Burley, G. A.; Gutmiedl, K.; Carell, T.; Ravoo, B. J.; Reinhoudt, D. N. Transfer Printing of DNA by “Click” Chemistry. *ChemBioChem* **2007**, *8*, 1997–2002.

(29) Fischler, M.; Simon, U.; Nir, H.; Eichen, Y.; Burley, G. A.; Gierlich, J.; Gramlich, P. M. E.; Carell, T. Formation of Bimetallic Ag-Au Nanowires by Metallization of Artificial DNA Duplexes. *Small* **2007**, *3*, 1049–1055.

(30) Fischler, M.; Sologubenko, A.; Mayer, J.; Clever, G.; Burley, G.; Gierlich, J.; Carell, T.; Simon, U. Chain-like Assembly of Gold

Nanoparticles on Artificial DNA Templates via ‘Click Chemistry’. *Chem. Commun.* **2008**, *44*, 169–171.

(31) Lundberg, E. P.; El-Sagheer, A. H.; Kocalka, P.; Wilhelmsson, L. M.; Brown, T.; Norden, B. A New Fixation Strategy for Addressable Nano-Network Building Blocks. *Chem. Commun.* **2010**, *46*, 3714–3716.

(32) Lundberg, E. P.; Plesa, C.; Wilhelmsson, L. M.; Lincoln, P.; Brown, T.; Norden, B. Nanofabrication Yields. Hybridization and Click-Fixation of Polycyclic DNA Nanoassemblies. *ACS Nano* **2011**, *5*, 7565–7575.

(33) Hein, J. E.; Fokin, V. V. Copper-Catalyzed Azide-Alkyne Cycloaddition (CuAAC) and Beyond: New Reactivity of Copper(I) Acetylides. *Chem. Soc. Rev.* **2010**, *39*, 1302–1315.

(34) Johansson, J. R.; Beke-Somfai, T.; Said Stalsmeden, A.; Kann, N. Ruthenium-Catalyzed Azide Alkyne Cycloaddition Reaction: Scope, Mechanism, and Applications. *Chem. Rev.* **2016**, *116*, 14726–14768.

(35) Sultana, J.; Sarma, D. Ag-Catalyzed Azide-Alkyne Cycloaddition: Copper Free Approaches for Synthesis of 1,4-Disubstituted 1,2,3-Triazoles. *Catal. Rev.: Sci. Eng.* **2020**, *62*, 96–117.

(36) Smith, C. D.; Greaney, M. F. Zinc Mediated Azide-Alkyne Ligation to 1,5- and 1,4,5-Substituted 1,2,3-Triazoles. *Org. Lett.* **2013**, *15*, 4826–4829.

(37) Himo, F.; Lovell, T.; Hilgraf, R.; Rostovtsev, V. V.; Noodleman, L.; Sharpless, K. B.; Fokin, V. V. Copper(I)-Catalyzed Synthesis of Azoles. DFT Study Predicts Unprecedented Reactivity and Intermediates. *J. Am. Chem. Soc.* **2005**, *127*, 210–216.

(38) Rodionov, V. O.; Fokin, V. V.; Finn, M. G. Mechanism of the Ligand-Free Cu<sup>I</sup>-Catalyzed Azide-Alkyne Cycloaddition Reaction. *Angew. Chem., Int. Ed.* **2005**, *44*, 2210–2215.

(39) Straub, B. F.  $\mu$ -Acetylide and  $\mu$ -Alkenylidene Ligands in “Click” Triazole Syntheses. *Chem. Commun.* **2007**, 3868–3870.

(40) Jin, L.; Tolentino, D. R.; Melaimi, M.; Bertrand, G. Isolation of Bis(Copper) Key Intermediates in Cu-Catalyzed Azide-Alkyne “Click” Reaction. *Sci. Adv.* **2015**, *1*, No. e1500304.

(41) Berg, R.; Straub, B. F. Advancements in the mechanistic understanding of the copper-catalyzed azide-alkyne cycloaddition. *Beilstein J. Org. Chem.* **2013**, *9*, 2715–2750.

(42) Diez-Gonzalez, S.; Nolan, S. P. [(NHC)<sub>2</sub>Cu]X Complexes as Efficient Catalysts for Azide-Alkyne Click Chemistry at Low Catalyst Loadings. *Angew. Chem., Int. Ed.* **2008**, *47*, 8881–8884.

(43) Lipshutz, B. H.; Frieman, B. A.; Tomaso, A. E., Jr. Copper-in-Charcoal (Cu/C): Heterogeneous, Copper-Catalyzed Asymmetric Hydrosilylations. *Angew. Chem., Int. Ed.* **2006**, *45*, 1259–1264.

(44) Meldal, M.; Tornøe, C. W. Cu-Catalyzed Azide-Alkyne Cycloaddition. *Chem. Rev.* **2008**, *108*, 2952–3015.

(45) Liu, P. Y.; Jiang, N.; Zhang, J.; Wei, X.; Lin, H. H.; Yu, X. Q. The Oxidative Damage of Plasmid DNA by Ascorbic Acid Derivatives *in Vitro*: the First Research on the Relationship between the Structure of Ascorbic Acid and the Oxidative Damage of Plasmid DNA. *Chem. Biodiversity* **2006**, *3*, 958–966.

(46) Tasdelen, M. A.; Yagci, Y. Light-Induced Copper(I)-Catalyzed Click Chemistry. *Tetrahedron Lett.* **2010**, *51*, 6945–6947.

(47) Adzima, B. J.; Tao, Y.; Kloxin, C. J.; DeForest, C. A.; Anseth, K. S.; Bowman, C. N. Spatial and Temporal Control of the Alkyne-Azide Cycloaddition by Photoinitiated Cu(II) Reduction. *Nat. Chem.* **2011**, *3*, 256–259.

(48) Zhan, W. H.; Barnhill, H. N.; Sivakumar, K.; Tian, T.; Wang, Q. Synthesis of Hemicyanine Dyes for ‘Click’ Bioconjugation. *Tetrahedron Lett.* **2005**, *46*, 1691–1695.

(49) Golas, P. L.; Tsarevsky, N. V.; Sumerlin, B. S.; Matyjaszewski, K. Catalyst Performance in “Click” Coupling Reactions of Polymers Prepared by ATRP: Ligand and Metal Effects. *Macromolecules* **2006**, *39*, 6451–6457.

(50) Presolski, S. I.; Hong, V. P.; Finn, M. G. Copper-Catalyzed Azide-Alkyne Click Chemistry for Bioconjugation. *Curr. Protoc. Chem. Biol.* **2011**, *3*, 153–162.

(51) Yamamoto, K.; Kawanishi, S. Site-Specific DNA Damage Induced by Hydrazine in the Presence of Manganese and Copper

Ions - the Role of Hydroxyl Radical and Hydrogen-Atom. *J. Biol. Chem.* **1991**, *266*, 1509–1515.

(52) Wang, Q.; Chan, T. R.; Hilgraf, R.; Fokin, V. V.; Sharpless, K. B.; Finn, M. G. Bioconjugation by Copper(I)-Catalyzed Azide-Alkyne [3 + 2] Cycloaddition. *J. Am. Chem. Soc.* **2003**, *125*, 3192–3193.

(53) Neumann, S.; Biewend, M.; Rana, S.; Binder, W. H. The CuAAC: Principles, Homogeneous and Heterogeneous Catalysts, and Novel Developments and Applications. *Macromol. Rapid Commun.* **2020**, *41*, 1900359.

(54) Greenberg, M. M. Reactivity of Nucleic Acid Radicals. *Adv. Phys. Org. Chem.* **2016**, *50*, 119–202.

(55) Pitie, M.; Pratviel, G. Activation of DNA Carbon-Hydrogen Bonds by Metal Complexes. *Chem. Rev.* **2010**, *110*, 1018–1059.

(56) Presolski, S. I.; Hong, V.; Cho, S. H.; Finn, M. G. Tailored Ligand Acceleration of the Cu-Catalyzed Azide-Alkyne Cycloaddition Reaction: Practical and Mechanistic Implications. *J. Am. Chem. Soc.* **2010**, *132*, 14570–14576.

(57) Chan, T. R.; Hilgraf, R.; Sharpless, K. B.; Fokin, V. V. Polytriazoles as Copper(I)-Stabilizing Ligands in Catalysis. *Org. Lett.* **2004**, *6*, 2853–2855.

(58) Lewis, W. G.; Magallon, F. G.; Fokin, V. V.; Finn, M. G. Discovery and Characterization of Catalysts for Azide-Alkyne Cycloaddition by Fluorescence Quenching. *J. Am. Chem. Soc.* **2004**, *126*, 9152–9153.

(59) Kallick, J.; Harris, S.; Udit, A. K.; Hill, M. G. Heterogeneous Catalysis for Azide-Alkyne Bioconjugation in Solution via Spin Column: Attachment of Dyes and Saccharides to Peptides and DNA. *BioTechniques* **2015**, *59*, 329–334.

(60) Heuer-Jungemann, A.; Kirkwood, R.; El-Sagheer, A. H.; Brown, T.; Kanaras, A. G. Copper-Free Click Chemistry as an Emerging Tool for The Programmed Ligation of DNA-Functionalized Gold Nanoparticles. *Nanoscale* **2013**, *5*, 7209–7212.

(61) Shelbourne, M.; Chen, X.; Brown, T.; El-Sagheer, A. H. Fast Copper-Free Click DNA Ligation by the Ring-Strain Promoted Alkyne-Azide Cycloaddition Reaction. *Chem. Commun.* **2011**, *47*, 6257–6259.

(62) Osman, E. A.; Gadzikwa, T.; Gibbs, J. M. Quick Click: The DNA-Templated Ligation of 3'-O-Propargyl- and 5'-Azide-Modified Strands Is as Rapid as and More Selective than Ligase. *ChemBioChem* **2018**, *19*, 2081–2087.

(63) Denis, M.; Goldup, S. M. The Active Template Approach to Interlocked Molecules. *Nat. Rev. Chem.* **2017**, *1*, 0061.

(64) Acevedo-Jake, A.; Ball, A. T.; Galli, M.; Kukwikila, M.; Denis, M.; Singleton, D. G.; Tavassoli, A.; Goldup, S. M. AT-CuAAC Synthesis of Mechanically Interlocked Oligonucleotides. *J. Am. Chem. Soc.* **2020**, *142*, 5985–5990.

(65) Akimova, G.; Chistokletov, V.; Petrov, A. 1,3-Bipolar Addition to Unsaturated Compounds XVIII. Reaction of Aliphatic and Aromatic Azides with the Iotsich Complexes Obtained from Acetylene, Diacetylene, and Their Homologs. *Zh. Obshch. Khim.* **1967**, *3*, 2241–2247.

(66) Akimova, G.; Chistokletov, V.; Petrov, A. 1,3-Bipolar Addition to Unsaturated Compounds XVII. The Reaction of Azides with Iotsich Complexes Obtained from Phenyl- and Alkenylacetylenes. *Zh. Obshch. Khim.* **1967**, *3*, 968–974.

(67) Akimova, G.; Chistokletov, V.; Petrov, A. 1,3-Dipolar Addition to Unsaturated Compounds XIX. Reactions of Aryl Azides with Lithium Acetylides. *Zh. Obshch. Khim.* **1968**, *4*, 389–394.

(68) Krasinski, A.; Fokin, V. V.; Sharpless, K. B. Direct Synthesis of 1,5-Disubstituted-4-Magnesium-1,2,3-Triazoles, Revisited. *Org. Lett.* **2004**, *6*, 1237–1240.

(69) *Ruthenium in Organic Synthesis*; Murahashi, S. I., Ed.; Wiley-VCH: Weinheim, Germany, 2004.

(70) Liu, P. N.; Li, J.; Su, F. H.; Ju, K. D.; Zhang, L.; Shi, C.; Sung, H. H. Y.; Williams, I. D.; Fokin, V. V.; Lin, Z. Y.; et al. Selective Formation of 1,4-Disubstituted Triazoles from Ruthenium-Catalyzed Cycloaddition of Terminal Alkynes and Organic Azides: Scope and Reaction Mechanism. *Organometallics* **2012**, *31*, 4904–4915.

(71) Boren, B. C.; Narayan, S.; Rasmussen, L. K.; Zhang, L.; Zhao, H.; Lin, Z.; Jia, G.; Fokin, V. V. Ruthenium-Catalyzed Azide-Alkyne Cycloaddition: Scope and Mechanism. *J. Am. Chem. Soc.* **2008**, *130*, 8923–8930.

(72) Zhang, L.; Chen, X.; Xue, P.; Sun, H. H. Y.; Williams, I. D.; Sharpless, K. B.; Fokin, V. V.; Jia, G. Ruthenium-Catalyzed Cycloaddition of Alkynes and Organic Azides. *J. Am. Chem. Soc.* **2005**, *127*, 15998–15999.

(73) Pribut, N.; Veale, C. G. L.; Basson, A. E.; van Otterlo, W. A. L.; Pelly, S. C. Application of the Huisgen Cycloaddition and 'Click' Reaction Toward Various 1,2,3-Triazoles as HIV Non-Nucleoside Reverse Transcriptase Inhibitors. *Bioorg. Med. Chem. Lett.* **2016**, *26*, 3700–3704.

(74) Majireck, M. M.; Weinreb, S. M. A Study of the Scope and Regioselectivity of the Ruthenium-Catalyzed [3 + 2]-Cycloaddition of Azides with Internal Alkynes. *J. Org. Chem.* **2006**, *71*, 8680–8683.

(75) Oakdale, J. S.; Fokin, V. V.; Umezaki, S.; Fukuyama, T. Preparation of 1,5-Disubstituted 1,2,3-Triazoles via Ruthenium-catalyzed Azide Alkyne Cycloaddition. *Org. Synth.* **2014**, *90*, 96–104.

(76) Mainardi, J. L.; Villet, R.; Bugg, T. D.; Mayer, C.; Arthur, M. Evolution of Peptidoglycan Biosynthesis under the Selective Pressure of Antibiotics in Gram-Positive Bacteria. *FEMS Microbiol. Rev.* **2008**, *32*, 386–408.

(77) Goffin, C.; Ghuysen, J. M. Biochemistry and Comparative Genomics of SxxK Superfamily Acyltransferases Offer a Clue to the Mycobacterial Paradox: Presence of Penicillin-Susceptible Target Proteins Versus Lack of Efficiency of Penicillin as Therapeutic Agent. *Microbiol. Mol. Biol. Rev.* **2002**, *66*, 702–738.

(78) Chemama, M.; Fonvielle, M.; Arthur, M.; Valery, J. M.; Etheve-Quellejeu, M. Synthesis of Stable Aminoacyl-tRNA Analogues Containing Triazole as a Bioisoster of Esters. *Chem. - Eur. J.* **2009**, *15*, 1929–1938.

(79) Agard, N. J.; Bertozzi, C. R. Chemical Approaches to Perturb, Profile, and Perceive Glycans. *Acc. Chem. Res.* **2009**, *42*, 788–797.

(80) Laughlin, S. T.; Baskin, J. M.; Amacher, S. L.; Bertozzi, C. R. In Vivo Imaging of Membrane-Associated Glycans in Developing Zebrafish. *Science* **2008**, *320*, 664–667.

(81) Devaraj, N. K.; Weissleder, R.; Hilderbrand, S. A. Tetrazine-Based Cycloadditions: Application to Pretargeted Live Cell Imaging. *Bioconjugate Chem.* **2008**, *19*, 2297–2299.

(82) Blackman, M. L.; Royzen, M.; Fox, J. M. Tetrazine Ligation: Fast Bioconjugation Based on Inverse-Electron-Demand Diels-Alder Reactivity. *J. Am. Chem. Soc.* **2008**, *130*, 13518–13519.

(83) Song, W.; Wang, Y.; Qu, J.; Lin, Q. Selective Functionalization of a Genetically Encoded Alkene-Containing Protein via "Photoclick Chemistry" in Bacterial Cells. *J. Am. Chem. Soc.* **2008**, *130*, 9654–9655.

(84) Ning, X.; Guo, J.; Wolfert, M. A.; Boons, G.-J. Visualizing Metabolically Labeled Glycoconjugates of Living Cells by Copper-Free and Fast Huisgen Cycloadditions. *Angew. Chem., Int. Ed.* **2008**, *47*, 2253–2255.

(85) Hamlin, T. A.; Levandowski, B. J.; Narsaria, A. K.; Houk, K. N.; Bickelhaupt, F. M. Structural Distortion of Cycloalkynes Influences Cycloaddition Rates both by Strain and Interaction Energies. *Chem. - Eur. J.* **2019**, *25*, 6342–6348.

(86) Dommerholt, J.; Rutjes, F. P. J. T.; van Delft, F. L. Strain-Promoted 1,3-Dipolar Cycloaddition of Cycloalkynes and Organic Azides. *Top. Curr. Chem.* **2016**, *374*, 16.

(87) Krebs, A.; Wilke, J. Angle Strained Cycloalkynes. *Top. Curr. Chem.* **1983**, *109*, 189–233.

(88) Baskin, J. M.; Prescher, J. A.; Laughlin, S. T.; Agard, N. J.; Chang, P. V.; Miller, I. A.; Lo, A.; Codelli, J. A.; Bertozzi, C. R. Copper-Free Click Chemistry for Dynamic In Vivo Imaging. *Proc. Natl. Acad. Sci. U. S. A.* **2007**, *104*, 16793–16797.

(89) Buhl, H.; Gugel, H.; Kolshorn, H.; Meier, H. Eine verbesserte Cyclooctyn-Synthese. *Synthesis* **1978**, *1978*, 536–537.

(90) Marks, I. S.; Kang, J. S.; Jones, B. T.; Landmark, K. J.; Cleland, A. J.; Taton, T. A. Strain-Promoted "Click" Chemistry for Terminal Labeling of DNA. *Bioconjugate Chem.* **2011**, *22*, 1259–1263.

- (91) Shelbourne, M.; Brown, T.; El-Sagheer, A. H.; Brown, T. Fast and Efficient DNA Crosslinking and Multiple Orthogonal Labelling by Copper-Free Click Chemistry. *Chem. Commun.* **2012**, *48*, 11184–11186.
- (92) van Delft, P.; Meeuwenoord, N. J.; Hoogendoorn, S.; Dinkelaar, J.; Overkleeft, H. S.; van der Marel, G. A.; Filippov, D. V. Synthesis of Oligoribonucleic Acid Conjugates Using a Cyclooctyne Phosphoramidite. *Org. Lett.* **2010**, *12*, 5486–5489.
- (93) Jayaprakash, K. N.; Peng, C. G.; Butler, D.; Varghese, J. P.; Maier, M. A.; Rajeev, K. G.; Manoharan, M. Non-Nucleoside Building Blocks for Copper-Assisted and Copper-Free Click Chemistry for the Efficient Synthesis of RNA Conjugates. *Org. Lett.* **2010**, *12*, 5410–5413.
- (94) Ren, X. M.; El-Sagheer, A. H.; Brown, T. Efficient Enzymatic Synthesis and Dual-Colour Fluorescent Labelling of DNA Probes Using Long Chain Azido-dUTP and BCN Dyes. *Nucleic Acids Res.* **2016**, *44*, No. e79.
- (95) Singh, I.; Freeman, C.; Madder, A.; Vyle, J. S.; Heaney, F. Fast RNA Conjugations on Solid Phase by Strain-Promoted Cycloadditions. *Org. Biomol. Chem.* **2012**, *10*, 6633–6639.
- (96) Debets, M. F.; Van Berkel, S. S.; Dommerholt, J.; Dirks, A. J.; Rutjes, F. P. J. T.; Van Delft, F. L. Bioconjugation with Strained Alkenes and Alkynes. *Acc. Chem. Res.* **2011**, *44*, 805–815.
- (97) Dommerholt, J.; Schmidt, S.; Temming, R.; Hendriks, L. J. A.; Rutjes, F. P. J. T.; van Hest, J. C. M.; Lefeber, D. J.; Friedl, P.; van Delft, F. L. Readily Accessible Bicyclononynes for Bioorthogonal Labeling and Three-Dimensional Imaging of Living Cells. *Angew. Chem., Int. Ed.* **2010**, *49*, 9422–9425.
- (98) Jawalekar, A. M.; Malik, S.; Verkade, J. M. M.; Gibson, B.; Barta, N. S.; Hodges, J. C.; Rowan, A.; van Delft, F. L. Oligonucleotide Tagging for Copper-Free Click Conjugation. *Molecules* **2013**, *18*, 7346–7363.
- (99) Gutmiedl, K.; Wirges, C. T.; Ehmke, V.; Carell, T. Copper-Free ‘Click’ Modification of Dna via Nitrile Oxide-Norbornene 1,3-Dipolar Cycloaddition. *Org. Lett.* **2009**, *11*, 2405–2408.
- (100) Graham, D.; Parkinson, J. A.; Brown, T. DNA Duplexes Stabilized by Modified Monomer Residues: Synthesis and Stability. *J. Chem. Soc., Perkin Trans. 1* **1998**, 1131–1138.
- (101) Ding, P.; Wunnicke, D.; Steinhoff, H. J.; Seela, F. Site-Directed Spin-Labeling of DNA by the Azide-Alkyne ‘Click’ Reaction: Nanometer Distance Measurements on 7-Deaza-2'-Deoxyadenosine and 2'-Deoxyuridine Nitroxide Conjugates Spatially Separated or Linked to a 'dA-dT' Base Pair. *Chem. - Eur. J.* **2010**, *16*, 14385–14396.
- (102) Gramlich, P. M. E.; Warncke, S.; Gierlich, J.; Carell, T. Click-Click-Click: Single to Triple Modification of DNA. *Angew. Chem., Int. Ed.* **2008**, *47*, 3442–3444.
- (103) Seela, F.; Ming, X. Oligonucleotides Containing 7-Deaza-2'-Deoxyinosine as Universal Nucleoside: Synthesis of 7-Halogenated and 7-Alkynylated Derivatives, Ambiguous Base Pairing, and Dye Functionalization by the Alkyne - Azide ‘Click’ Reaction. *Helv. Chim. Acta* **2008**, *91*, 1181–1200.
- (104) Seela, F.; Sirivolu, V. R.; Chitpepu, P. Modification of DNA with Octadiynyl Side Chains: Synthesis, Base Pairing, and Formation of Fluorescent Coumarin Dye Conjugates of Four Nucleobases by the Alkyne-Azide “Click” Reaction. *Bioconjugate Chem.* **2008**, *19*, 211–224.
- (105) Wamberg, M. C.; Wiczorek, R.; Brier, S. B.; de Vries, J. W.; Kwak, M.; Herrmann, A.; Monnard, P. A. Functionalization of Fatty Acid Vesicles through Newly Synthesized Bolaamphiphile-DNA Conjugates. *Bioconjugate Chem.* **2014**, *25*, 1678–1688.
- (106) Seela, F.; Xiong, H.; Leonard, P.; Budow, S. 8-Aza-7-Deazaguanine Nucleosides and Oligonucleotides with Octadiynyl Side Chains: Synthesis, Functionalization by the Azide-Alkyne ‘Click’ Reaction and Nucleobase Specific Fluorescence Quenching of Coumarin Dye Conjugates. *Org. Biomol. Chem.* **2009**, *7*, 1374–1387.
- (107) Gierlich, J.; Gutmiedl, K.; Gramlich, P. M. E.; Schmidt, A.; Burley, G. A.; Carell, T. Synthesis of Highly Modified DNA by a Combination of PCR with Alkyne-Bearing Triphosphates and Click Chemistry. *Chem. - Eur. J.* **2007**, *13*, 9486–9494.
- (108) Gramlich, P. M. E.; Wirges, C. T.; Gierlich, J.; Carell, T. Synthesis of Modified DNA by PCR with Alkyne-Bearing Purines Followed by a Click Reaction. *Org. Lett.* **2008**, *10*, 249–251.
- (109) Maciáková-Cahová, H.; Pohl, R.; Hocek, M. Cleavage of Functionalized DNA Containing 5-Modified Pyrimidines by Type II Restriction Endonucleases. *ChemBioChem* **2011**, *12*, 431–438.
- (110) Ren, X.; El-Sagheer, A. H.; Brown, T. Azide and Trans-Cyclooctene dUTPs: Incorporation into DNA Probes and Fluorescent Click-Labeling. *Analyst* **2015**, *140*, 2671–2678.
- (111) Balintová, J.; Čpaček, J.; Pohl, R.; Brázdová, M.; Havran, L.; Fojta, M.; Hocek, M. Azidophenyl as a Click-Transformable Redox Label of DNA Suitable for Electrochemical Detection of DNA-Protein Interactions. *Chem. Sci.* **2015**, *6*, 575–587.
- (112) Ren, X.; El-Sagheer, A. H.; Brown, T. Efficient Enzymatic Synthesis and Dual-Colour Fluorescent Labelling of DNA Probes Using Long Chain Azido-dUTP and BCN Dyes. *Nucleic Acids Res.* **2016**, *44*, No. e79.
- (113) Ren, X. M.; Gerowska, M.; El-Sagheer, A. H.; Brown, T. Enzymatic Incorporation and Fluorescent Labelling of Cyclooctyne-Modified Deoxyuridine Triphosphates in DNA. *Bioorg. Med. Chem.* **2014**, *22*, 4384–4390.
- (114) Seo, T. S.; Li, Z.; Ruparel, H.; Ju, J. Click Chemistry to Construct Fluorescent Oligonucleotides for DNA Sequencing. *J. Org. Chem.* **2003**, *68*, 609–612.
- (115) Gerowska, M.; Hall, L.; Richardson, J.; Shelbourne, M.; Brown, T. Efficient Reverse Click Labeling of Azide Oligonucleotides with Multiple Alkynyl Cy-Dyes Applied to the Synthesis of HyBeacon Probes for Genetic Analysis. *Tetrahedron* **2012**, *68*, 857–864.
- (116) Steger, J.; Graber, D.; Moroder, H.; Geiermann, A. S.; Aigner, M.; Micura, R. Efficient Access to Nonhydrolyzable Initiator tRNA Based on The Synthesis of 3'-Azido-3'-Deoxyadenosine RNA. *Angew. Chem., Int. Ed.* **2010**, *49*, 7470–7472.
- (117) Slavickova, M.; Janouskova, M.; Simonova, A.; Cahova, H.; Kambova, M.; Sanderova, H.; Krasny, L.; Hocek, M. Turning Off Transcription with Bacterial RNA Polymerase through CuAAC Click Reactions of DNA Containing 5-Ethynyluracil. *Chem. - Eur. J.* **2018**, *24*, 8311–8314.
- (118) Ingale, S. A.; Mei, H.; Leonard, P.; Seela, F. Ethynyl Side Chain Hydration During Synthesis and Workup of “Clickable” Oligonucleotides: Bypassing Acetyl Group Formation by Triisopropylsilyl Protection. *J. Org. Chem.* **2013**, *78*, 11271–11282.
- (119) Neef, A. B.; Pernot, L.; Schreier, V. N.; Scapozza, L.; Luedtke, N. W. A Bioorthogonal Chemical Reporter of Viral Infection. *Angew. Chem., Int. Ed.* **2015**, *54*, 7911–7914.
- (120) Neef, A. B.; Luedtke, N. W. Dynamic Metabolic Labeling of DNA *in Vivo* with Arabinosyl Nucleosides. *Proc. Natl. Acad. Sci. U. S. A.* **2011**, *108*, 20404–20409.
- (121) Samanta, A.; Krause, A.; Jaschke, A. A Modified Dinucleotide for Site-Specific RNA-Labeling by Transcription Priming and Click Chemistry. *Chem. Commun.* **2014**, *50*, 1313–1316.
- (122) Winz, M. L.; Samanta, A.; Benzinger, D.; Jaschke, A. Site-Specific Terminal and Internal Labeling of RNA by Poly(A) Polymerase Tailing and Copper-Catalyzed or Copper-Free Strain-Promoted Click Chemistry. *Nucleic Acids Res.* **2012**, *40*, No. e78.
- (123) Dojahn, C. M.; Hesse, M.; Arenz, C. A Chemo-Enzymatic Approach to Specifically Click-Modified RNA. *Chem. Commun.* **2013**, *49*, 3128–3130.
- (124) Seela, F.; Sirivolu, V. R. Nucleosides and Oligonucleotides with Diynyl Side Chains: Base Pairing and Functionalization of 2'-Deoxyuridine Derivatives by the Copper(I)-Catalyzed Alkyne-Azide ‘Click’ Cycloaddition. *Helv. Chim. Acta* **2007**, *90*, 535–552.
- (125) Seela, F.; Sirivolu, V. R. DNA Containing Side Chains with Terminal Triple Bonds: Base-Pair Stability and Functionalization of Alkynylated Pyrimidines and 7-Deazapurines. *Chem. Biodiversity* **2006**, *3*, 509–514.

- (126) Seela, F.; Ingale, S. A. Double Click" Reaction on 7-Deazaguanine DNA: Synthesis and Excimer Fluorescence of Nucleosides and Oligonucleotides with Branched Side Chains Decorated with Proximal Pyrenes. *J. Org. Chem.* **2010**, *75*, 284–295.
- (127) Sirivolu, V. R.; Chittepudi, P.; Seela, F. DNA with Branched Internal Side Chains: Synthesis of 5-Tripropargylamine-dU and Conjugation by an Azide-Alkyne Double Click Reaction. *ChemBioChem* **2008**, *9*, 2305–2316.
- (128) Panattoni, A.; Pohl, R.; Hocke, M. Flexible Alkyne-Linked Thymidine Phosphoramidites and Triphosphates for Chemical or Polymerase Synthesis and Fast Postsynthetic DNA Functionalization through Copper-Catalyzed Alkyne Azide 1,3-Dipolar Cycloaddition. *Org. Lett.* **2018**, *20*, 3962–3965.
- (129) Krishna, H.; Caruthers, M. H. Alkynyl Phosphonate DNA: A Versatile "Click"able Backbone for DNA-Based Biological Applications. *J. Am. Chem. Soc.* **2012**, *134*, 11618–11631.
- (130) Obeid, S.; Bußkamp, H.; Welte, W.; Diederichs, K.; Marx, A. Interactions of Non-Polar and "Click-able" Nucleotides in the Confines of a DNA Polymerase Active Site. *Chem. Commun.* **2012**, *48*, 8320–8322.
- (131) Obeid, S.; Baccaro, A.; Welte, W.; Diederichs, K.; Marx, A. Structural Basis for the Synthesis of Nucleobase Modified DNA by *Thermus Aquaticus* DNA Polymerase. *Proc. Natl. Acad. Sci. U. S. A.* **2010**, *107*, 21327–21331.
- (132) Ranasinghe, R. T.; Brown, T. Fluorescence Based Strategies for Genetic Analysis. *Chem. Commun.* **2005**, 5487–5502.
- (133) Ranasinghe, R. T.; Brown, T. Ultrasensitive Fluorescence-Based Methods for Nucleic Acid Detection: Towards Amplification-Free Genetic Analysis. *Chem. Commun.* **2011**, *47*, 3717–3735.
- (134) Shendure, J.; Mitra, R. D.; Varma, C.; Church, G. M. Advanced Sequencing Technologies: Methods and Goals. *Nat. Rev. Genet.* **2004**, *5*, 335–344.
- (135) Berndt, S.; Herzig, N.; Kele, P.; Lachmann, D.; Li, X. H.; Wolfbeis, O. S.; Wagenknecht, H. A. Comparison of a Nucleosidic vs Non-Nucleosidic Postsynthetic "Click" Modification of DNA with Base-Labile Fluorescent Probes. *Bioconjugate Chem.* **2009**, *20*, 558–564.
- (136) Holzhauser, C.; Wagenknecht, H. A. DNA and RNA "Traffic Lights": Synthetic Wavelength-Shifting Fluorescent Probes Based on Nucleic Acid Base Substitutes for Molecular Imaging. *J. Org. Chem.* **2013**, *78*, 7373–7379.
- (137) Holzhauser, C.; Rubner, M. M.; Wagenknecht, H. A. Energy-Transfer-Based Wavelength-Shifting DNA Probes with "Clickable" Cyanine Dyes. *Photochem. Photobiol. Sci.* **2013**, *12*, 722–724.
- (138) Jorgensen, A. S.; Gupta, P.; Wengel, J.; Astakhova, I. K. Clickable" LNA/DNA Probes for Fluorescence Sensing of Nucleic Acids and Autoimmune Antibodies. *Chem. Commun.* **2013**, *49*, 10751–10753.
- (139) Willibald, J.; Harder, J.; Sparrer, K.; Conzelmann, K. K.; Carell, T. Click-Modified Anandamide siRNA Enables Delivery and Gene Silencing in Neuronal and Immune Cells. *J. Am. Chem. Soc.* **2012**, *134*, 12330–12333.
- (140) Husken, N.; Gasser, G.; Koster, S. D.; Metzler-Nolte, N. Four-Potential" Ferrocene Labeling of PNA Oligomers via Click Chemistry. *Bioconjugate Chem.* **2009**, *20*, 1578–1586.
- (141) Gasser, G.; Pinto, A.; Neumann, S.; Sosniak, A. M.; Seitz, M.; Merz, K.; Heumann, R.; Metzler-Nolte, N. Synthesis, Characterisation and Bioimaging of a Fluorescent Rhenium-Containing PNA Bioconjugate. *Dalton Trans.* **2012**, *41*, 2304–2313.
- (142) Gasser, G.; Jäger, K.; Zenker, M.; Bergmann, R.; Steinbach, J.; Stephan, H.; Metzler-Nolte, N. Preparation, <sup>99m</sup>Tc-Labeling and Biodistribution Studies of a PNA Oligomer Containing a New Ligand Derivative of 2,2'-Dipicolylamine. *J. Inorg. Biochem.* **2010**, *104*, 1133–1140.
- (143) Panattoni, A.; El-Sagheer, A. H.; Brown, T.; Kellett, A.; Hocke, M. Oxidative DNA Cleavage with Clip-Phenanthroline Triplex-Forming Oligonucleotide Hybrids. *ChemBioChem* **2020**, *21*, 991.
- (144) Bales, B. C.; Kodama, T.; Weledji, Y. N.; Pitie, M.; Meunier, B.; Greenberg, M. M. Mechanistic Studies on DNA Damage by Minor Groove Binding Copper-Phenanthroline Conjugates. *Nucleic Acids Res.* **2005**, *33*, 5371–5379.
- (145) Sigman, D. S.; Mazumder, A.; Perrin, D. M. Chemical Nucleases. *Chem. Rev.* **1993**, *93*, 2295–2316.
- (146) Lauria, T.; Slatore, C.; McKee, V.; Müller, M.; Stazzoni, S.; Crisp, A. L.; Carell, T.; Kellett, A. A Click Chemistry Approach to Developing Molecularly Targeted DNA Scissors. *Chem.—Eur. J.* **2020**, *26*, 16782–16792.
- (147) Fantoni Zuin, N.; McGorman, B.; Molphy, Z.; Singleton, D.; Walsh, S.; El-Sagheer, A. H.; McKee, V.; Brown, T.; Kellett, A. Development of Gene-Targeted Polypyridyl Triplex Forming Oligonucleotide Hybrids. *ChemBioChem* **2020**, *21*, 3563–3574.
- (148) Gratzner, H. G. Monoclonal-Antibody to 5-Bromodeoxyuridine and 5-Iododeoxyuridine - a New Reagent for Detection of DNA-Replication. *Science* **1982**, *218*, 474–475.
- (149) Waldman, F. M.; Chew, K.; Ljung, B. M.; Goodson, W.; Hom, J.; Duarte, L.; Smith, H. S.; Mayall, B. A Comparison between Bromodeoxyuridine and <sup>3</sup>H Thymidine Labeling in Human Breast-Tumors. *Mod. Pathol.* **1991**, *4*, 718–722.
- (150) Uddin, M.; Altmann, G. G.; Leblond, C. P. Radioautographic visualization of differences in the pattern of [<sup>3</sup>H]uridine and [<sup>3</sup>H]orotic acid incorporation into the RNA of migrating columnar cells in the rat small intestine. *J. Cell Biol.* **1984**, *98*, 1619–1629.
- (151) Cmarko, D.; Verschure, P. J.; Martin, T. E.; Dahmus, M. E.; Krause, S.; Fu, X. D.; van Driel, R.; Fakan, S. Ultrastructural Analysis of Transcription and Splicing in the Cell Nucleus after Bromo-UTP Microinjection. *Mol. Biol. Cell* **1999**, *10*, 211–223.
- (152) Meneni, S.; Ott, I.; Sergeant, C. D.; Sniady, A.; Gust, R.; Dembinski, R. 5-Alkynyl-2'-Deoxyuridines: Chromatography-Free Synthesis and Cytotoxicity Evaluation Against Human Breast Cancer Cells. *Bioorg. Med. Chem.* **2007**, *15*, 3082–3088.
- (153) Neef, A. B.; Luedtke, N. W. An Azide-Modified Nucleoside for Metabolic Labeling of DNA. *ChemBioChem* **2014**, *15*, 789–793.
- (154) Jao, C. Y.; Salic, A. Exploring RNA Transcription and Turnover *In Vivo* by Using Click Chemistry. *Proc. Natl. Acad. Sci. U. S. A.* **2008**, *105*, 15779–15784.
- (155) Curanovic, D.; Cohen, M.; Singh, I.; Slagle, C. E.; Leslie, C. S.; Jaffrey, S. R. Global Profiling of Stimulus-Induced Polyadenylation in Cells Using a Poly(A) Trap. *Nat. Chem. Biol.* **2013**, *9*, 671–673.
- (156) Grammel, M.; Hang, H.; Conrad, N. K. Chemical Reporters for Monitoring RNA Synthesis and Poly(A) Tail Dynamics. *ChemBioChem* **2012**, *13*, 1112–1115.
- (157) Feng, H. J.; Zhang, X. G.; Zhang, C. L. mRIN for Direct Assessment of Genome-Wide and Gene-Specific mRNA Integrity from Large-Scale RNA-Sequencing Data. *Nat. Commun.* **2015**, *6*, 7816.
- (158) Nainar, S.; Beasley, S.; Fazio, M.; Kubota, M.; Dai, N.; Correa, I. R.; Spitale, R. C. Metabolic Incorporation of Azide Functionality into Cellular RNA. *ChemBioChem* **2016**, *17*, 2149–2152.
- (159) Sawant, A. A.; Tanpure, A. A.; Mukherjee, P. P.; Athavale, S.; Kelkar, A.; Galande, S.; Srivatsan, S. G. A Versatile Toolbox for Posttranscriptional Chemical Labeling and Imaging of RNA. *Nucleic Acids Res.* **2016**, *44*, No. e16.
- (160) Zhang, Y.; Kleiner, R. E. A Metabolic Engineering Approach to Incorporate Modified Pyrimidine Nucleosides into Cellular RNA. *J. Am. Chem. Soc.* **2019**, *141*, 3347–3351.
- (161) Nainar, S.; Cuthbert, B. J.; Lim, N. M.; England, W. E.; Ke, K.; Sophal, K.; Quechol, R.; Mobley, D. L.; Goulding, C. W.; Spitale, R. C. An Optimized Chemical-Genetic Method for Cell-Specific Metabolic Labeling of RNA. *Nat. Methods* **2020**, *17*, 311–318.
- (162) Wang, D. Y.; Zhang, Y.; Kleiner, R. E. Cell- and Polymerase-Selective Metabolic Labeling of Cellular RNA with 2'-Azidocytidine. *J. Am. Chem. Soc.* **2020**, *142*, 14417–14421.
- (163) Motorin, Y.; Burhenne, J.; Teimer, R.; Koynov, K.; Willnow, S.; Weinhold, E.; Helm, M. Expanding the Chemical Scope of

RNA:Methyltransferases to Site-Specific Alkynylation of RNA for Click Labeling. *Nucleic Acids Res.* **2011**, *39*, 1943–1952.

(164) Hartstock, K.; Nilges, B. S.; Ovcharenko, A.; Cornelissen, N. V.; Pullen, N.; Lawrence-Dorner, A. M.; Leidel, S. A.; Rentmeister, A. Enzymatic or *In Vivo* Installation of Propargyl Groups in Combination with Click Chemistry for the Enrichment and Detection of Methyltransferase Target Sites in RNA. *Angew. Chem., Int. Ed.* **2018**, *57*, 6342–6346.

(165) Holstein, J. M.; Schulz, D.; Rentmeister, A. Bioorthogonal Site-Specific Labeling of the 5'-Cap Structure in Eukaryotic mRNAs. *Chem. Commun.* **2014**, *50*, 4478–4481.

(166) Schulz, D.; Holstein, J. M.; Rentmeister, A. A Chemo-Enzymatic Approach for Site-Specific Modification of the RNA Cap. *Angew. Chem., Int. Ed.* **2013**, *52*, 7874–7878.

(167) Nakahara, M.; Kuboyama, T.; Izawa, A.; Hari, Y.; Imanishi, T.; Obika, S. Synthesis and base-pairing properties of C-nucleotides having 1-substituted 1H-1,2,3-triazoles. *Bioorg. Med. Chem. Lett.* **2009**, *19*, 3316–3319.

(168) Chittepu, P.; Sirivolu, V. R.; Seela, F. Nucleosides and Oligonucleotides Containing 1,2,3-Triazole Residues with Nucleobase Tethers: Synthesis via the Azide-Alkyne 'Click' Reaction. *Bioorg. Med. Chem.* **2008**, *16*, 8427–8439.

(169) Ma, S. Y.; Saaem, I.; Tian, J. D. Error Correction in Gene Synthesis Technology. *Trends Biotechnol.* **2012**, *30*, 147–154.

(170) Luebke, K. J.; Dervan, P. B. Nonenzymatic Sequence-Specific Ligation of Double-Helical DNA. *J. Am. Chem. Soc.* **1991**, *113*, 7447–7448.

(171) Sokolova, N. I.; Ashirbekova, D. T.; Dolinnaya, N. G.; Shabarova, Z. A. Chemical-Reactions in Nucleic-Acid Duplexes.4. Cyanogen-Bromide as an Efficient Reagent in Condensation of Oligodeoxyribonucleotides. *Bioorg. Khim.* **1987**, *13*, 1286–1288.

(172) Nuzzi, A.; Massi, A.; Dondoni, A. Model Studies toward the Synthesis of Thymidine Oligonucleotides with Triazole Internucleosidic Linkages via Iterative Cu(I)-Promoted Azide-Alkyne Ligation Chemistry. *QSAR Comb. Sci.* **2007**, *26*, 1191–1199.

(173) Fujino, T.; Yamazaki, N.; Hasome, A.; Endo, K.; Isobe, H. Efficient and Improved Synthesis of Triazole-Linked DNA ((TL)-DNA) Oligomers. *Tetrahedron Lett.* **2012**, *53*, 868–870.

(174) Fujino, T.; Suzuki, T.; Ooi, T.; Ikemoto, K.; Isobe, H. Duplex-Forming Oligonucleotide of Triazole-Linked RNA. *Chem. - Asian J.* **2019**, *14*, 3380–3385.

(175) Varizhuk, A. M.; Chizhov, A.; Smirnov, I.; Kaluzhny, D.; Florentiev, V. Triazole-Linked Oligonucleotides with Mixed-Base Sequences: Synthesis and Hybridization Properties. *Eur. J. Org. Chem.* **2012**, *2012*, 2173–2179.

(176) Dallmann, A.; El-Sagheer, A. H.; Dehmel, L.; Mugge, C.; Griesinger, C.; Ernsting, N. P.; Brown, T. Structure and Dynamics of Triazole-Linked DNA: Biocompatibility Explained. *Chem. - Eur. J.* **2011**, *17*, 14714–14717.

(177) El-Sagheer, A. H.; Brown, T. Combined Nucleobase and Backbone Modifications Enhance DNA Duplex Stability and Preserve Biocompatibility. *Chem. Sci.* **2014**, *5*, 253–259.

(178) Varizhuk, A. M.; Kaluzhny, D. N.; Novikov, R. A.; Chizhov, A. O.; Smirnov, I. P.; Chuvilin, A. N.; Tatarinova, O. N.; Fisunov, G. Y.; Pozmogova, G. E.; Florentiev, V. L. Synthesis of Triazole-Linked Oligonucleotides with High Affinity to DNA Complements and an Analysis of Their Compatibility with Biosystems. *J. Org. Chem.* **2013**, *78*, 5964–5969.

(179) Baker, Y. R.; Traore, D.; Wanat, P.; Tyburn, A.; El-Sagheer, A. H.; Brown, T. Searching for the Ideal Triazole: Investigating the 1,5-Triazole as a Charge Neutral DNA Backbone Mimic. *Tetrahedron* **2020**, *76*, 130914.

(180) El-Sagheer, A. H.; Brown, T. Synthesis and Polymerase Chain Reaction Amplification of DNA Strands Containing an Unnatural Triazole Linkage. *J. Am. Chem. Soc.* **2009**, *131*, 3958–3964.

(181) El-Sagheer, A. H.; Brown, T. Efficient RNA Synthesis by *in Vitro* Transcription of a Triazole-Modified DNA Template. *Chem. Commun.* **2011**, *47*, 12057–12058.

(182) Birts, C. N.; Sanzone, A. P.; El-Sagheer, A. H.; Blaydes, J. P.; Brown, T.; Tavassoli, A. Transcription of Click-Linked DNA in Human Cells. *Angew. Chem., Int. Ed.* **2014**, *53*, 2362–2365.

(183) Kukwikila, M.; Gale, N.; El-Sagheer, A. H.; Brown, T.; Tavassoli, A. Assembly of a Biocompatible Triazole-Linked Gene by One-Pot Click-DNA Ligation. *Nat. Chem.* **2017**, *9*, 1089–1098.

(184) Chen, X.; El-Sagheer, A. H.; Brown, T. Reverse Transcription through a Bulky Triazole Linkage in RNA: Implications for RNA Sequencing. *Chem. Commun.* **2014**, *50*, 7597–7600.

(185) Li, Y.; Korolev, S.; Waksman, G. Crystal Structures of Open and Closed Forms of Binary and Ternary Complexes of the Large Fragment of *Thermus Aquaticus* DNA Polymerase I: Structural Basis for Nucleotide Incorporation. *EMBO J.* **1998**, *17*, 7514–7525.

(186) Shivalingam, A.; Tyburn, A. E. S.; El-Sagheer, A. H.; Brown, T. Molecular Requirements of High-Fidelity Replication-Competent DNA Backbones for Orthogonal Chemical Ligation. *J. Am. Chem. Soc.* **2017**, *139*, 1575–1583.

(187) Weng, Y. H.; Xiao, H. H.; Zhang, J. C.; Liang, X. J.; Huang, Y. Y. RNAi Therapeutic and its Innovative Biotechnological Evolution. *Biotechnol. Adv.* **2019**, *37*, 801–825.

(188) Aartsma-Rus, A.; Krieg, A. M. FDA Approves Eteplirsen for Duchenne Muscular Dystrophy: The Next Chapter in the Eteplirsen Saga. *Nucleic Acid Ther.* **2017**, *27*, 1–3.

(189) Aartsma-Rus, A. FDA Approval of Nusinersen for Spinal Muscular Atrophy Makes 2016 the Year of Splice Modulating Oligonucleotides. *Nucleic Acid Ther.* **2017**, *27*, 67–69.

(190) Palframan, M. J.; Alharthy, R. D.; Powalowska, P. K.; Hayes, C. J. Synthesis of Triazole-Linked Morpholino Oligonucleotides via Cu Catalysed Cycloaddition. *Org. Biomol. Chem.* **2016**, *14*, 3112–3119.

(191) Kumar, P.; El-Sagheer, A. H.; Truong, L.; Brown, T. Locked Nucleic Acid (LNA) Enhances Binding Affinity of Triazole-Linked DNA towards RNA. *Chem. Commun.* **2017**, *53*, 8910–8913.

(192) Kumar, P.; Truong, L.; Baker, Y. R.; El-Sagheer, A. H.; Brown, T. Synthesis, Affinity for Complementary RNA and DNA, and Enzymatic Stability of Triazole-Linked Locked Nucleic Acids (t-LNAs). *ACS Omega* **2018**, *3*, 6976–6987.

(193) Sharma, V. K.; Singh, S. K.; Krishnamurthy, P. M.; Alterman, J. F.; Haraszti, R. A.; Khvorova, A.; Prasad, A. K.; Watts, J. K. Synthesis and Biological Properties of Triazole-Linked Locked Nucleic Acid. *Chem. Commun.* **2017**, *53*, 8906–8909.

(194) Rees, H. A.; Liu, D. R. Base Editing: Precision Chemistry on the Genome and Transcriptome of Living Cells. *Nat. Rev. Genet.* **2018**, *19*, 770–788.

(195) Fellmann, C.; Gowen, B. G.; Lin, P. C.; Doudna, J. A.; Corn, J. E. Cornerstones of CRISPR-Cas in Drug Discovery and Therapy. *Nat. Rev. Drug Discovery* **2017**, *16*, 89–100.

(196) He, K. Z.; Chou, E. T.; Begay, S.; Anderson, E. M.; Smith, A. V. Conjugation and Evaluation of Triazole-Linked Single Guide RNA for CRISPR-Cas9 Gene Editing. *ChemBioChem* **2016**, *17*, 1809–1812.

(197) Taemaitree, L.; Shivalingam, A.; El-Sagheer, A. H.; Brown, T. An Artificial Triazole Backbone Linkage Provides a Split-and-Click Strategy to Bioactive Chemically Modified CRISPR sgRNA. *Nat. Commun.* **2019**, *10*, 1610.

(198) Seeman, N. C. Nanomaterials Based on DNA. *Annu. Rev. Biochem.* **2010**, *79*, 65–87.

(199) Jacobsen, M. F.; Ravnsbaek, J. B.; Gothelf, K. V. Small Molecule Induced Control in Duplex and Triplex DNA-Directed Chemical Reactionst. *Org. Biomol. Chem.* **2010**, *8*, 50–52.

(200) Xu, Y.; Suzuki, Y.; Komiyama, M. Click Chemistry for the Identification of G-Quadruplex Structures: Discovery of a DNA-RNA G-Quadruplex. *Angew. Chem., Int. Ed.* **2009**, *48*, 3281–3284.

(201) Xiong, H.; Seela, F. Stepwise "Click" Chemistry for the Template Independent Construction of a Broad Variety of Cross-Linked Oligonucleotides: Influence of Linker Length, Position, and Linking Number on DNA Duplex Stability. *J. Org. Chem.* **2011**, *76*, 5584–5597.

(202) Pujari, S. S.; Xiong, H.; Seela, F. Cross-Linked DNA Generated by “Bis-Click” Reactions with Bis-Functional Azides: Site Independent Ligation of Oligonucleotides via Nucleobase Alkynyl Chains. *J. Org. Chem.* **2010**, *75*, 8693–8696.

(203) Seela, F.; Sirivolu, V. R. Nucleosides and Oligonucleotides with Diynyl Side Chains: The Huisgen-Sharpless Cycloaddition “Click Reaction” Performed on DNA and their Constituents. *Nucleosides, Nucleotides Nucleic Acids* **2007**, *26*, 597–601.

(204) Xiong, H.; Seela, F. Cross-Linked DNA: Site-Selective “Click” Ligation in Duplexes with Bis-Azides and Stability Changes Caused by Internal Cross-Links. *Bioconjugate Chem.* **2012**, *23*, 1230–1243.

(205) Nordell, P.; Westerlund, F.; Reymer, A.; El-Sagheer, A. H.; Brown, T.; Norden, B.; Lincoln, P. DNA Polymorphism as an Origin of Adenine-Thymine Tract Length-Dependent Threading Intercalation Rate. *J. Am. Chem. Soc.* **2008**, *130*, 14651–14658.

(206) El-Sagheer, A. H.; Brown, T. Synthesis, Serum Stability and Cell Uptake of Cyclic and Hairpin Decoy Oligonucleotides for TCF/LEF and GLI Transcription Factors. *Int. J. Pept. Res. Ther.* **2008**, *14*, 367–372.

(207) Nakane, M.; Ichikawa, S.; Matsuda, A. Triazole-Linked Dumbbell Oligodeoxynucleotides with NF-Kappa B Binding Ability as Potential Decoy Molecules. *J. Org. Chem.* **2008**, *73*, 1842–1851.

(208) Romling, U.; Gomelsky, M.; Galperin, M. Y. C-di-GMP: the Dawning of a Novel Bacterial Signalling System. *Mol. Microbiol.* **2005**, *57*, 629–639.

(209) Danilchanka, O.; Mekalanos, J. J. Cyclic Dinucleotides and the Innate Immune Response. *Cell* **2013**, *154*, 962–970.

(210) Dialer, C. R.; Stazzoni, S.; Drexler, D. J.; Müller, F. M.; Veth, S.; Pichler, A.; Okamura, H.; Witte, G.; Hopfner, K. P.; Carell, T. A Click-Chemistry Linked 2'3'-cGAMP Analogue. *Chem. - Eur. J.* **2019**, *25*, 2089–2095.